2020

Analysis Of The Role For Antioxidant Enzyme Heme Oxygenase-1 In Brain Regional Hiv Neuropathogenesis And Blood-Brain Barrier Function

Analise L. Gruenewald
University of Pennsylvania

Analysis Of The Role For Antioxidant Enzyme Heme Oxygenase-1 In Brain Regional Hiv Neuropathogenesis And Blood-Brain Barrier Function

Abstract

HIV-associated neurocognitive impairment (HIV NCI) persists in persons living with HIV (PLWH) despite the availability of suppressive combination antiretroviral therapy. Chronic inflammation, oxidative stress, and blood-brain barrier (BBB) disruption are well-known in HIV infection and likely contribute to the development of HIV NCI. Post-mortem and neuroimaging studies in PLWH demonstrate region-specific neuroinflammation, injury, and BBB damage within the brain, indicating that the processes causing HIV NCI might therefore be region-specific. We previously identified the highly inducible antioxidant enzyme heme oxygenase-1 (HO-1) as a potential mediator of HIV neuropathogenesis, showing that HO-1 expression in the prefrontal cortex is reduced in PLWH with HIV NCI compared to both HIV-negative individuals and PLWH without HIV NCI, and this reduction associates with increased CSF HIV RNA, type I interferon-stimulated gene expression, and immunoproteasome expression. HO-1 is expressed throughout the brain, and its expression in brain microvascular endothelial cells has been shown to support BBB functions. This thesis expounds our understanding of the role for HO-1 in HIV neuropathogenesis through two approaches: i) Regional ex vivo analysis of autopsied brains of PLWH without HIV NCI; and ii) manipulation of HO-1 expression in in vitro models of the BBB using human brain microvascular endothelial cells. We show that PLWH without HIV NCI have stable or increased HO-1 expression compared to HIV-negative individuals that associates positively with CSF and plasma HIV RNA consistently throughout the brain. HO-1 expression also associates positively with type I interferon-stimulated gene, immunoproteasome subunit, and endothelial adhesion marker expression. We also noted distinct patterns of neuroinflammation in certain brain regions (posterior cingulate cortex, cerebellum, and globus pallidus). Finally, we demonstrate manipulation of HO-1 expression in a human endothelial cell line and primary human brain microvascular endothelial cells, outlining experimental parameters for future experiments to determine the role for endothelial HO-1 in BBB functioning during HIV infection. Our work suggests that in PLWH without HIV NCI, HO-1 is driven by HIV replication as a component of an inflammatory response throughout the brain, including within the BBB, and that the role for HO-1 within this process can be modeled using primary human cell culture systems.

Degree Type

Dissertation

Degree Name

Doctor of Philosophy (PhD)

Graduate Group

Neuroscience

First Advisor

Dennis L. Kolson

Keywords

antioxidant, blood-brain barrier, heme oxygenase, HIV, HIV-associated neurocognitive disorders, neuroinflammation

Subject Categories

Neuroscience and Neurobiology | Virology

ANALYSIS OF THE ROLE FOR ANTIOXIDANT ENZYME HEME OXYGENASE-1 IN BRAIN REGIONAL HIV NEUROPATHOGENESIS AND BLOOD-BRAIN BARRIER FUNCTION

Analise L. Gruenewald

A DISSERTATION

In

Neuroscience

Presented to the Faculties of the University of Pennsylvania

In

Partial Fulfillment of the Requirements for the
Degree of Doctor of Philosophy

2020

Supervisor of Dissertation

Dennis Kolson MD/PhD

Dennis L. Kolson, MD, PhD
Professor of Neurology, Perelman School of Medicine at the University of Pennsylvania

Graduate Group Chairperson

Joshua Gold

Joshua I. Gold, PhD
Professor of Neuroscience, Perelman School of Medicine at the University of Pennsylvania

Dissertation Committee:

Harry Ischiropoulos, PhD, (Committee Chair) Research Professor of Pediatrics and Pharmacology, Children's Hospital of Philadelphia

Edward B. Lee, Assistant Professor of Pathology and Laboratory Medicine, Perelman School of Medicine at the University of Pennsylvania

Amit Bar-Or, Professor of Neurology, Perelman School of Medicine at the University of Pennsylvania

T. Dianne Langford, Professor of Neuroscience, Lewis Katz School of Medicine at Temple University

ANALYSIS OF THE ROLE FOR ANTIOXIDANT ENZYME HEME OXYGENASE-1 IN BRAIN REGIONAL HIV NEUROPATHOGENESIS AND BLOOD-BRAIN BARRIER FUNCTION

ACKNOWLEDGMENT

I first want to thank Dr. Dennis Kolson, my PI and mentor, for his support and encouragement throughout my PhD. Dennis' passion for science and medicine has shown me the true meaning of dedication. Dennis is an outstanding scientist and educator, and I am grateful for the time had to learn from him. I will take this, a favorite adage of his, with me: "If it's not worth doing well, then it's not worth doing."

To past and present members of the Kolson lab, I thank you for helping me get through some difficult experiments and some difficult times over the years. Alex and Colleen, whose work I reference ad nauseam within this thesis, thank you for your contributions to the Kolson lab's body of work and for your mentorship. Pat, thank you for being a friend and answering every annoying question I ever had. Rolando, thank you for your commiserations and your humor. Finally, Yoelvis, thank you for helping me through the final years of my PhD. I have learned a lot from you, and will miss having you as a colleague.

Thank you to my thesis committee, Drs. Harry Ischiropoulos, Eddie Lee, and Amit Bar-Or for steering me in the right direction and for supporting me throughout. Thank you to Dr. Dianne Langford for joining my committee as I defend this thesis. I am grateful for the support and collaboration of Dr. Ben Gelman and the resources of the National NeuroAIDS Tissue Consortium, and to Dr. Joan Berman and her lab for their generosity in teaching me techniques new to our lab. Thank you to the NGG and CFAR for endless educational resources.

Finally, I thank my family and friends for their unwavering love and support. To my fiancé Chris (who will be my husband by the time I defend this thesis), you have been with me from the first day to the last. Thank you for keeping me sane and for loving me even when I am acting insane.

ABSTRACT

ANALYSIS OF THE ROLE FOR ANTIOXIDANT ENZYME HEME OXYGENASE-1 IN BRAIN REGIONAL HIV NEUROPATHOGENESIS AND BLOOD-BRAIN BARRIER FUNCTION

Analise L. Gruenewald

Dennis L. Kolson

HIV-associated neurocognitive impairment (HIV NCI) persists in persons living with HIV (PLWH) despite the availability of suppressive combination antiretroviral therapy. Chronic inflammation, oxidative stress, and blood-brain barrier (BBB) disruption are well-known in HIV infection and likely contribute to the development of HIV NCI. Post-mortem and neuroimaging studies in PLWH demonstrate region-specific neuroinflammation, injury, and BBB damage within the brain, indicating that the processes causing HIV NCI might therefore be region-specific. We previously identified the highly inducible antioxidant enzyme heme oxygenase-1 (HO-1) as a potential mediator of HIV neuropathogenesis, showing that HO-1 expression in the prefrontal cortex is reduced in PLWH with HIV NCI compared to both HIV-negative individuals and PLWH without HIV NCI, and this reduction associates with increased CSF HIV RNA, type I interferon-stimulated gene expression, and immunoproteasome expression. HO-1 is expressed throughout the brain, and its expression in brain microvascular endothelial cells has been shown to support BBB functions. This thesis expounds our understanding of the role for HO-1 in HIV neuropathogenesis through two approaches: i) Regional *ex vivo* analysis of autopsied brains of PLWH without HIV NCI; and ii) manipulation of HO-1 expression in *in vitro* models of the BBB using human brain microvascular endothelial cells. We show that PLWH without HIV NCI have stable or increased HO-1 expression compared to HIV-negative individuals that associates positively with CSF and plasma HIV RNA consistently throughout the brain. HO-1 expression also associates positively with type I interferon-stimulated gene, immunoproteasome subunit, and endothelial adhesion marker expression. We also noted distinct patterns of neuroinflammation in certain brain regions (posterior cingulate cortex,

cerebellum, and globus pallidus). Finally, we demonstrate manipulation of HO-1 expression in a human endothelial cell line and primary human brain microvascular endothelial cells, outlining experimental parameters for future experiments to determine the role for endothelial HO-1 in BBB functioning during HIV infection. Our work suggests that in PLWH without HIV NCI, HO-1 is driven by HIV replication as a component of an inflammatory response throughout the brain, including within the BBB, and that the role for HO-1 within this process can be modeled using primary human cell culture systems.

TABLE OF CONTENTS

LIST OF TABLES

LIST OF FIGURES

CHAPTER 1: Introduction

1.1 HIV-associated neurocognitive impairment in the era of combination antiretroviral therapy

The World Health Organization estimates that 75 million people have been infected and 32 million people have died of HIV/AIDS since the outset of the pandemic in the 1980s. With access and adherence to combination antiretroviral therapy (cART) regimens, persons living with HIV (PLWH) have a good prognosis and life expectancy nearly on par with the general population (1). However, various barriers to treatment prevent many PLWH from achieving viral suppression, and the pandemic persists: at the end of 2018, almost 38 million people worldwide were living with HIV and there were 1.7 million new infections (WHO). To combat this continuing global public health challenge, in 2014 the United Nations Program on HIV and AIDS published the 90-90-90 treatment target: 90% of PLWH knowing their HIV status, 90% of diagnosed PLWH receiving cART, and 90% of those on cART achieving viral suppression by 2020 (2). A report synthesizing data from 60 countries showed that through 2018, 79% of PLWH worldwide knew their HIV status; 78% of those individuals were receiving cART, and 86% of those individuals were virally suppressed (3). The global percentages of PLWH who know their status and are receiving cART has significantly improved since 2015, but the percentage of cART-treated PLWH who have achieved viral suppression has remained stable (3). While many countries will not reach the 90-90-90 target in 2020, the advances in model-based approaches to national estimates will be beneficial for years to come (3). Furthermore, the global 90-90-90 framework will continue to identify which populations and countries require additional investment to reach testing and treatment goals. Though reaching the UNAIDS 90-90-90 target will certainly limit the human and economic costs of HIV/AIDS, tens of millions of individuals will be living with HIV on cART long-term, as cure strategies that would allow interruption or cessation of cART remain out of reach.

Persons living with chronic HIV have increased risk for many comorbid conditions, including cardiovascular disease, non-AIDS-related cancers, diabetes mellitus, hepatic and renal disease,

and metabolic disorders, many of which will increase in prevalence as the population of PLWH ages (4). HIV infection is also associated with a number of neurologic complications, including meningitis, acute inflammatory polyneuropathy, immune reconstitution inflammatory syndrome, chronic inflammatory polyneuropathy, distal symmetric polyneuropathy, progressive multifocal leukoencephalopathy, HIV encephalitis (HIVE), and a spectrum of neurocognitive impairment collectively termed HIV-associated neurocognitive disorders (HAND) (5). Similar to systemic outcomes, neurologic outcomes with HIV infection have improved dramatically with cART. In the pre-cART era, 20% of PLWH died with HIVE, histopathologically defined by astrogliosis and HIV p24-positive multinucleated giant cells (6-8). HIVE rarely, if ever, occurs in PLWH on suppressive cART, but some form of HAND persists in up to 50% of PLWH (9). Importantly, HAND is exclusively *clinically* diagnosed. In contrast to HIVE, which has a clearly delineated neuropathologic signature, HAND does not have any definitive associated pathology (10).

HAND is diagnosed through a battery of neuropsychological tests spanning at least five of the seven following neurocognitive domains: verbal/language; attention/working memory; abstraction/executive function; memory (learning; recall); speed of information processing; sensory-perceptual; motor skills (11). The criteria for HAND diagnosis are as follows: Performance one standard deviation below the mean for demographically adjusted normative scores in two or more domains, wherein neurocognitive impairment cannot be attributed to a comorbid condition, qualifies as asymptomatic neurocognitive impairment (ANI). Individuals who meet the criteria for ANI and also have impairment in activities of daily living (ADLs) are diagnosed with mild neurocognitive disorder (MND). Finally, individuals who perform two standard deviations below the mean for demographically adjusted normative scores in at least two cognitive domains and have impairment in ADLs are diagnosed with HIV-associated dementia, or HAD. Presently, the majority of individuals diagnosed with HAND fall within the ANI category. Still, 10-15% of PLWH experience *functional* neurocognitive impairment in the form of either MND or HAD, and diagnosis of ANI

increases risk for future diagnosis of MND or HAD by two- to six-fold (9, 12). Emerging data emphasize the significance of differentiating between ANI more severe HAND subtypes MND and HAD when studying HIV-associated neurocognitive impairment (HIV NCI), as ANI criteria can positively diagnose more than 30% of a normative reference population (13).

There are no definitive diagnostic or prognostic biomarkers for HIV NCI, and the understanding of its cause is incomplete. Among the potential biomarkers of CNS injury in HIV, neurofilament light chain (NFL), a major structural component of axons, has perhaps shown the most promise. CSF NFL is elevated in PLWH with both severe and mild HIV NCI (14, 15). CSF NFL is transiently elevated during primary HIV infection, and increased CSF NFL associates negatively with blood CD4 T-cell count in neuroasymptomatic PLWH, demonstrating its sensitivity to fluctuating neuronal injury throughout the course of HIV infection (15). NFL levels within CSF and plasma are strongly associated, suggesting that plasma NFL can be used as a surrogate marker for CSF NFL (16). This eliminates the necessity for invasive lumbar puncture procedures when measuring NFL as a biomarker (16). Plasma NFL associates negatively with neuropsychological test performance, but it has not been fully vetted in the cART-treated population (16, 17).

In terms of the cause of HIV NCI, neurological symptoms associate with HIV RNA in cerebrospinal fluid (CSF) during primary infection, but in the context of viral suppression with cART, ongoing active viral replication is not a feasible cause of HIV NCI (18). There are several known risk factors to HIV NCI including CD4 nadir, duration of HIV disease, age, co-infections, diabetes mellitus, substance abuse, and poor adherence to antiretroviral therapy (9, 19), and several alternative drivers of HIV NCI in cART-treated PLWH have been proposed. One is the ‘legacy effect’ of irreversible neuronal damage incurred during the initial HIV infection within the CNS prior to treatment, that translates to development of HIV NCI during chronic infection (20). Next is chronic

low-level inflammation and oxidative stress within the CNS, which persists even in cART-treated PLWH (discussed below) (21). Finally, direct neurotoxicity of CNS-penetrating antiretroviral drugs has been supported by various *in vitro* studies, though relevance of these mechanisms *in vivo* is controversial (22). Despite these advances, there remains a great incentive to fully elucidate the mechanistic drivers of HIV NCI and develop adjunctive therapies to cART that will further improve quality of life for PLWH.

1.2 Inflammation and oxidative stress at the blood-brain barrier in HIV infection

Among the potential drivers of HIV NCI is the state of persistent inflammation, immune activation, and oxidative stress systemically and within the CNS experienced by PLWH (21, 23). HIV RNA is detectable in CSF and brain parenchyma within weeks of infection (24-28). The most likely mechanism of HIV entry into the CNS is trafficking of infected CD4+ lymphocytes or monocytes across the blood-brain barrier (BBB) by transendothelial migration, although permeation of cell-free virus is plausible (27, 29-31). The cellular makeup of the BBB consists of highly specialized brain microvascular endothelial cells (BMECs), supported by smooth muscle-like pericytes embedded within the basement membrane, and astrocyte endfeet that secrete supportive and regulatory factors (32, 33). These cells work in concert to protect the brain from the circulation and tightly regulate which molecules and cells are permitted to enter and leave the CNS. The BBB is unique among vascular endothelial barriers due to the selectivity of its tight junctions, high transendothelial electrical resistance, and tight regulation of transendothelial cellular migration (33, 34).

Once in the CNS, HIV infects resident perivascular macrophages and microglia, which comprise the HIV reservoir within the CNS (35). Productively infected macrophages secrete neurotoxic factors including viral proteins and glutamate, as well as pro-inflammatory cytokines (9, 36). Concurrently, depletion of CD4+ lymphocytes in the gut-associated lymphoid tissue during acute

HIV infection contributes to compromise of the gut epithelial barrier, resulting in microbial translocation (37). Subsequent immune activation of circulating monocytes is evidenced by increased soluble CD14, sCD163, and monocyte-associated CD14 and CD16 in plasma (38-41). The BBB is inevitably exposed to microbial translocation products in the circulation, including bacterial nucleic acids and lipopolysaccharide (LPS), which disrupts tight junction integrity and promotes trafficking of immune cells into the CNS (39, 42). In HIV, this equates to exacerbation of infected and/or activated immune cell transmigration and increased permeability of the BBB to cell-free virus and other harmful factors in the circulation (43). Thus, during primary HIV infection (Fiebig stages I-II), the brain is challenged by *i)* active viral replication and release of neurotoxic viral proteins; *ii)* compromise of its protective barrier; and *iii)* influx of pro-inflammatory cytokines and oxidative stress as a result of the aforementioned processes (44).

BBB disruption during HIV infection often involves inflammation oxidative stress, and associates with HIV NCI in many studies (45-48). Perivascular inflammation independent of productive HIV infection has been observed in acute, asymptomatic HIV infection (45). Upregulated endothelial transcripts accompany HIV NCI without demonstrable neuropathological changes (46). The HIV DNA reservoir is associated with CSF immune activation, gliosis, neuronal damage, and cognitive impairment in treatment-naïve individuals (23). Boven et al. demonstrated immunohistochemical staining for nitrotyrosine in perivascular areas (indicating free radical nitric oxide production) in HIV NCI patients that was accompanied by damaged blood vessels and abnormal staining of tight junction protein ZO-1, indicating oxidative stress associating with a leaky barrier (47, 48). PLWH have decreased glutathione levels both in the CNS and systemically, which associates with impaired survival, underlining the significance of oxidative stress in HIV infection (48-51).

Introduction of effective cART eliminates productive viral replication, fundamentally changing the immune challenge to the CNS. Nonetheless, inflammation, oxidative stress, and BBB disruption persist within the CNS in treated PLWH. Elevated CSF/plasma albumin ratio, indicative of increased BBB permeability, associates with CSF HIV RNA and immune activation marker neopterin in untreated PLWH; in CSF-controlled patients, CSF/plasma albumin ratio instead associates with neuronal damage and astrocytosis (52, 53). One longitudinal study indicated that while neopterin decreased over time with treatment, most PLWH still had elevated neopterin in CSF after more than three years of viral suppression (CSF HIV RNA <50 copies/ml) (54). Persistent neuroinflammation at the BBB in treated PLWH is also indicated by metabolic signatures and post-contrast enhancement in magnetic resonance spectroscopy (MRS) that associate with HIV NCI in some cases (55-58). Finally, while antiretroviral therapy decreases levels of soluble endothelial activation markers (ICAM-1, VCAM-1, von Willebrand factor) in plasma of PLWH, they remain elevated in comparison to HIV-negative individuals (59).

The mechanisms by which blood-brain barrier damage, persistent oxidative stress, and inflammation contribute to HIV NCI are not entirely clear. It may be important to consider not just damage to the endothelial blood-brain barrier, but to the neurovascular unit (NVU), which describes the entire CNS blood vessel compartment and extends, critically, to include perivascular neuronal processes and synapses. In total, the NVU includes astrocytic endfeet, neuronal processes and synapses, microvascular endothelial cells, pericytes, pervascular macrophages and microglia, CNS extracellular spaces, subarachnoid spaces and CSF, and blood plasma (10). Evidence of direct innervation of microvascular endothelial cells and/or astrocytic endfeet suggests bidirectional communication between neurons and the CNS vasculature that regulates blood flow and BBB permeability (32). GABAergic transmission specifically is known to control microvascular blood flow through regulation of pericyte contractility (60, 61), and is abnormally low in neocortex of PLWH, suggesting a mechanism by which NVU dysregulation impacts BBB function (46). Abnormal

cerebral blood flow is observed in PLWH with and without HIV NCI, which may indicate early neurovascular injury (62). A supportive role for astrocytes within the NVU has long been suggested, as injection of astrocytes induced BBB properties in non-neural endothelial cells in the rat eye *in vivo*, and co-culture of astrocytes with brain microvascular endothelial cells enhances BBB characteristics *in vitro* (63-65). Astrocytic secretion of soluble factors, notably Sonic Hedgehog, directly support BBB properties of microvascular endothelial cells *in vitro* and *in vivo* (66). Exposure of astrocytes in an *in vitro* BBB model to HIV disrupts BBB functions through endothelial apoptosis and altered astrocyte endfeet signaling (67). This is recapitulated in brain tissue of SIV-infected macaques, where apoptotic endothelia cells are observed in contact with astrocytes containing SIV-p41 antigen (67). Recent work has emphasized the relevance of "vascular cognitive impairment" to our evolving understanding of HIV NCI, with the NVU as the proposed common mechanistic target of these conditions, and a worthy target for neurotherapeutics in PLWH (68).

1.3 Antioxidant response enzyme heme oxygenase-1 in HIV neuropathogenesis

Because of the persistence of inflammation and oxidative stress in the CNS in PLWH and their association with HIV NCI, our group has investigated of the role for the host antioxidant response in HIV neuropathogenesis. The endogenous host antioxidant response consists of cytoprotective and detoxifying effector proteins whose genes have a common regulatory element within their promoter regions termed the antioxidant response element (ARE), which is regulated by the Kelch-like ECH associated protein (Keap1)/nuclear factor erythroid 2-related factor (Nrf2) pathway (69-71). Under basal conditions, Nrf2 is sequestered in the cytoplasm by Keap1, which forms a homodimer and binds to actin and Nrf2 (**Fig. 1.1**). In this conformation, Nrf2 is targeted for ubiquitination and proteomic degradation. Keap1 contains several reactive cysteine residues that allow it to act as a chemical sensor (72). In response to changes in cellular redox state due to reactive oxygen species, electrophilic species, or reduced antioxidant capacity, conformational change in Keap1 results in release of Nrf2 (71). Nrf2 then translocates to the nucleus and binds

AREs, inducing transcription of target genes (72, 73). Nrf2 target gene products have diverse effector functions that provide multifaceted protection to the cell including direct antioxidant activity, xenobiotic transport, glutathione synthesis and regeneration, synthesis of reducing species, inhibition of inflammation, and repair and removal of damaged proteins (72).

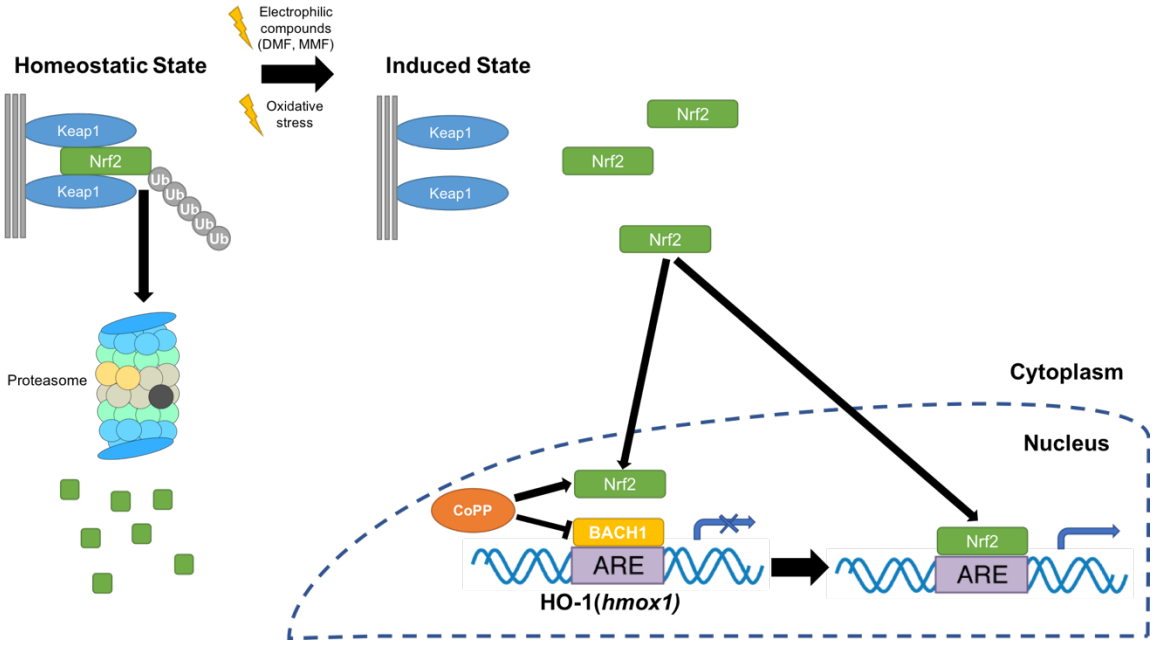

Figure 1.1 The Nrf2-Keap1-ARE Pathway

Illustration of Nrf2-Keap-1 interactions leading to induction of antioxidant response element-containing genes, specifically HO-1. Adapted from (72) and (74)

Within our studies of the host antioxidant response in HIV infection, we have identified antioxidant enzyme heme oxygenase (HO) as an important factor in the development of HIV NCI. HO executes the rate limiting step of heme catabolism, oxygenating heme to ferrous iron, biliverdin, and carbon monoxide (CO). Ferrous iron is sequestered by ferritin, and biliverdin is transformed to bilirubin by biliverdin reductase (**Fig. 1.1**). HO exists in two isoforms, heme oxygenase-1 (HO-1) and heme oxygenase-2 (HO- 2), which have identical enzymatic activity and 45% sequence homology (75).

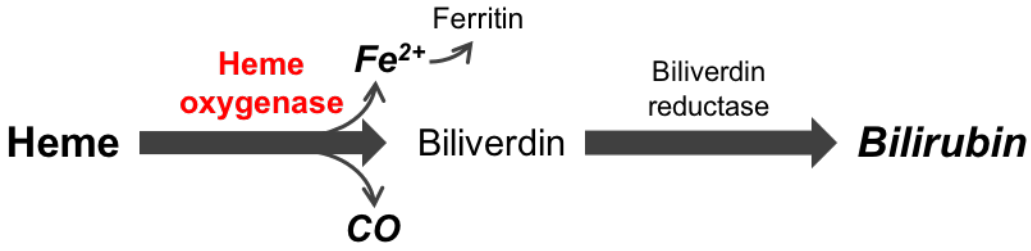

Figure 1.2 Heme catabolism

Schematic depicting catabolism of heme by HO. Oxygenation of heme by HO yields carbon monoxide, iron, and biliverdin. Iron is bound by ferritin and biliverdin reductase converts biliverdin to bilirubin.

HO-1 transcription is primarily regulated as a part of the Nrf2-antioxidant response element (ARE) signaling pathway (71), but several other transcription factors can bind the HO-1 promoter and regulate its transcription: activator protein-1 and -2 (AP-1, AP-2), nuclear factor kappa-light-chain-enhancer of activated B cells (NFκB), hypoxia-inducible factor-1 (HIF-1), signal transducer and activator of transcription 3 (STAT3), and broad complex-tramtrack-bric-a-brac-domain and cap'n'collar homology 1 (BACH1) (**Fig. 1.2**) (76-81). Critically, BACH1 binds the same antioxidant response element as Nrf2 within the HO-1 promoter, preventing Nrf2 from binding and thus suppressing HO-1 transcription (**Fig. 1.1**). BACH1 dissociates from the HO-1 promoter with exposure to heme and oxidative stress, allowing Nrf2 to bind and activate HO-1 transcription (82, 83). BACH1 serves as a semi-specific transcriptional repressor of HO-1 through this mechanism (84).

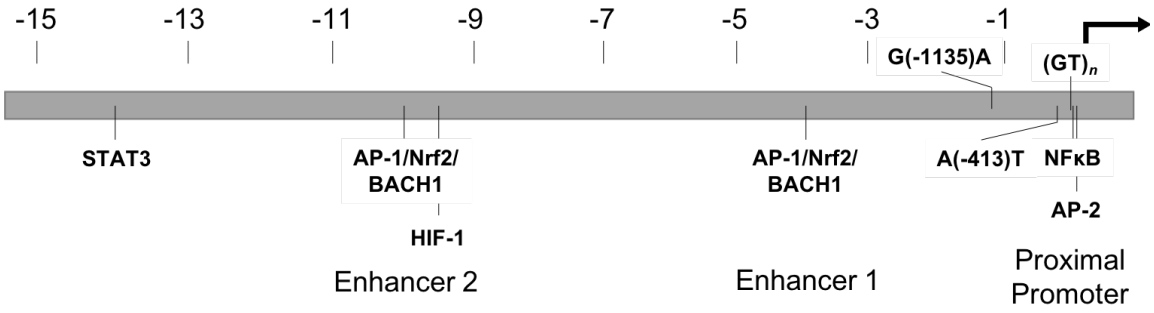

Figure 1.3 The heme oxygenase-1 promoter

Illustration of the heme oxygenase-1 promoter. Putative Nrf2, AP-1, AP-2, NFκB HIF-1 STAT-3, and BACH1 binding sites are indicated. Loci of (GT)n microsatellite dinucleotide repeat polymorphism and single nucleotide polymorphisms A(-413)T (rs2071746) and G(-1135)A (rs2071747) are also represented. The arrow indicates the transcription initiation site, and distance from this site is shown in kilobase pairs. Adapted from (76).

In addition to the described transcription factor binding sites, the HO-1 promoter contains a few polymorphisms (**Fig. 1.2**): a $(GT)_n$ microsatellite dinucleotide repeat polymorphism and two single nucleotide polymorphisms (SNPs), A(-413)T (rs2071746) and G(-1135)A (rs2071747) (85-87). The T(-413)A SNP and the $(GT)_n$ dinucleotide repeat polymorphism have each been shown to affect HO-1 transcription. In a luciferase assay testing the activity of promoters with each allele of the T(-413)A SNP in bovine aortic endothelial cells, the 'A' allele promoter had higher activity. The 'AA' genotype for this SNP associates with reduced risk for ischemic heart disease, suggesting a protective effect of higher HO-1 promoter activity (86). The $(GT)_n$ dinucleotide repeat polymorphism similarly impacts transcription in that 'short' repeat length alleles are associated with increased basal transcriptional activity and inducibility of HO-1 expression using luciferase reporter assays (88, 89). Lymphoblastoid cell lines derived from individuals with either 'short/short' repeat length alleles demonstrated significantly higher HO-1 mRNA expression and enzymatic activity in response to oxidative stress compared to those with 'long/long' repeat length alleles, and furthermore 'short/short' cell lines were more resistant to apoptosis induced by oxidative stress

(90). These observations have also been recapitulated in human umbilical vein endothelial cells (91).

Given the numerous factors governing HO-1 transcription, its expression is thus induced in response to not only heme levels but many other cellular stressors including cytokines and reactive oxygen species that are relevant to HIV infection (92). In contrast, HO-2 is not regulated through the ARE pathway and is considered to be constitutively expressed, although its expression levels can change in response to a few factors (93-95). In the brain, HO-2 is expressed in neuronal and glial cells and is the predominant isoform. HO-1 is expressed in glial cells and not in neurons, which demonstrate little to no HO-1 expression even in response to cellular stressors (96, 97).

The antioxidative and anti-inflammatory effects of HO-1 are multifactorial, through regulation of intracellular heme levels and the properties of its metabolites. Heme has many important biological roles as a prosthetic moiety on hemoproteins, e.g. hemoglobin, myoglobin, and cytochromes. However, free heme is a potent pro-oxidant and its lipophilic properties allow it to intercalate into and disrupt the cell membrane (98, 99). The byproducts of heme catabolism, i.e. carbon monoxide and bilirubin each exert their own antioxidative and anti-inflammatory effects. Carbon monoxide generated by HO-1 enzymatic activity suppresses endothelial apoptosis (100). Carbon monoxide also affects cytokine secretion, inhibiting TNFα and IL-1β via the p38 MAPK pathway, and increasing expression of anti-inflammatory cytokine IL-10 (101). Bilirubin scavenges reactive oxygen species and inhibits TNFα-induced adhesion molecule expression (102, 103). Bilirubin can also modulate innate immunity by interfering with the complement system and regulating Fc receptor and MHC class II expression (98).

In recent years, our group has defined a novel role for HO-1 in HIV neuropathogenesis and identified it as a potential therapeutic target for HIV NCI. In a study of autopsied brains of PLWH

and HIV-negative individuals from the National NeuroAIDS Tissue Consortium (NNTC), we observed that PLWH with HIV NCI and/or HIV encephalitis had reduced prefrontal cortex HO-1 expression compared to both neurocognitively normal PLWH and HIV-negative individuals. Lower HO-1 protein in prefrontal cortex associated with higher parenchymal and CSF HIV load, type I interferon-stimulated gene expression, and macrophage activation (36). *In vitro* studies showed that HIV infection of monocyte-derived macrophages (MDM) leads to reduced expression of HO-1 RNA and protein in a replication-dependent manner. Deficient HO-1 in HIV-infected MDM associated with release of neurotoxic levels of glutamate into the supernatant, and this was rescued with pharmacologic induction of HO-1 in HIV-infected MDM (36). These studies identified deficient HO-1 expression in brains of PLWH that associates with HIV NCI and encephalitis and furthermore linked HO-1 deficiency in HIV-infected MDM to glutamate-mediated neurotoxicity, suggesting a mechanism by which HO-1 deficiency *in vivo* might yield neuronal death and NCI.

Interestingly, further study within this cohort showed that PLWH with HIV NCI and/or encephalitis had *increased* HO-1 RNA compared to neurocognitively normal PLWH and HIV-negative individuals, and that HO-1 RNA and protein were negatively associated (104). This discordance was not consistent with the RNA and protein HO-1 deficiency observed *in vitro* in HIV-infected MDM (36). Alternatively, *in vitro* studies using human fetal astrocytes chronically exposed to IFNγ demonstrated post-translational degradation of HO-1 by the immunoproteasome (**Fig. 4**) (104). Others have demonstrated that PLWH have increased immunoproteasome subunit expression in prefrontal cortex that associates with HIV loads, HIV NCI and HIV-encephalitis (105). Indeed, increased immunoproteasome subunit expression in prefrontal cortex of PLWH with HIV encephalitis associated negatively with HO-1 protein (104). As IFNγ is an HIV-associated immune activator, this study identified a plausible mechanism for post-translational degradation in brains of PLWH.

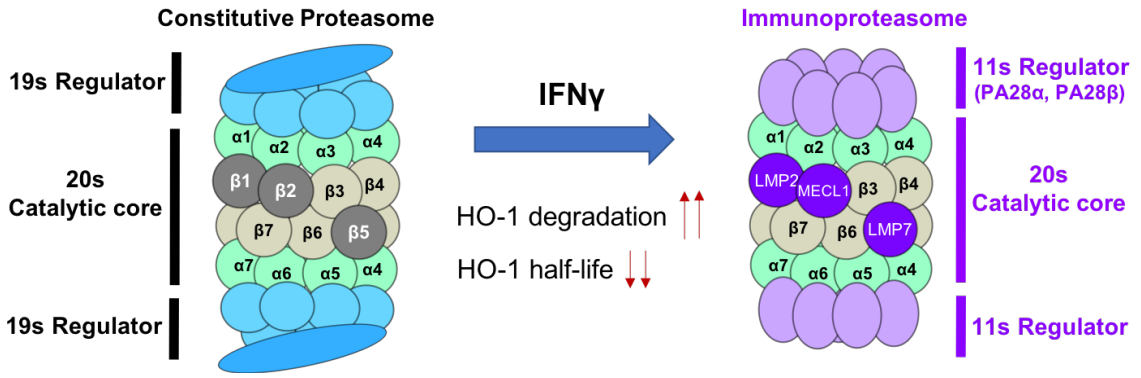

Figure 1.4 Immunoproteasome-mediated HO-1 degradation

Illustration of HO-1 degradation by the immunoproteasome in human fetal astrocytes. Chronic exposure (15 days) to IFNγ leads to replacement of constitutive proteasome subunits with immunoproteasome subunits. The immunoproteasome enhances post-translational HO-1 degradation and decreases its half-life. Adapted from CE Kovacsics (104).

We also addressed the potential role for the previously mentioned $(GT)_n$ dinucleotide repeat polymorphism in the HO-1 promoter region in HIV NCI. Along with increased promoter activity, shorter repeat length alleles of this polymorphism associate with better outcomes in numerous diseases that have inflammation and oxidative stress as critical elements to their pathogeneses (106). Examples of disease states in which shorter repeat length alleles are protective include ischemic stroke, ischemic heart disease, hypertension, coronary heart disease, coronary artery disease in diabetic patients, necrotizing acute pancreatitis, rheumatoid arthritis, sepsis, pneumonia, and emphysema (86-89, 107-112). Seu et al. demonstrated that longer $(GT)_n$ repeat length alleles associated with higher monocyte activation and viral loads in African-American PLWH, suggesting that this polymorphism can modulate systemic HIV disease outcomes (113). We found significant associations between this polymorphism and risk for HIV-encephalitis, as well as type I interferon-stimulated gene expression and T-lymphocyte activation within the prefrontal cortex of PLWH (114). In a separate clinical cohort study of PLWH, we observed modulating effects of the HO-1 $(GT)_n$ promoter dinucleotide repeat on risk for HIV NCI (115). These observations suggest a balance between transcriptional and post-translational mechanisms of HO-1 modulation that

determine parenchymal HO-1 levels in the setting of neuroinflammation in prefrontal cortex, and they also suggest a role for HO-1 expression in modulating risk for HIV NCI.

Our previous work has established that HO-1 modulates risk for HIV NCI and HIV encephalitis and has identified mechanisms by which HIV replication or HIV-associated chronic inflammation reduce HO-1 expression in macrophages and astrocytes, respectively. HO-1 has also been shown to support BMEC function in various models by limiting oxidative stress and inflammation. Administration of curcumin and resultant induction of HO-1 in a model of oxygen glucose deprivation reduced barrier permeability through restoration of tight junction protein expression (116). Pharmacologic upregulation of HO-1 by cobalt protoporphyrin (CoPP), a potent inducer of HO-1 through destabilization of BACH1 and stabilization of Nrf2 (117), ameliorated glutamate-mediated oxidative stress and apoptosis in murine BMECs (118). These data suggest that deficient HO-1 at the BBB might contribute to its dysfunction, and equally that therapeutic induction of HO-1 at the BBB could support its function in HIV infection.

1.4 Region-specific brain vulnerability to HIV infection: implications for HIV NCI

As previously mentioned, HIV NCI does not have a defined neuropathology. Still, researchers have long sought to characterize histopathologic, neuroimaging, and CSF biomarker abnormalities in PLWH, with the hope of identifying key diagnostic or prognostic correlates of HIV NCI. While this goal has not yet been met, these studies have shed light on region-specific effects of HIV infection on the brain in treated and untreated PLWH, identifying distinct cortical and sub-cortical abnormalities and their relevance to HIV NCI. With the implementation of cART, not only has the severity of HIV NCI decreased, but the clinical presentation of HIV NCI has also shifted. Pre-cART, individuals with HIV NCI commonly presented with motor dysfunction and memory deficits pointing to sub-cortical involvement, and without treatment, HIV NCI would commonly progress to severe

dementia (119, 120). In PLWH on cART, however, HIV NCI typically presents with deficits to executive functioning and working memory, suggesting involvement of the prefrontal cortex (121). HIV NCI is not typically progressive in PLWH on cART; in one longitudinal study of PLWH, 77% of those individuals were neurocognitively stable, while 13% declined and 10% improved over the course of 4 years (122). Thus, evolution of clinical presentation of HIV NCI with cART suggests potential change for its etiology, with regards to both the particular regions damaged and the source of that damage.

Studies to identify regional distribution of HIV RNA and capsid protein (p24 antigen) have shown higher levels of HIV in the basal ganglia (dorsal striatum [caudate + putamen], ventral striatum [olfactory tubercle + nucleus accumbens], globus pallidus, subthalamic nucleus, substantia nigra) compared to neocortex (123-125). Perhaps because they harbor comparatively more virus, the basal ganglia are exceptionally vulnerable to BBB damage and atrophy in untreated PLWH. Indeed, higher CSF HIV RNA associates with atrophy of the caudate in individuals with HIV NCI (126). In MRI studies, smaller basal ganglia volume differentiates PLWH with dementia or encephalitis from those without (127, 128), and lower caudate volume specifically associates with worse performance on neuropsychological tests and/or dementia (129-131). Furthermore, progressive volume loss in the caudate has been linked to disease stage and rate of CD4 count decline (132). Vulnerability of the basal ganglia is suggested even in treated PLWH in some studies; Chaganti et al. described BBB disruption measured by contrast enhanced perfusion MRA in basal ganglia that associates with CSF neopterin and CSF/serum albumin ratio in virally suppressed PLWH (56). Smaller volumes in the basal ganglia associate with executive function deficits in PLWH on cART, indicating relevance of the basal ganglia to HIV NCI even in treated individuals (133). More pronounced atrophy of sub-cortical regions including the basal ganglia has been observed in older PLWH, suggesting the relevance of these abnormalities will only increase as the population of PLWH ages (134, 135).

Because of the prevalence of executive function deficits in HIV NCI, the prefrontal cortex has also been of particular interest to the neuroHIV field. PLWH have cortical thinning in prefrontal cortex, among other cortical areas, that associates with HIV NCI (136). In women living with HIV, stress can exacerbate prefrontal cortical volume loss that associates with learning and memory deficits (137). Using blood oxygen level dependent functional MRI (fMRI) to measure real-time changes in brain metabolism, Ann et al. showed that resting-state functional connectivity between the prefrontal cortex and precuneus also decreased in PLWH with HIV NCI (138), and multiple studies have identified impaired frontostriatal circuitry in PLWH. In treatment-naïve PLWH, prefrontal cortical thinning associates with impaired striatal functioning (139). Another fMRI study demonstrated impaired functional connectivity between the prefrontal cortex and basal ganglia regions in PLWH with mild NCI (140). Ipser et al. made similar observations of reduced connectivity between prefrontal cortex and caudate in PLWH on cART that associated with NCI, and particularly in younger participants (141). Together, these data point to the prefrontal cortex and basal ganglia/striatum as key regions for pathogenesis of HIV NCI. Indeed, our previous studies showed reduced HO-1 protein in the prefrontal cortex and striatum (caudate), but not occipital cortex or cerebellum of PLWH with HIV NCI and HIV-encephalitis, suggesting that a deficient HO-1 response in those regions might contribute to dysfunction (36).

Still, the potential for significance of dysfunction in other regions remains, especially in the post-cART era when brain structural changes in HIV NCI are less pronounced and less consistent (142). Besides prefrontal cortex, which has been studied at length in HIV, other cortical abnormalities have been observed that could impact HIV NCI. Cortical thinning has been observed in temporal (143), sensory, and motor cortices in PLWH (136). Poorer fine motor performance associated with reduced cerebral blood flow in occipital cortex in a study of PLWH on protease inhibitor monotherapy (144). Altered fMRI signal in anterior cingulate cortex associates with executive

function deficits in cART-treated PLWH (145), and volume loss has also been reported in cingulate cortices in PLWH (143, 146). Microglial activation in the posterior cingulate cortex associates with poorer executive function in cART-treated PLWH (147). Abnormalities in additional sub-cortical regions beyond striatum/basal ganglia (caudate, putamen, globus pallidus) have also been reported in PLWH, including the amygdala (146). Atrophy of the brainstem and cerebellum has also been observed in PLWH (134, 148). Finally, white matter abnormalities are frequently observed in HIV and associate with neuroinflammation and HIV NCI (149-152). Together, these data indicate it is valuable to study regions whose functions reflect a range of neurocognitive domains to identify the subtler neurocognitive abnormalities observed in PLWH on cART.

CHAPTER 2: Neuroinflammation associates with antioxidant heme oxygenase-1 response throughout the brain in persons living with HIV

Analise L. Gruenewald, BS[1], Yoelvis Garcia-Mesa, PhD[1], Alexander J Gill, MD, PhD[1], Rolando Garza, BS[1], Benjamin B. Gelman, MD, PhD[2], Dennis L. Kolson, MD, PhD*[1]

[1]Department of Neurology, Perelman School of Medicine, University of Pennsylvania Philadelphia, PA

[2]Department of Pathology, University of Texas Medical Branch, Galveston, TX

Submitted for publication to the Journal of NeuroVirology

2.1 Abstract

Previous studies showed that persons living with HIV (PLWH) demonstrate higher brain prefrontal cortex neuroinflammation and immunoproteasome expression compared to HIV-negative individuals; these associate positively with HIV levels. Lower expression of the antioxidant enzyme heme oxygenase-1 (HO-1) was observed in PLWH with HIV-associated neurocognitive impairment (NCI) compared to neurocognitively normal PLWH. We hypothesized that similar expression patterns occur throughout cortical, sub-cortical and brainstem regions in PLWH, and that neuroinflammation and immunoproteasome expression associate with lower expression of neuronal markers. We analyzed autopsied brains (15 regions) from 9 PLWH without HIV NCI and 7 matched HIV-negative individuals. Using Western blot and RT-qPCR, we quantified synaptic, inflammatory, immunoproteasome, endothelial, and antioxidant biomarkers, including HO-1 and its isoform heme oxygenase-2 (HO-2). In these PLWH without HIV NCI, we observed higher expression of neuroinflammatory, endothelial, and immunoproteasome markers in multiple cortical and sub-cortical regions compared to HIV-negative individuals, suggesting a global brain inflammatory response to HIV. Several regions, including posterior cingulate cortex, globus pallidus, and cerebellum showed a distinct pattern of higher type I interferon (IFN)-stimulated gene and immunoproteasome expression. PLWH without HIV NCI also had *i*) stable or higher HO-1 expression; and positive associations between *ii*) HO-1 and HIV levels (CSF, plasma); and *iii)* HO-1 expression and neuroinflammation, in multiple cortical, sub-cortical and brainstem regions. We observed no differences in synaptic marker expression, suggesting little, if any, associated neuronal injury. We speculate that this may reflect a neuroprotective effect of a concurrent HO-1 antioxidant response despite global neuroinflammation, which will require further investigation.

2.2 Introduction

Persistent oxidative stress and inflammation within the brain of persons living with HIV (PLWH) are thought to contribute to development of HIV-associated neurocognitive impairment (HIV NCI) (9, 31, 153-156). In the absence of HIV infection, such potentially pathological processes typically induce expression of antioxidant response genes, which execute cytoprotective responses to acute cellular injury in the brain. Among those most strongly linked to neuronal injury and recovery in various models is the antioxidant/anti-inflammatory enzyme, heme oxygenase (HO), which exists in two isoforms, heme oxygenase-1 and -2 (HO-1, HO-2) (97, 118, 157-160). HO-1 is highly inducible by a variety of factors and predominates in non-neuronal cells, while HO-2 is considered to be constitutively expressed and only slowly inducible by a few factors. In the brain, HO-2 predominates in neurons. The protective effects of HO-1 and HO-2 are downstream of their selective catabolism of heme, a highly toxic, pro-oxidative factor. Heme is released as a byproduct of hemoglobin degradation, or, in the context of cellular stress, from cellular metabolic enzymes for which it serves as a critical cofactor. HO-mediated heme catabolism produces the anti-inflammatory, cytoprotective metabolites carbon monoxide and bilirubin (98, 161-163). In the human brain, expression of HO-1 and HO-2 RNA is reportedly higher in cortical areas (frontal, temporal, occipital) compared to pons and cerebellum (164), which suggests that HO enzymatic cytoprotective capacity may vary among brain regions.

We previously demonstrated that decreased HO-1 protein expression in the prefrontal cortex of PLWH associates with HIV NCI and encephalitis, and that this HO-1 reduction is associated with the level of HIV expression, type I interferon (IFN)-stimulated gene expression, and macrophage activation (36, 165). Notably, we observed a marked discordance (negative association) between HO-1 protein and RNA expression, which suggests post-transcriptional loss of HO-1 protein (104). In *in vitro* studies, we linked HO-1 expression to dysregulation of glutamate release from glial cells, further suggesting a direct link between HO-1 deficiency and excitotoxic injury as a mechanism of HIV-induced neuronal injury *in vivo* (165, 166). HO-1 protein reduction was also observed in the

striatum, but not in the occipital cortex or cerebellum, which suggests regional brain variability in HO-1 expression in response to HIV infection. Upregulation of IFN-stimulated genes and endothelia-associated genes have also been reported in the striatum in PLWH, which suggests concurrent host antioxidant responses and neuroinflammatory responses that extend beyond the prefrontal cortex (46).

We addressed several potential mechanisms by which HO-1 expression might be reduced by HIV infection in PLWH. PLWH have increased immunoproteasome subunit expression in prefrontal cortex that associates with HIV load, HIV NCI and HIV-encephalitis (105). We found evidence *in vitro* that degradation of HO-1, but not HO-2, is enhanced through IFN-induced immunoproteasome expression (104), thus potentially explaining the observed discordance between HO-1 protein and RNA expression in the prefrontal cortex of PLWH. We also addressed the potential role for known regulatory variations in the HO-1 promoter region [a $(GT)_n$ dinucleotide repeat polymorphism]. We found significant associations between this polymorphism and type I IFN-stimulated genes and T-lymphocyte activation within the prefrontal cortex of PLWH (114). In a separate clinical cohort study of PLWH, we observed modulating effects of the HO-1 $(GT)_n$ promoter dinucleotide repeat on risk for HIV NCI (115). These observations suggest a balance between transcriptional and post-translational mechanisms of HO-1 modulation that determine parenchymal HO-1 levels in the setting of neuroinflammation in prefrontal cortex, and they also suggest a role for HO-1 expression in modulating risk for HIV NCI.

In this study, we sought to determine whether neuroinflammation and a concurrent HO-1 antioxidant response in PLWH extend to additional cortical and deep brain regions, and whether those processes associate with synaptic integrity. We analyzed 15 brain regions in an autopsy cohort of PLWH without HIV NCI (n=9) and HIV-negative individuals (n=7). We determined expression of HO-1 and HO-2, and defined their associations with plasma and cerebrospinal fluid (CSF) HIV levels, markers of neuroinflammation, synaptic integrity, endothelial adhesion, and

immunoproteasome expression. Similar to our prior observations in prefrontal cortex of PLWH, we observed higher expression of markers of neuroinflammation, endothelial activation and adhesion, and immunoproteasome expression in multiple cortical, sub-cortical and brainstem regions compared to HIV-negative individuals. Notably, posterior cingulate cortex, globus pallidus, and cerebellum expressed similar neuroinflammatory patterns. We also observed *i)* similar or increased HO-1 expression levels in all brain regions in PLWH compared to HIV-negative individuals; *ii)* positive association between HO-1 expression and HIV levels in CSF and plasma; *iii)* positive association between HO-1 and neuroinflammatory markers; and *iv)* no difference in expression of synaptic markers.

2.3 Materials and Methods

National NeuroAIDS Tissue Consortium brain autopsy cohort and viral loads

A cohort consisting of 9 PLWH and 7 HIV-negative individuals was selected from the National NeuroAIDS Tissue Consortium (NNTC) (**Table 2.1**). We selected individuals on the basis of several criteria: *i)* the availability of brain tissue specimens from multiple brain regions; *ii)* absence of neurocognitive impairment attributable to HIV infection (i.e., HIV NCI) and HIV encephalitis; and, if possible, *iii)* homozygosity for either 'short' (S/S) or 'long' (L/L) HO-1 promoter region $(GT)_n$ dinucleotide repeat allele genotype. The rationale for seeking individuals with either the S/S or L/L genotype is that *HMOX1* promoters with short HO-1 $(GT)_n$ repeats express higher basal *HMOX1* gene transcriptional activity and inducibility (89, 90, 110, 113), and short HO-1 $(GT)_n$ repeat alleles associate with less brain inflammation and lower risk for HIV NCI in PLWH (114). This could potentially allow us to identify differences in HO-1 protein expression in various brain regions on the basis of the individual's promoter genotype in the presence and absence of HIV infection.

Among the 9 PLWH studied, none had diagnosed HIV NCI, according to the Frascati Criteria (11). Four were categorized as "Neuropsychological impairment-other (NPIO)," indicating impairment that can be attributed to another comorbid condition distinct from HIV infection or AIDS-related CNS

disease (co-infection, tumor, metabolic disease, other acquired neurological disease). The remaining 5 PLWH were categorized as neurocognitively normal. Eight of the PLWH were antiretroviral therapy (ART)-experienced. PLWH and HIV-negative individuals (n=7) did not differ significantly by age, sex, race, ethnicity, or postmortem autopsy interval. Blood (n=9) and CSF (n=6) samples were obtained within 6 months of death and on the same day that neurocognitive testing was completed. Plasma and CSF HIV RNA levels were determined with the Amplicor HIV-1 Monitor test v1.1 through v1.5 (Roche).

Monocyte-derived macrophage culture and siRNA transfection

Peripheral blood mononuclear cells (PBMC) were isolated from volunteer donors by Ficoll density gradient centrifugation, and monocytes were isolated by adherence to gelatin-coated flasks (167). Isolated monocytes were plated at $10.5x10^4$ cells/cm^3 on Cell-Bind plates (Corning) and cultured in Dulbecco's Modified Eagle Medium (DMEM) supplemented with 10% fetal bovine serum (Thermo Scientific), 10% horse serum (Invitrogen), 1% non-essential amino acids (Invitrogen), 2mM glutamine (Invitrogen), and 50U/ml penicillin/streptomycin at 37ºC, 6% CO_2. Monocyte-derived macrophages (MDM) were cultured for 7 days *in vitro* and inspected for differentiation. Silencer® Select siRNAs (Ambion) were transfected at a final concentration of 20nM using Lipofectamine RNAiMax (Invitrogen).

Brain tissue sampling

Fresh frozen brain tissue samples from frontal cortex (FC), temporal cortex (TC), occipital cortex (OC), motor cortex (MC), sensory cortex (SC), anterior cingulate cortex (ACC), posterior cingulate cortex (PCC), amygdala (AM), caudate nucleus/putamen (CN), globus pallidus (GP), pons (PN), midbrain (MB), medulla (MED), cerebellum (CB), frontal white matter (FWM), and spinal cord (SPC) (**Table 2.2**) stored at -80°C were dissected on dry ice. Samples from each region were divided into two pieces (i.e. adjacent pieces) for analysis of protein and RNA expression, respectively.

Western blot

Protein lysates were prepared from 100mg of tissue homogenized by silica bead beating and sonication in 7 volumes of buffer (10mM Tris-HCl pH 7.8, 0.5mM Dithiothreitol [DTT], 5mM $MgCl_2$, 0.03% Triton X-100) containing Complete Protease Inhibitor Cocktail (Roche Applied Science) and PhosSTOP Phosphatase Inhibitor Cocktail (Roche). Protein concentration was quantified using the Detergent Compatible (DC) protein assay (BioRad). Proteins were resolved by SDS-PAGE and transferred to polyvinylidene fluoride (PVDF) membranes. Membranes were incubated with primary antibody (**Table 2.3**) overnight at 4°C. For infrared fluorescent detection of protein expression, membranes were incubated with IRDye-conjugated secondary antibody (**Table 2.4**) for one hour at room temperature and scanned with the Odyssey CLx Infrared Imagine System (LI-COR Biosciences). Background-corrected signal intensity of protein bands was measured using Image Studio Lite software (LI-COR Biosciences).

HO-1 promoter $(GT)_n$ repeat genotyping

HO-1 $(GT)_n$ repeat lengths were determined by PCR of the $(GT)_n$ repeat region with a 6-FAM labeled forward primer, followed by fragment size determination on a capillary sequencer. In a subset of samples, PCR products were run on a 2% agarose gel to assess amplification of the target sequence predicted sizes (homozygotes, heterozygotes). All samples were run at least twice from independent PCR reactions to ensure accurate and reproducible sizing and were determined to be accurate within +/- 1 GT repeats. In rare (<4%) cases where identical $(GT)_n$ repeat lengths were not obtained in duplicate, samples were run additional times to confirm accurate repeat lengths. We assigned HO-1 $(GT)_n$ alleles as short 'S' (< 27), medium 'M' (27-34) or long 'L' (> 34) $(GT)_n$ repeats (114).

In-gel digestion and mass spectrometry analysis and confirmation of HO-1 detection

Human brain lysates were resolved by SDS-PAGE, with an identical lysate added to two lanes of a symmetrically organized gel. One half of the gel was stained for protein with Coomassie blue,

while the other half was transferred to PVDF membrane and probed for HO-1 as described above. Gel bands for digestion were chosen by exact size according to corresponding bands recognized by the primary antibody used to probe the PVDF membrane. Each gel band was excised and further cut into 1 mm cubes (168). These were de-stained with 50% Methanol/1.25% Acetic Acid, reduced with 5mM Dithiothreitol (DTT) (Thermo), and alkylated with 20mM iodoacetamide (Sigma). Gel pieces were then washed with 20mM ammonium bicarbonate (Sigma) and dehydrated with acetonitrile (Fisher). Trypsin (Promega) (5ng/mL in 20mM ammonium bicarbonate) was added to the gel pieces and proteolysis was allowed to proceed overnight at 37ºC. Peptides were extracted with 0.3% triflouroacetic acid (J.T. Baker), followed by 50% acetonitrile. Extracts were combined and the volume was reduced by vacuum centrifugation.

Extracted samples were analyzed on a QExactive HF mass spectrometer (Thermofisher Scientific San Jose, CA) coupled with an Ultimate 3000 nano UPLC system and an EasySpray source. Peptides were separated by reverse phase (RP)-HPLC on Easy-Spray RSLC C18 2µm 75µm id × 50cm column at 50C. Mobile phase A consisted of 0.1% formic acid and mobile phase B of 0.1% formic acid/acetonitrile. Peptides were eluted into the mass spectrometer at 210nL/min with each RP-LC run comprising a 125-minute gradient from 1 to 5 % B in 15 min, 5-45%B in 110 min. The mass spectrometer was set to repetitively scan m/z from 300 to 1400 (R=240,000) followed by data-dependent MS/MS scans on the twenty most abundant ions, minimum AGC 1e4, dynamic exclusion with a repeat count of 1, repeat duration of 30s, (R=15000) FTMS full scan AGC target value was 3e6, while MSn AGC was 1e5, respectively. MSn injection time was 160 ms; microscans were set at one. Rejection of unassigned and 1+,6-8 charge states was set.

Peptide and protein identification were performed with the Sequest search engine accessed through Proteome Discoverer 2.0 (Thermo Fisher Scientific) using human reference proteome database from Uniprot (canonical and isoform proteins; downloaded on 20180104). Carbamidomethyl of Cys was defined as a fixed modification. Oxidation of Met and acetylation of protein N-termini were set as variable modifications. Trypsin was selected as the digestion enzyme,

and a maximum of two missed cleavages per peptide was allowed. The precursor mass tolerance was set at 10 ppm and the MS/MS fragment mass tolerance was set at 0.02 DA. The minimum peptide length was set at 7 amino acids. The False Discovery Rate (FDR) for peptides and proteins was set at 1%. The rest of the parameters were kept as default. The search results were exported and visualized in Scaffold 4.8.4 (Proteome Software). Mass spectrometry analysis and data processing were performed with support of the Children's Hospital of Philadelphia Proteomics Core.

Quantitative real-time qPCR (qPCR)

Total RNA was prepared from 50mg of fresh-frozen brain tissue (adjacent to tissue section used for preparation of protein lysates) using the RNeasy Lipid Tissue Mini Kit. RNA purity and concentration were determined with NanoDrop One UV-Vis spectrophotometer (ThermoFisher Scientific) and 1µg of total RNA was reverse transcribed to single-stranded cDNA using the High Capacity RNA-to-cDNA Kit (Applied Biosciences). Relative RNA expression was determined by qPCR using 25ng cDNA, Taqman Fast Universal Master Mix (Applied Biosciences) and TaqMan primer/probe sets (*HMOX1*: Hs01110250_m1; *GAPDH*: Hs02786624_g1; *ISG15*: Ha00192713_m1; *MX1*: Hs00182073_m1; Applied Biosystems) in 10µL reaction volumes. Reactions were run in triplicate on a StepOnePlus (ThermoFisher Scientific). *GAPDH* was used as the reference gene and RNA expression was calculated for each sample relative to the average expression of that gene across all brain samples.

Statistical analysis

All quantifications are expressed as mean ± standard error of the mean (SEM). Protein and RNA expression data were log transformed. Differences in expression of markers within individual brain regions between HIV-negative individuals and PLWH were evaluated by Student's unpaired t-test. Differences in mean expression of markers throughout the brain between HIV-negative individuals and PLWH were analyzed by Student's paired t-test, whereby mean expression of a marker in a given region within HIV-negative individuals was paired with mean expression of that marker in the

same region within PLWH. Linear trends were analyzed by Pearson's correlation with line of best fit determined by linear regression. Statistical significance was defined as $p<0.05$. All statistical tests were performed using GraphPad Prism version 8.

2.4 Results

HO-1 expression in multiple brain regions associates with CSF and plasma HIV levels in PLWH

We previously showed that HO-1 protein levels are lower in prefrontal cortex and caudate of PLWH with HIV NCI compared to HIV-negative individuals while HO-1 RNA levels are higher, suggesting an induction of HO-1 gene expression associated with post-translational HO-1 protein loss that may contribute to HIV NCI (36). No such pattern was seen in occipital cortex or cerebellum. In this study, we examined a broad distribution of brain regions (15 regions) and spinal cord in PLWH without HIV NCI. We confirmed the relative specificity of the anti-HO-1 antibody used for our analyses (**Fig. 2.1**). We analyzed human and transgenic mouse brain and spleen lysates (**Fig. 2.1A, C, D**) and used mass spectrometry (**Fig. 2.1B**) to confirm antibody specificity for HO-1 in human brain tissue. Comparing HO-1 protein expression within each brain region, we found higher HO-1 levels only in the midbrain in PLWH compared to HIV-negative individuals (**Fig. 2.2A**). However, the average of the means of HO-1 protein expression by region was significantly higher in PLWH, suggesting that increased HO-1 expression likely occurs in multiple brain regions (**Fig. 2.2B**). We also observed a positive association between HO-1 RNA and HO-1 protein expression in PLWH in 7 of 15 brain regions analyzed (temporal cortex, occipital cortex, motor cortex, sensory cortex, anterior cingulate cortex, posterior cingulate cortex, frontal white matter; **Table 2.5**).

Detection of CSF HIV RNA was successful in 6 of 9 PLWH while brain parenchymal HIV RNA was not detected in 8 of 9 PLWH, precluding comprehensive analysis of HIV levels in brain parenchyma. Nonetheless, CSF HIV RNA associated positively with brain HO-1 RNA, in 9 of 15 brain regions, including frontal cortex (**Fig. 2.2C**), five other cortical regions, amygdala, globus pallidus, and cerebellum (**Table 2.6**), similar to our prior observations in prefrontal cortex (36). We also found

positive associations between plasma HIV RNA and HO-1 RNA in all brain regions except midbrain and frontal white matter (**Fig. 2.2D, Table 2.6**). CSF HIV RNA associated positively with HO-1 protein expression in 5 of 15 brain regions, including frontal cortex (**Fig. 2.2E**), and four other cortical regions (**Table 2.6**). Finally, we observed positive associations between plasma HIV RNA and HO-1 protein in 7 of 15 brain regions, including frontal cortex (**Fig. 2.2F**), five other cortical regions, and the pons (**Table 2.6**). These results confirm positive associations between plasma and CSF HIV expression and the host HO-1 response in multiple brain regions.

Expression of the constitutive HO-2 isoform is higher in frontal white matter in PLWH than in HIV-negative individuals

The HO-2 isoform is considered to be constitutively expressed, but expression can change in response to certain stimuli (hypoxia, glucocorticoids) (93-95, 169). In contrast to HO-1 expression in the brain, HO-2 is the predominant isoform expressed in neurons. We observed significantly higher HO-2 expression only in frontal white matter in PLWH compared to HIV-negative individuals (**Fig. 2.3A**). However, similar to our HO-1 expression observation (**Fig. 2.2B**), when we compared the means of HO-2 expression for each region we found higher HO-2 expression in PLWH (**Fig. 2.3B**).

Immunoproteasome expression is higher in multiple brain regions in PLWH than in HIV-negative individuals

Our prior studies of PLWH showed increased immunoproteasome expression in the prefrontal cortex that associates with HIV NCI and HIV encephalitis (105). We also showed a negative association between HO-1 protein and immunoproteasome expression in prefrontal cortex in PLWH and evidence for immunoproteasome-associated degradation of HO-1 (104). To determine whether this association is consistent throughout the brain in PLWH, we quantified expression of immunoproteasomes (LMP7 and Pa28α subunits) and constitutive proteasomes (β5 subunit) in additional brain regions.

HIV infection associated with higher expression of immunoproteasome subunits in multiple cortical and sub-cortical regions (LMP7: temporal cortex, occipital cortex, sensory cortex, posterior cingulate cortex, globus pallidus, cerebellum, frontal white matter; Pa28α: temporal cortex, sensory cortex, posterior cingulate cortex, globus pallidus, cerebellum; **Fig. 2.4A-D**). These immunoproteasome associations stand in contrast to the lack of changes in constitutive proteasome expression (β5 subunit), in PLWH compared to HIV-negative individuals with the exception of lower β5 expression in the pons (**Fig. 2.4E-F**). We did not find a consistent relationship between HO-1 and LMP7 expression across brain regions in PLWH (**Table 2.7**).

HO-1 expression in multiple brain regions associates with type I IFN-stimulated genes in PLWH

We next determined the association between HIV infection, type I IFN-stimulated genes (*ISG15* and *MX1*), and HO-1 expression. We found increased type I IFN-stimulated gene expression in multiple cortical and sub-cortical regions (**Fig. 2.5A-D**). We observed higher *MX1* ([**Fig. 2.5A-B**]: frontal and posterior cingulate cortices, globus pallidus, cerebellum, and frontal white matter) and higher *ISG15* ([**Fig. 2.5C-D**]: frontal cortex and frontal white matter). We also identified several positive associations between *ISG15* and *i)* HO-1 RNA (temporal cortex, anterior and posterior cingulate cortices, frontal white matter [**Table 2.8**]); *ii)* HO-1 protein (anterior cingulate cortex, amygdala, frontal white matter, spinal cord [**Table 2.8**]) in PLWH. *MX1* also associated positively with HO-1 RNA: temporal, occipital, anterior cingulate cortices, amygdala, cerebellum, frontal white matter, spinal cord (**Table 2.8**) in PLWH. In contrast, in HIV-negative individuals, we did not find clear evidence of an association between HO-1 and *ISG15* or *MX1* (**Table 2.9**).

HO-1 expression in multiple brain regions associates with markers of endothelial activation and adhesion in PLWH

Dysfunction and/or injury to the neurovascular unit (defined as capillary endothelia, pericytes, astrocytic foot processes, neuronal processes, perivascular macrophages, along with the CNS

extracellular space, subarachnoid space, and blood plasma) is thought to be a major contributor to the development of HIV NCI, perhaps independently from brain neuroinflammation (10, 46, 60, 170). We examined several endothelial adhesion molecules (ICAM-1, VCAM-1, PECAM-1) and observed higher expression of each overall, and in multiple cortical and sub-cortical regions in PLWH compared to HIV-negative individuals: *i)* ICAM-1: frontal, sensory, and temporal cortices, and cerebellum (**Fig. 2.6A-B**); *ii)* VCAM-1: motor cortex and globus pallidus (**Fig. 2.6C-D**); and *iii)* PECAM-1: anterior cingulate cortex (**Fig. 2.6E-F**).

We determined the associations of these endothelial markers with HO-1 expression. VCAM-1 and PECAM-1, but not ICAM-1, associated positively with HO-1 protein expression in PLWH in multiple cortical, sub-cortical and brainstem regions (VCAM-1: frontal, temporal, anterior cingulate cortices, pons, midbrain, spinal cord; PECAM-1: temporal, occipital and posterior cingulate cortices, globus pallidus [**Table 2.10**]). Each also associated positively with HO-1 RNA in multiple cortical, sub-cortical and brainstem regions in PLWH (VCAM-1: amygdala, caudate; PECAM-1: six cortical regions, caudate, pons **[Table 2.10]**). We did not find consistent associations between HO-1 and endothelial adhesion molecules in HIV-negative individuals (**Table 2.11**).

Synaptic marker expression in multiple brain regions is similar in PLWH and in HIV-negative individuals

Because the induction of HO-1 expression is associated with neuroprotection in various injury response models including HIV infection (36, 166), we measured markers of synaptic integrity in PLWH. To do this, we analyzed expression of presynaptic (synaptophysin) and postsynaptic (PSD95) markers. Expression of each was similar in PLWH compared to HIV-negative individuals (**Fig. 2.7A-D**) and neither associated with HO-1 protein or RNA expression in PLWH (**Tables 2.12-13**).

*The HO-1 promoter region (*GT$)_n$ *variant genotype does not associate with brain HO-1 expression*

The HO-1 promoter region contains a $(GT)_n$ dinucleotide repeat that modulates basal HO-1 expression and gene inducibility, specifically with shorter HO-1 $(GT)_n$ repeats associating with higher basal HO-1 promoter activity (89, 90, 110, 113), as well as better outcomes in inflammatory and oxidative stress-associated diseases (107, 108, 110, 111, 113). Short (S) $(GT)_n$ repeat length alleles are defined as those with less than 27 $(GT)_n$ repeats, while long (L) alleles are defined as those with more than 34 $(GT)_n$ repeats (114, 171, 172). Our current study cohort included 5 'SS' homozygous individuals (3 PLWH, 2 HIV-negative) and 4 'LL' homozygous individuals (3 PLWH, 1 HIV-negative). We did not find a significant difference in HO-1 protein or RNA expression in any individual brain region in PLWH based upon HO-1 $(GT)_n$ repeat allele genotype (**Fig. 2.8A-B**).

2.5 Discussion

Neuroinflammation and oxidative stress are considered central to the pathogenesis of neurocognitive impairment in PLWH and analyses of associated biomarkers are typically limited to only a few brain regions. In previous studies of prefrontal cortex in PLWH compared to HIV-negative individuals, we and others observed increased expression of markers of neuroinflammation (IFN-stimulated genes, endothelial markers) and immunoproteasome expression that associate with HIV NCI and HIV-encephalitis (46, 105, 173, 174). In prefrontal cortex, we also observed reduced protein levels of the antioxidant/anti-inflammatory enzyme, HO-1 (36); despite increased levels of HO-1 RNA (104). This discordant HO-1 protein and RNA expression associated with HIV load in brain and CSF, neuroinflammation, immunoproteasome expression, and HIV NCI. Notably, PLWH with HIV NCI had significantly lower HO-1 expression in prefrontal cortex compared to PLWH without HIV NCI in the same cohort. In *in vitro* studies, we showed that HIV infection drives decreased HO-1 expression in monocyte-derived macrophages, and that immunoproteasome expression enhances HO-1 degradation (36, 104). We subsequently linked this reduced glial cell HO-1 expression with release of neurotoxic levels of glutamate, which has been associated with HIV NCI (46, 165, 175-182). We concluded that HIV infection and HIV-driven neuroinflammation and immunoproteasome induction could lead to accelerated HO-1 protein degradation and loss,

leading to neuronal injury and, ultimately, HIV NCI. Finally, we also showed that the HO-1 gene promoter region $(GT)_n$ dinucleotide repeat genetic variation, which is known to modulate HO-1 transcriptional activity, associates with risk for HIV NCI and neuroinflammation in PLWH in a pattern consistent with a role for HO-1 in reducing risk for HIV NCI (114, 115).

We thus hypothesized that PLWH have HIV-driven neuroinflammation and immunoproteasome expression throughout the brain that associates with HO-1 expression, and that this might associate with synaptic integrity in multiple regions, or even predominantly in selected regions. Based upon our prior observations in prefrontal cortex comparing PLWH with and without HIV NCI and abundant literature defining HO-1 induction in response to inflammation and oxidative stress, we hypothesized that this cohort of PLWH without HIV NCI would have normal or even increased levels of brain HO-1 expression along with increased neuroinflammation and immunoproteasome expression. Our results indeed showed stable or increased HO-1 expression, and increased neuroinflammation, endothelial marker expression, and immunoproteasome expression in multiple cortical, sub-cortical, and brainstem regions in PLWH compared to HIV-negative individuals (see schematic **Fig. 2.9**). We felt that examining individuals with predictably distinct HO-1 $(GT)_n$ genotypes might allow us to identify differences in regional brain HO-1 expression that might be influenced by the individual's promoter genotype translational HO-1 expression capacity, both in the presence and absence of HIV infection. However, we could identify only 6 PLWH individuals of 'SS' and 'LL' allele genotypes who met all three inclusion criteria. Among the HIV-negative individuals, 3 had these genotypes, thus limiting the statistical powering of the analysis.

The observed stable or increased HO-1 expression in PLWH without HIV NCI is in contrast to our previously reported decreased HO-1 expression in prefrontal cortex in PLWH with HIV NCI. These data suggest that although induction of pathological neuroinflammation occurs in multiple brain regions, induction of a protective HO-1 response also occurs in such regions in PLWH without HIV NCI. These data also suggest that the HO-1 response is pathologically suppressed in PLWH who

develop HIV NCI, in part through immunoproteasome-mediated degradation of HO-1 (104). Thus, in conjunction with our previous findings, this study is consistent with the hypothesis that therapeutic induction of HO-1 in PLWH may limit neuroinflammation and provide neuroprotection against HIV NCI (see schematic **Fig. 2.9**). We did not observe differences in synaptic marker expression in this cohort, which suggests that these concurrent inflammatory and antioxidant responses were not associated with synaptic neuronal injury in these individuals, albeit as determined only by the level of sensitivity of detection of differences in expression levels of synaptic proteins.

We also noted some specific differences in these responses among different brain regions and we speculate that there are likely functional consequences, as has been suggested in previous studies of PLWH (183-190). While immunoproteasome subunit expression (LMP7, Pa28α) was higher in 7/15 brain regions, three of these regions (globus pallidus, cerebellum, and posterior cingulate cortex [PCC]) also showed significantly higher type I IFN-stimulated gene expression (*MX1*).

We speculate that our data reflect particular vulnerability of the PCC to HIV-induced neuroinflammation, which could have consequences for neurocognitive functioning. The prevalence of deficits in executive functioning is high in PLWH, even in those not meeting the full diagnostic criteria for HIV NCI (133) Indeed, functional neuroimaging studies have identified metabolic abnormalities in the PCC that associate with HIV infection and with progression of HIV NCI, as well as abnormal aging and amyloid pathology in the HIV-negative population (186, 191, 192). In a previous study of PLWH, microglial activation in PCC associated specifically with poorer executive function, suggesting clinical significance to neuroinflammation in that region even in PLWH who do not meet the strict Frascati criteria for the diagnosis of HIV NCI (193). Cysique et al (186, 188) used Magnetic Resonance Spectroscopy to detect neuronal injury (reduced N-acetyl-aspartate/NAA) and neuroinflammation (increased myoinositol/mI) in PCC in virally-suppressed PLWH compared to HIV-negative individuals. However, we cannot attribute deficits in executive

function solely to involvement of the PCC in our PLWH cohort, as such dysfunction is also affected by other brain regions, including frontal cortex and white matter, precuneus, accumbens, putamen, and globus pallidus (133, 189).

Other sub-cortical brain regions have also been implicated in selective vulnerability to HIV and associated NCI. Vulnerability of the striatum (caudate + putamen) to HIV-associated blood-brain barrier disruption and impaired function has been observed, especially in individuals with HIV-associated dementia and HIV-encephalitis (56, 140, 194-197). Our study also implicates the globus pallidus, which, along with caudate and putamen, show neuroinflammation (microglial activation) in PLWH despite suppressive combination antiretroviral therapy (198). Similar to our findings in the PCC, our data demonstrate neuroinflammation (*MX1*) and immunoproteasome expression (LMP7, Pa28α) in globus pallidus, extending neuropathological observations to this region within the basal ganglia (caudate + putamen + globus pallidus), and they further suggest its potential vulnerability to neuroinflammation in PLWH. Although we cannot specifically link our globus pallidus findings to NCI in our PLWH cohort, the links between basal ganglia dysfunction, neuroinflammation and HIV NCI are the subject of many studies (128, 132, 199-203). Finally, cerebellar atrophy, degeneration, and decreased functional connectivity have also been reported in PLWH (204-206).

Whether the specific neuroinflammatory changes (type I IFN-stimulated genes, endothelial activation) or immunoproteasome induction identified in this study contribute specifically to dysfunction in these brain regions in PLWH will require further investigation. We speculate that the increase of endothelial adhesion molecules might promote increased immune cell adhesion and migration through the blood-brain barrier, which could promote local neuroinflammation. The clustering of ICAM-1 and VCAM-1 at the apical surface of endothelial cells and facilitation of leukocyte adhesion prior to diapedesis is well known (207-211). Expression of type I IFN (IFNα) has been linked to HIV NCI presumably by promoting a pro-inflammatory state (212). Finally, increased immunoproteasome expression in the prefrontal cortex in PLWH is associated with HIV

NCI (104, 105, 174), and increased immunoproteasome expression is associated with enhanced autoimmunity and neurodegeneration in other CNS disease states (213, 214). In total, our data suggest that HIV infection of the brain broadly induces neuroinflammatory responses and antioxidant responses that are more pronounced in certain regions, which may promote more global or more regionally-influenced features of NCI, respectively.

We have demonstrated expression of neuroinflammatory and immunoproteasome markers that associate with expression of the antioxidant response (HO-1 expression) in multiple cortical, sub-cortical and brainstem regions in PLWH without HIV NCI. These observations extend previous findings of HIV-associated responses in the prefrontal cortex, and they suggest a ubiquitous response pattern throughout the brain to HIV infection. We speculate that the absence of synaptic protein loss in the setting of neuroinflammation may reflect a protective effect of the antioxidant response. We further speculate that more robust regional responses, such as those within the PCC, globus pallidus, and cerebellum might disrupt normal circuitry, with effects that may be detected only with more selective clinical assessments targeting such regions. Finally, we speculate that targeting the regulation of the HO-1 antioxidant response might offer therapeutic options for neuroprotection against HIV throughout the brain.

Declarations

Ethics approval and consent to participate

NNTC studies were conducted in accordance with human subject protection protocols at participating institutions. Written informed consent was obtained for subjects at four collection sites in the USA. The following offices maintained the Institutional Review Boards that provided oversight for the protection of human subjects: (1) The University of Texas Medical Branch Office of Research Subject Protections; (2) Mount Sinai Medical Center Program for the Protection of Human Subjects; (3) University of California, San Diego Human Research Protections Program; and (4) University of California, Los Angeles Office of the Human Research Protection Program.

Acknowledgements

We acknowledge the support of Dr. Anupam Agarwal at The University of Alabama at Birmingham in providing transgenic mouse tissues. We also acknowledge the support of the National NeuroAIDS Tissue Consortium for providing all human brain tissue samples and cohort clinical and paraclinical data.

2.6 Figures

A

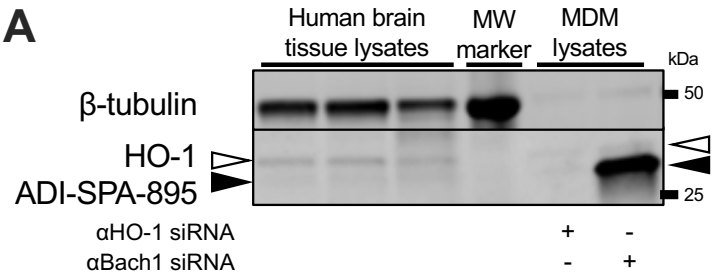

B

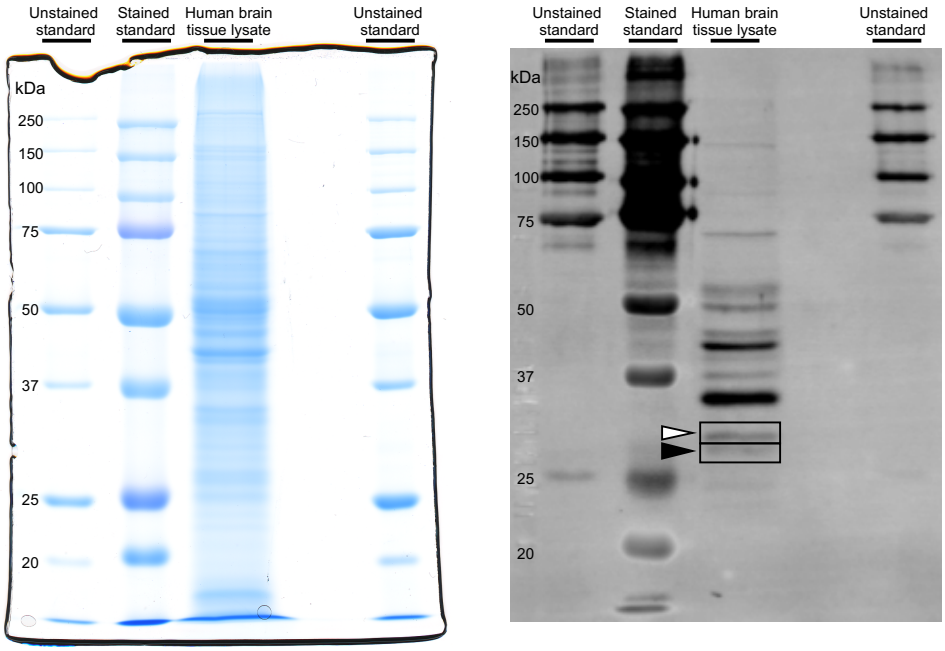

HO-1 sequence: Red font indicates the 4 unique peptides detected by mass spectrometry.

N-terminus-
MERPQPDSMPQDLSEALKEATKEVHTQAENAEFMRNFQKGQVTRDGFKLVMASLYHIYVALEEE
IERNKESPVFAPVYFPEELHRKAALEQDLAFWYGPRWQEVIPYTPAMQRYVKRLHEVGRTEPEL
LVAHAYTRYLGDLSGGQVLKKIAQKALDLPSSGEGLAFFTFPNIASATKFKQLYRSRMNSLEMTPA
VRQRVIIQLFEELQELLTHDTKDQSPSRAPGLRQRASNKVQDSAPVETPRGKPPLNTRSQAPLLR
WVLTLSFLVATVAVGLYAM **-C-terminus**

C

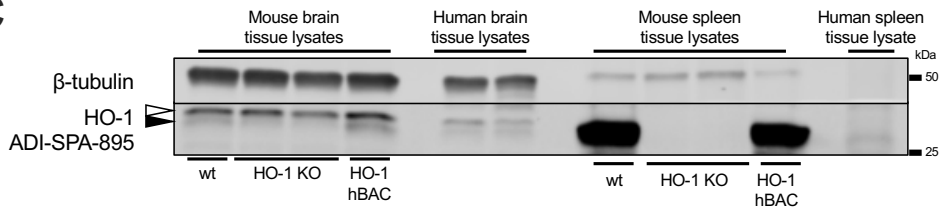

D

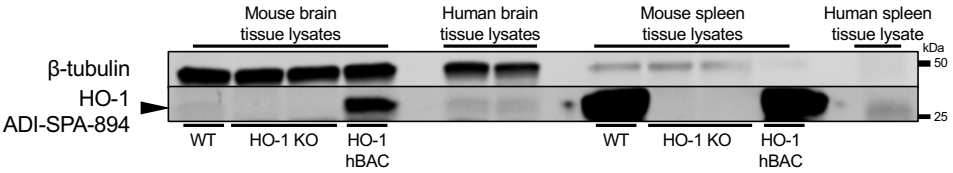

Figure 2.1 Validation of a rabbit polyclonal HO-1 antibody for Western blot

(**A**) Human brain tissue lysates were probed for β-tubulin and HO-1 (Enzo ADI-SPA-895) by Western blot. For a control comparator, we used differentiated human monocyte-derived macrophages (MDMs), which express high levels of HO-1 after siRNA knock-down of the Nrf2 repressor protein BACH-1 (36, 215). MDMs were treated with siRNAs targeting HO-1 or BACH1 for 6 days. In human brain lysates, we observed two bands at ~32kDa (white and black arrows), of which the higher molecular weight band (white arrow) was consistently more intense. In human MDMs, we observed the same two bands, but only the lower molecular weight band (black arrow) was enhanced as expected by anti-BACH1 siRNA transfection. (**B**) Human brain lysate was resolved by SDS-PAGE in two identically loaded lanes. One half of SDS-PAGE gel was stained with Coomassie blue (left) and the other was transferred to PVDF membrane and probed for HO-1 with ADI-SPA-895 (right). Two bands were dissected from the stained gel (left) based on location of bands in 32kDa range on the membrane (white and black arrows), trypsin-digested, and subjected to mass spectrometric analysis. Sequence-to-spectrum peptide assignments generated by SEQUEST in Proteome Discoverer were loaded into Scaffold to validate MS/MS peptide and protein identification. Four unique peptides with Xcorr scores >2.0 and delta Cn >0.1 representing 21% coverage of the HO1 sequence were identified in the two gel bands. Each MS/MS spectrum was also manually evaluated and contained contiguous series of y-series fragment ions. (**C**) Human and wild-type C57Bl/6 (WT), HO-1 knockout (HO-1 KO), and human HO-1 overexpressing (HO-1 hBAC) mouse brain and spleen lysates (courtesy of Dr. Anupam Agarwal, UAB) were probed for β-tubulin and HO-1 using Enzo ADI-SPA-895. Two bands were detected at ~32kDa in human brain tissue lysates (white and black arrows), and a similar banding pattern was observed in transgenic mouse brain tissue lysates. The higher molecular weight band (white arrow) was detected in HO-1 knockout mouse brain tissue lysates, indicating a protein other than HO-1 at 32kDa. No such band was observed in spleen lysates from mouse or human, or in the HO-1 knockout mouse lysates. These results suggest that ADI-SPA-895 detects HO-1 protein in both bands, as well as another protein in the higher molecular weight band. (**D**) Human and wild-type C57Bl/6 (WT), HO-1

knockout (HO-1 KO), and human HO-1 overexpressing (HO-1 hBAC) mouse brain and spleen lysates were probed for β-tubulin and HO-1 using Enzo ADI-SPA-894. A single band was detected at 32kDa in mouse brain tissue lysates (black arrow), which was not present in HO-1 knockout mouse brain or spleen. We confirmed HO-1 content in this band, and therefore used this antibody in all subsequent experiments.

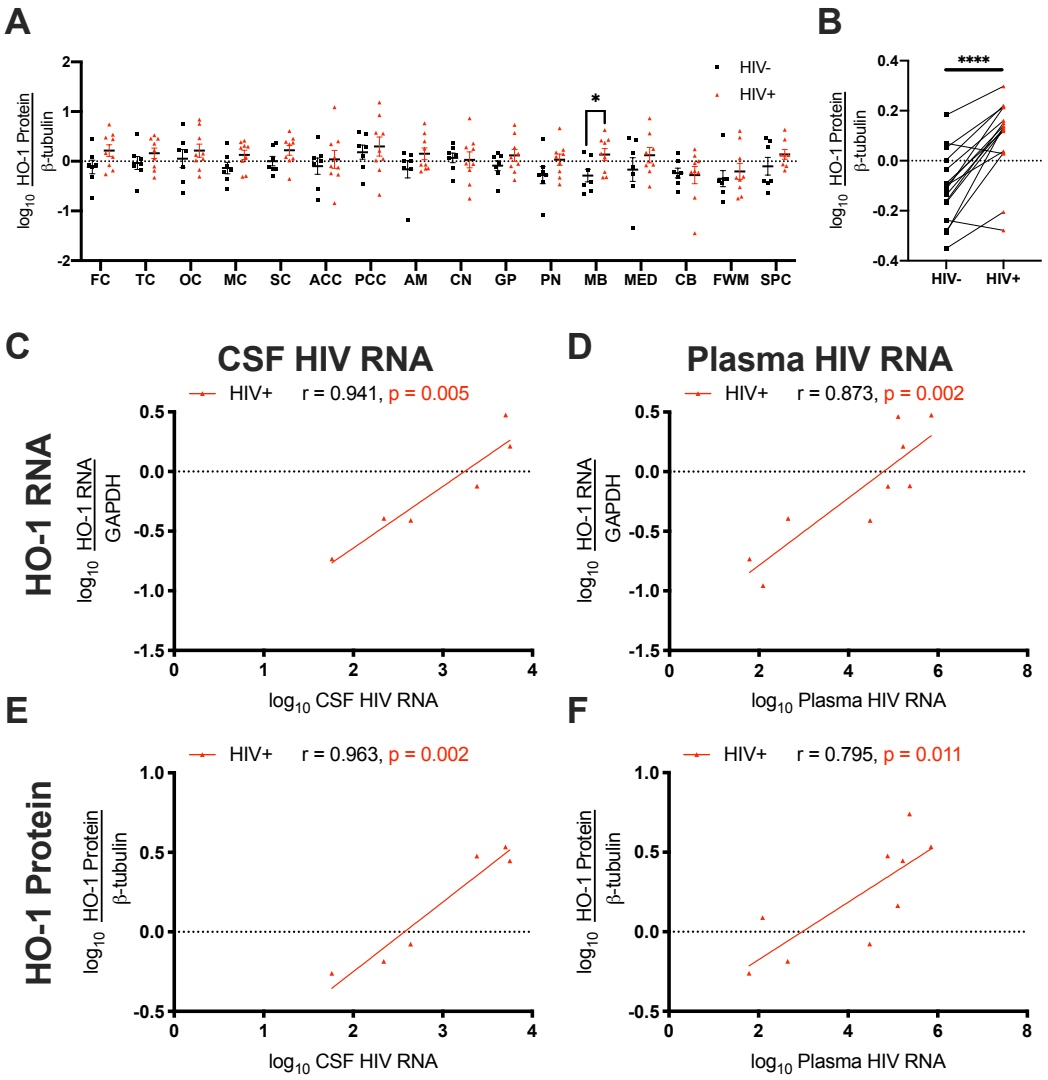

Figure 2.2 HO-1 expression in multiple cortical and deep brain regions associates with CSF and plasma HIV levels in PLWH

HO-1 protein **(A-B, E-F)** and RNA **(C-D)** were measured by Western blot and RT-qPCR, respectively. **(A)** Effect of HIV infection on HO-1 expression in individual brain regions was measured by Student's unpaired t-test. **(B)** Effect of HIV infection on whole brain HO-1 expression was measured by Student's paired t-test, where the mean expression of HO-1 in each region in HIV-negative individuals was compared to the mean expression of HO-1 that region in in PLWH. **(C, E)** CSF and **(D, F)** plasma HIV RNA were measured by RT-qPCR. Associations between frontal

cortex HO-1 protein or RNA expression and plasma or CSF HIV RNA were analyzed by Pearson's correlation with line of best fit by linear regression.

*p<0.05, ** p<0.01, ***p<0.001, ****p<0.0001

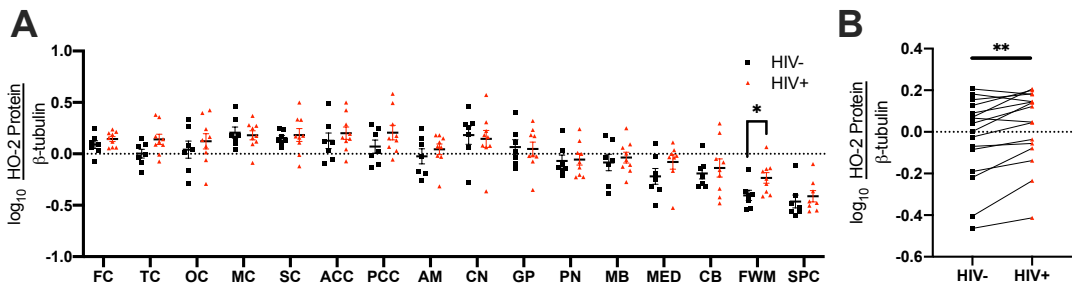

Figure 2.3 Expression of the HO-2 isoform is higher in frontal white matter in PLWH than in HIV-negative individuals

HO-2 protein was measured by Western blot. **(A)** Effect of HIV infection on HO-2 expression in individual brain regions was measured by Student's unpaired t-test. **(B)** Effect of HIV infection on whole brain HO-2 expression was measured by Student's paired t-test, where the mean expression of HO-2 in each region in HIV-negative individuals was compared to the mean expression of HO-2 that region in in PLWH. *p<0.05, ** p<0.01, ***p<0.001, ****p<0.0001

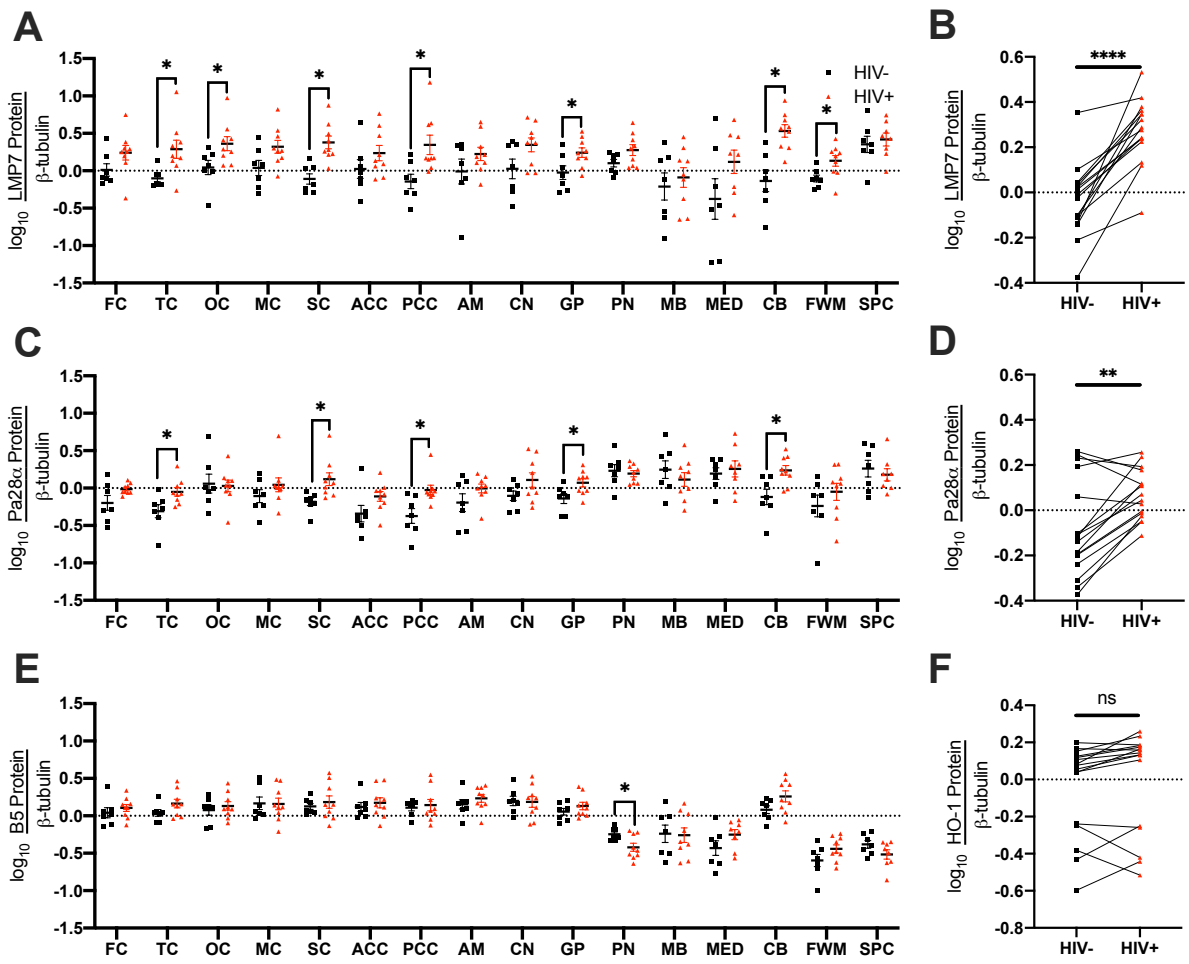

Figure 2.4 Immunoproteasome expression is higher in multiple brain regions in PLWH than in HIV-negative individuals

LMP7 **(A-B)**, Pa28α **(C-D)**, and B5 **(E-F)** protein expression were measured by Western blot. **(A, C, E)** Effect of HIV infection on proteasome subunit expression in individual brain regions was measured by Student's unpaired t-test. **(B, D, F)** Effect of HIV infection on whole brain proteasome subunit expression was measured by Student's paired t-test. *p<0.05, ** p<0.01, ***p<0.001, ****p<0.0001

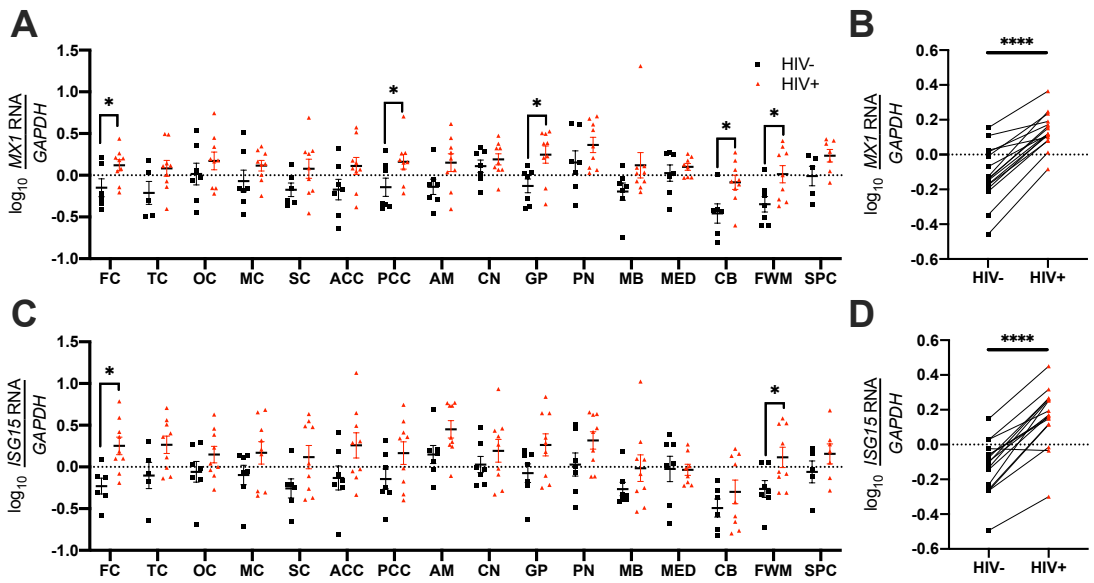

Figure 2.5 Type I IFN-stimulated gene expression is higher in multiple brain regions in PLWH than in HIV-negative individuals

(A-B) *MX1* and **(C-D)** *ISG15* RNA expression were measured by RT-qPCR. **(A,C)** Effect of HIV infection on type I IFN-stimulated gene expression in individual brain regions was measured by Student's unpaired t-test. **(B, D)** Effect of HIV infection on whole brain IFN-stimulated gene expression was measured by Student's paired t-test. *p<0.05, ** p<0.01, ***p<0.001, ****p<0.0001

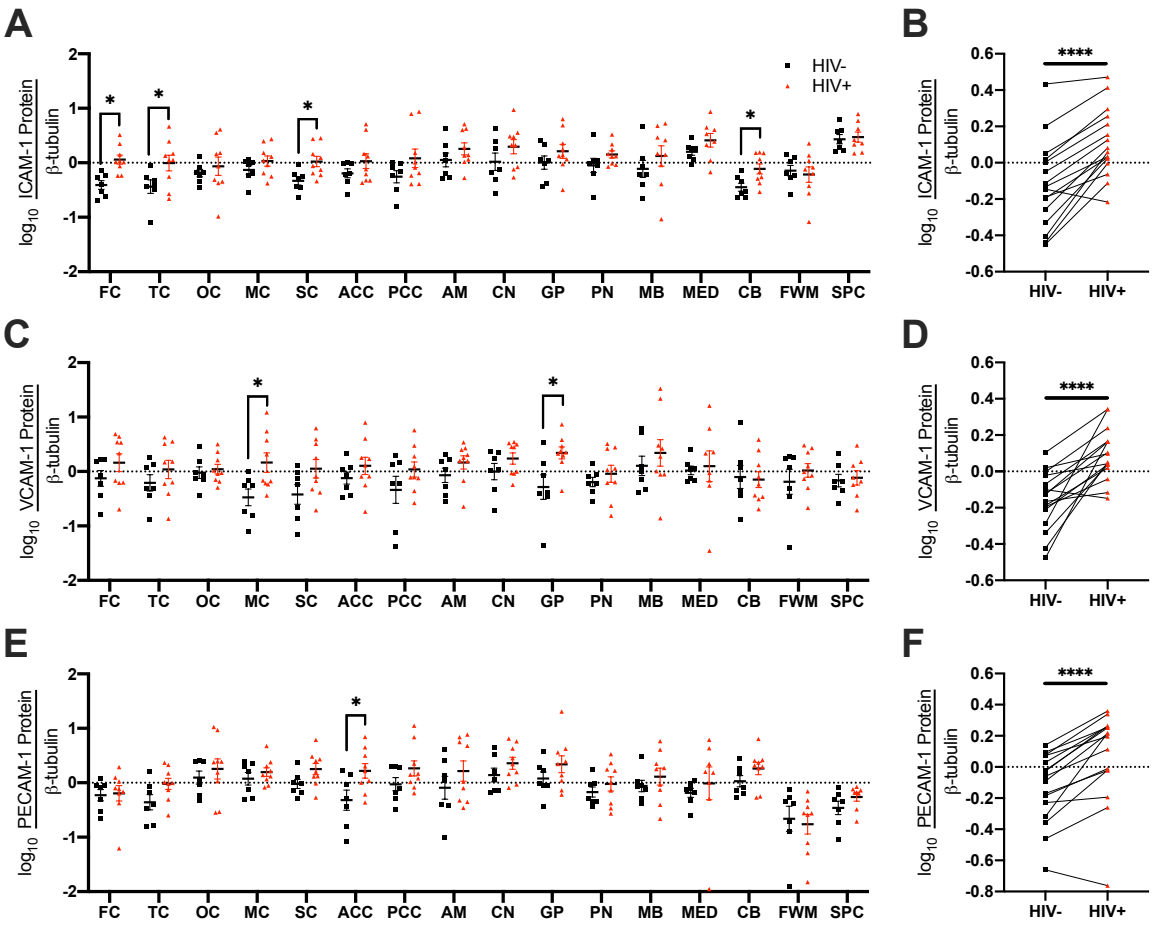

Figure 2.6 Endothelial activation and adhesion marker expression is higher in multiple brain regions in PLWH than in HIV-negative individuals

ICAM-1 **(A-B)**, VCAM-1 **(C-D)**, and PECAM-1 **(E-F)** protein expression were measured by Western blot. **(A, C, E)** Effect of HIV infection on endothelial adhesion molecule expression in individual brain regions was measured by Student's unpaired t-test. **(B, D, F)** Effect of HIV infection on whole brain endothelial adhesion molecule expression was measured by Student's paired t-test. *p<0.05, ** p<0.01, ***p<0.001, ****p<0.0001

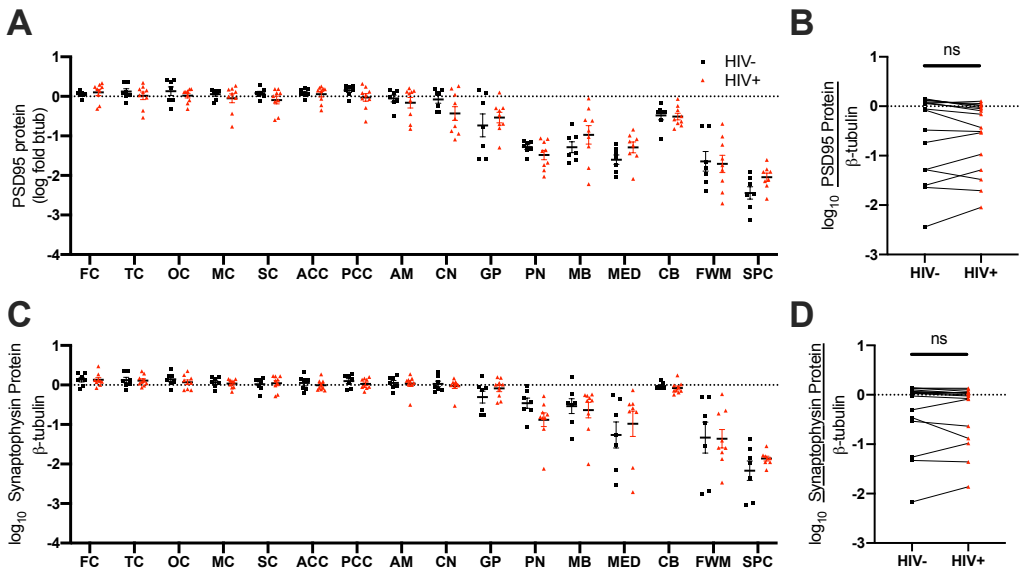

Figure 2.7 Synaptic marker expression is similar in PLWH and HIV-negative individuals

(A-B) PSD95 and **(C-D)** synaptophysin protein expression were measured by Western blot. **(a, c)** Effect of HIV infection on synaptic marker expression in individual brain regions was measured by Student's unpaired t-test. **(B, D)** Effect of HIV infection on synaptic marker expression was measured by Student's paired t-test. *p<0.05, ** p<0.01, ***p<0.001, ****p<0.0001

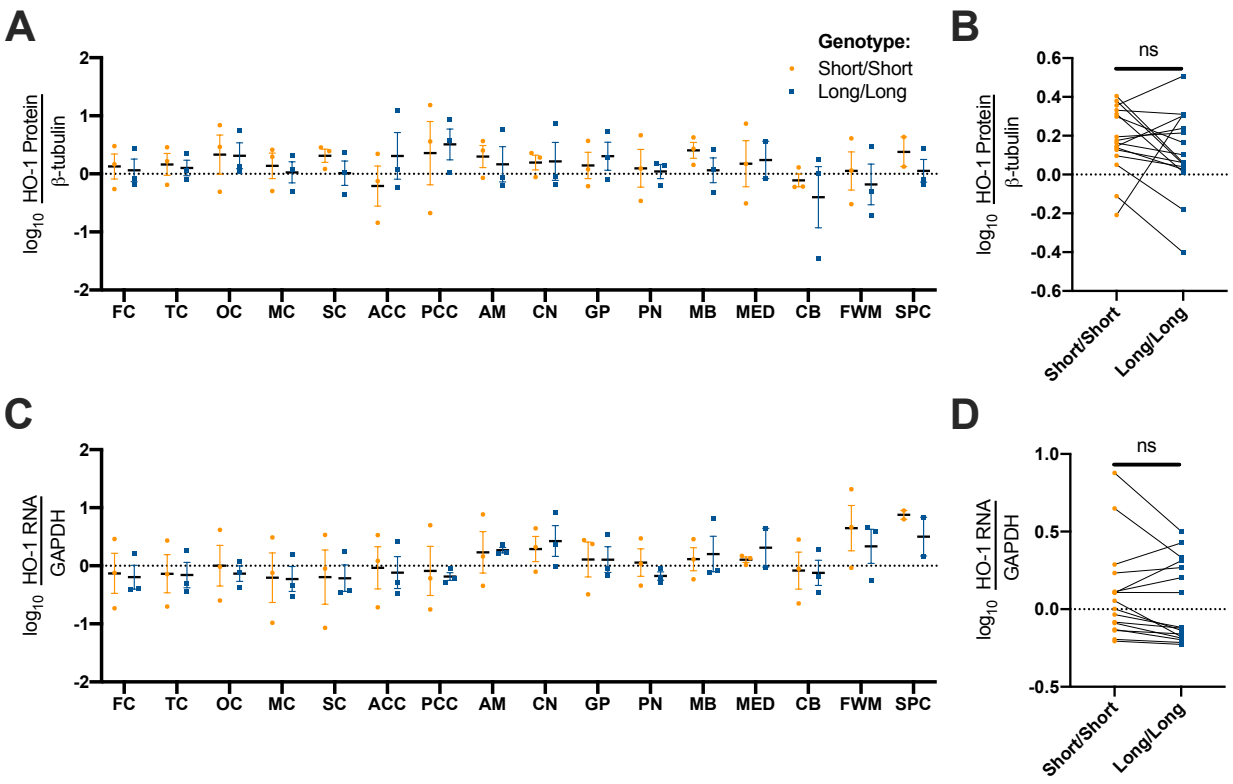

Figure 2.8 HO-1 $(GT)_n$ promoter genotype does not associate with HO-1 expression

(**A**) HO-1 protein and (**B**) RNA expression were measured by Western blot and RT-qPCR, respectively. PLWH were stratified by promoter genotype (orange circles: short/short [S/S]; blue squares: long/long [L/L]). (**A, C**) Effect of HO-1 $(GT)_n$ promoter genotype on HO-1 expression in individual brain regions was measured by Student's unpaired t-test. (**B, D**) Effect of HO-1 $(GT)_n$ promoter genotype on whole brain HO-1 expression was measured by Student's paired t-test. *p<0.05, ** p<0.01, ***p<0.001, ****p<0.0001

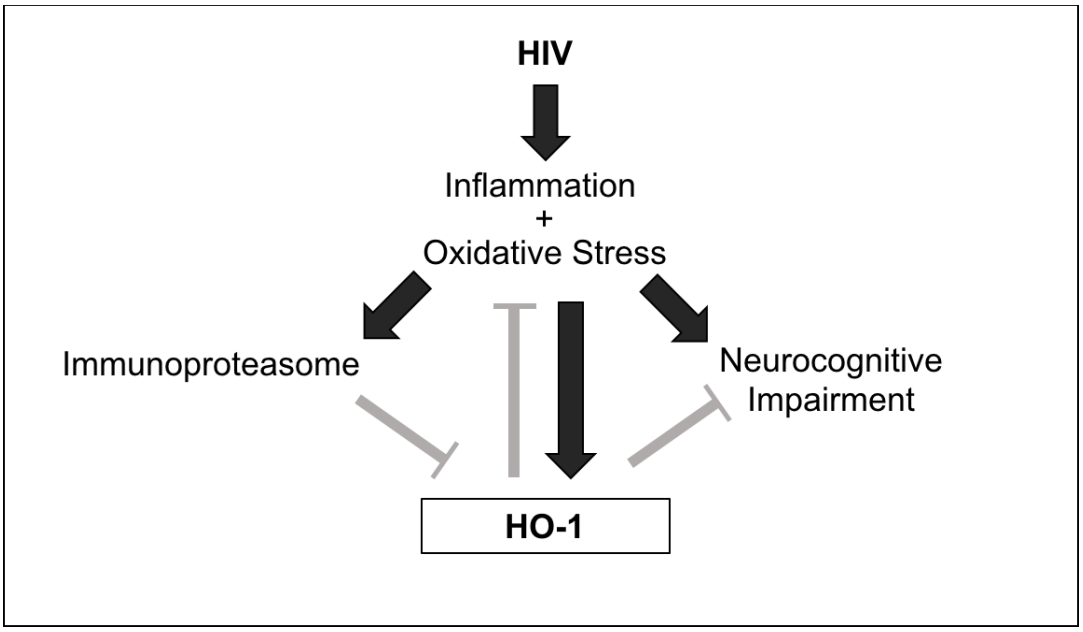

Figure 2.9 Hypothesized role for HO-1 in the development of HIV NCI

Schematic depicting proposed relationships between inflammation and oxidative stress, HO-1, immunoproteasome, and NCI in PLWH. HIV infection increases inflammation and oxidative stress, which associates with HIV NCI. Inflammation and oxidative stress also stimulate immunoproteasome and HO-1 expression. HO-1 induction limits inflammation, oxidative stress, and may protect against HIV NCI. Immunoproteasome induction drives down HO-1, decrease of which associates with HIV NCI.

2.7 Tables

	HIV-	HIV+	p-value
Demographic Data, mean ± SD			
Number of Subjects	7	9	
Age at death (mean ± SD)	60 ± 15.7	51 ± 11.0	0.196 §
Hours postmortem (mean ± SD)	18 ± 9.9	19 ± 8.0	0.850 §
Sex, N (%)			
Male	5 (71%)	8 (89%)	0.37 †
Female	2 (29%)	1 (11%)	
Race, N (%)			
White	5 (71%)	6 (67%)	0.84 †
Black	2 (29%)	3 (33%)	
Other/Unknown	0 (0%)	0 (0%)	
Ethnicity, N (%)			
Hispanic	0 (0%)	0 (0%)	
Not Hispanic	7 (100%)	9 (100%)	
Disease Parameters, mean ± SD ¶			
Log plasma HIV c/mL	-	4.2 ± 1.5	
Log CSF HIV c/mL	-	2.9 ± 0.7	
CD4+ lymphocytes/mm^3	-	120 ± 148.2	
Neurocognitive Impairment, N (%)			
HIV-NCI	-	0 (0%)	
Neuropsychological Impairment-Other	-	4 (44%)	
Neurocognitive Normal	-	5 (56%)	
No Neurocognitive Data	-	0 (0%)	
ART, N (%)			
ART-experienced	-	8 (89%)	
ART-naïve	-	0 (0%)	
Unknown ART	-	1 (11%)	

Table 2.1 Demographic and clinical data for PLWH cohort

Data are presented as mean ± standard deviation (SD) or as population percentages. Abbreviations: Cerebrospinal fluid (CSF), HIV-associated neurocognitive impairment (HIV NCI), antiretroviral therapy (ART). Statistical analyses: § Student's t-test; † Chi-square Test.

Regions Analyzed	Abbreviation
Frontal Cortex	FC
Temporal Cortex	TC
Occipital Cortex	OC
Motor Cortex	MC
Sensory Cortex	SC
Anterior Cingulate Cortex	ACC
Posterior Cingulate Cortex	PCC
Amygdala	AM
Caudate Nucleus/Putamen	CN
Globus Pallidus	GP
Pons	PN
Midbrain	MB
Medulla	MED
Cerebellum	CB
Frontal White Matter	FWM
Spinal Cord	SPC

Table 2.2 CNS regions analyzed and abbreviations

Primary Antibodies

Antibody	Type	Source	Catalog #	Dilution
β-tubulin	Rabbit mAb	Cell Signaling Technology	2128L	1:3000
Proteasome subunit LMP7	Mouse mAb	Enzo Life Sciences	BML-PW8845	1:500
Proteasome subunit β5	Rabbit pAb	Invitrogen	PA1-977	1:1000
GAPDH	Mouse mAb	Calbiochem	CB1001	1:20000
VCAM-1	Rabbit mAb	Abcam	ab134047	1:2000
PECAM-1	Rabbit pAb	Abcam	ab28364	1:500
ICAM-1	Rabbit mAb	Abcam	ab109361	1:1000
PSD95	Mouse mAb	EMD Millipore	MAB1596	1:1000
Synaptophysin	Mouse mAb	Abcam	Ab8049	1:1000
HO-2	Rabbit pAb	Enzo Life Sciences	SPA-897	1:1000
HO-1	Rabbit pAb	Enzo Life Sciences	SPA-895	1:500
HO-1	Rabbit pAb	Enzo Life Sciences	SPA-894	1:500
Proteasome subunit Pa28α	Rabbit pAb	Enzo Life Sciences	BML-PW8185	1:1000

Table 2.3 Primary antibodies used for Western blot

Abbreviations: monoclonal antibody (mAb); polyclonal antibody (pAb).

Secondary Antibodies

Antibody	Type	Source	Catalog #	Dilution
IRDye 680RD	Goat anti-mouse IgG	LI-COR Biosciences	926-68070	1:20,000
IRDye 680RD	Goat anti-rabbit IgG	LI-COR Biosciences	926-68071	1:20,000
IRDye 800CW	Goat anti-mouse IgG	LI-COR Biosciences	926-32210	1:15,000
IRDye 800CW	Goat anti-rabbit IgG	LI-COR Biosciences	926-32211	1:15,000

Table 2.4 Secondary antibodies used for Western blot

	HO-1 protein vs. HO-1 RNA			
	HIV-negative		PLWH	
Region	**Pearson r**	**p-value**	**Pearson r**	**p-value**
FC	0.301	0.563	0.586	0.097
TC	0.298	0.626	0.813	***0.008***
OC	0.612	0.144	0.673	***0.047***
MC	0.666	0.103	0.808	***0.008***
SC	0.150	0.776	0.686	***0.041***
ACC	-0.009	0.985	0.667	***0.050***
PCC	0.470	0.287	0.675	***0.046***
AM	0.725	0.065	0.537	0.136
CN	0.240	0.605	0.577	0.104
GP	-0.067	0.887	0.633	0.068
PN	0.192	0.679	0.534	0.139
MB	0.146	0.754	0.167	0.668
MED	0.162	0.728	0.525	0.182
CB	0.273	0.601	0.132	0.736
FWM	0.287	0.533	0.683	***0.043***
SPC	0.800	0.104	0.731	0.062

Table 2.5 HO-1 protein associates positively with HO-1 RNA in PLWH

Correlations between HO-1 RNA and protein were analyzed by Pearson's correlation. Bold and italicized text: $p<0.05$

	HO-1 RNA vs. CSF HIV RNA		HO-1 protein vs. CSF HIV RNA		HO-1 RNA vs. plasma HIV RNA		HO-1 protein vs. plasma HIV RNA	
Region	**Pearson r**	**p-value**	**Pearson r**	**p-value**	**Pearson r**	**p-value**	**Pearson r**	**p-value**
FC	0.941	***0.005***	0.963	***0.002***	0.873	***0.002***	0.795	***0.011***
TC	0.936	***0.006***	0.957	***0.003***	0.903	***0.001***	0.930	***0.000***
OC	0.766	0.076	0.843	***0.035***	0.822	***0.007***	0.670	***0.048***
MC	0.955	***0.003***	0.910	***0.012***	0.942	***0.000***	0.875	***0.002***
SC	0.969	***0.001***	0.764	0.077	0.876	***0.002***	0.759	***0.018***
ACC	0.988	***0.000***	0.935	***0.006***	0.866	***0.003***	0.634	0.067
PCC	0.782	0.066	0.791	0.061	0.741	***0.022***	0.709	***0.033***
AM	0.812	***0.050***	0.799	0.056	0.745	***0.021***	0.532	0.140
CN	0.540	0.269	0.779	0.068	0.650	0.058	0.506	0.164
GP	0.986	***0.000***	0.808	0.052	0.870	***0.002***	0.428	0.251
PN	0.792	0.061	0.770	0.073	0.730	***0.026***	0.770	***0.015***
MB	0.276	0.596	0.421	0.405	0.317	0.407	0.355	0.348
MED	0.804	0.101	0.845	0.071	0.750	***0.032***	0.663	0.073
CB	0.975	***0.001***	0.261	0.617	0.740	***0.023***	0.236	0.542
FWM	0.596	0.212	0.640	0.171	0.390	0.299	0.499	0.171
SPC	0.824	0.176	0.723	0.168	0.760	***0.048***	0.494	0.214

Table 2.6 Brain HO-1 RNA and protein associate with CSF and plasma HIV RNA in PLWH

Correlations between HO-1 RNA or protein and CSF or HIV RNA in individual regions were analyzed by Pearson's correlation. Bold and italicized text: $p<0.05$

	HO-1 RNA vs. LMP7 protein				HO-1 protein vs. LMP7 protein			
	HIV-negative		PLWH		HIV-negative		PLWH	
Region	Pearson r	p-value	Pearson r	p-value	Pearson r	p-value	Pearson r	p-value
FC	-0.114	0.830	0.288	0.452	0.360	0.428	0.676	***0.046***
TC	-0.229	0.711	0.202	0.602	0.219	0.637	0.474	0.198
OC	0.686	0.089	0.295	0.441	0.374	0.408	0.213	0.582
MC	0.754	0.050	0.003	0.994	0.190	0.683	-0.094	0.810
SC	0.011	0.984	0.105	0.789	0.111	0.812	-0.093	0.812
ACC	0.688	0.088	0.378	0.317	0.129	0.783	0.202	0.602
PCC	0.109	0.8163	0.065	0.8681	0.400	0.3745	0.289	0.4506
AM	0.559	0.192	0.009	0.982	0.827	***0.022***	-0.134	0.732
CN	0.180	0.699	0.023	0.953	0.065	0.890	0.068	0.863
GP	0.056	0.905	0.195	0.615	-0.665	0.104	0.372	0.324
PN	-0.265	0.566	0.552	0.124	0.092	0.844	0.347	0.360
MB	-0.173	0.711	0.014	0.972	0.623	0.135	0.151	0.698
MED	0.095	0.839	0.449	0.264	0.635	0.125	0.339	0.412
CB	0.151	0.775	-0.446	0.229	0.169	0.718	0.232	0.549
FWM	-0.224	0.629	-0.239	0.535	0.568	0.183	-0.247	0.521
SPC	0.147	0.814	0.885	***0.008***	0.558	0.193	0.627	0.096

Table 2.7 Associations between brain HO-1 and immunoproteasome subunit LMP7 in PLWH and HIV-negative individuals

Correlations between HO-1 RNA or protein and LMP7 in individual regions were analyzed by Pearson's correlation. Bold and italicized text: $p<0.05$

	ISG15 RNA vs. HO-1 RNA		*ISG15* RNA vs. HO-1 protein		*MX1* RNA vs. HO-1 RNA		*MX1* RNA vs. HO-1 protein	
Region	**Pearson r**	**p-value**	**Pearson r**	**p-value**	**Pearson r**	**p-value**	**Pearson r**	**p-value**
FC	0.497	0.173	0.311	0.415	0.510	0.161	-0.239	0.535
TC	0.712	***0.032***	0.605	0.085	0.706	***0.034***	0.435	0.241
OC	0.588	0.096	0.559	0.118	0.670	***0.048***	0.412	0.270
MC	0.589	0.096	0.588	0.096	0.355	0.348	0.347	0.361
SC	0.615	0.078	0.213	0.583	0.350	0.355	-0.044	0.910
ACC	0.755	***0.019***	0.725	***0.027***	0.736	***0.024***	0.472	0.199
PCC	0.714	***0.031***	0.613	0.080	0.630	0.069	0.480	0.191
AM	0.634	0.067	0.724	***0.027***	0.741	***0.022***	0.466	0.207
CN	0.204	0.599	0.556	0.120	0.481	0.190	0.590	0.094
GP	0.540	0.134	0.655	0.055	0.403	0.282	0.505	0.166
PN	0.247	0.522	0.203	0.600	0.107	0.783	-0.153	0.695
MB	0.634	0.067	-0.297	0.438	0.563	0.115	-0.308	0.420
MED	0.489	0.219	0.191	0.650	0.000	>0.999	-0.516	0.191
CB	0.559	0.117	-0.216	0.577	0.750	***0.020***	0.128	0.744
FWM	0.738	***0.023***	0.802	***0.009***	0.768	***0.016***	0.650	0.058
SPC	0.680	0.093	0.839	***0.018***	0.798	***0.031***	0.583	0.170

Table 2.8 Associations between brain HO-1 and type I IFN-stimulated genes in PLWH

Correlations between HO-1 RNA or protein and *ISG15* or *MX1* RNA in individual regions were analyzed by Pearson's correlation. Bold and italicized text: $p<0.05$

	***ISG15* RNA vs. HO-1 RNA**		***ISG15* RNA vs. HO-1 protein**		***MX1* RNA vs. HO-1 RNA**		***MX1* RNA vs. HO-1 protein**	
Region	**Pearson r**	**p-value**	**Pearson r**	**p-value**	**Pearson r**	**p-value**	**Pearson r**	**p-value**
FC	-0.100	0.850	-0.276	0.597	-0.446	0.376	-0.680	0.138
TC	-0.097	0.876	-0.602	0.282	-0.189	0.761	-0.920	***0.027***
OC	0.068	0.884	-0.412	0.358	-0.185	0.691	-0.567	0.184
MC	0.165	0.724	-0.110	0.815	-0.100	0.831	-0.370	0.414
SC	0.099	0.852	-0.293	0.573	0.214	0.684	-0.478	0.337
ACC	0.077	0.871	-0.584	0.169	-0.292	0.526	-0.617	0.140
PCC	-0.163	0.727	-0.061	0.896	-0.264	0.567	-0.229	0.6218
AM	0.102	0.828	-0.130	0.781	0.082	0.862	-0.118	0.801
CN	-0.630	0.130	-0.025	0.958	-0.279	0.544	0.390	0.387
GP	-0.569	0.182	-0.374	0.408	-0.773	***0.042***	-0.110	0.814
PN	-0.385	0.394	0.110	0.815	-0.383	0.396	-0.222	0.632
MB	-0.427	0.339	-0.065	0.889	-0.550	0.201	0.305	0.507
MED	0.558	0.193	0.210	0.651	0.654	0.111	0.350	0.441
CB	-0.484	0.331	-0.029	0.956	-0.732	0.098	-0.729	0.101
FWM	-0.079	0.867	-0.346	0.447	-0.553	0.198	-0.632	0.128
SPC	-0.248	0.687	-0.686	0.201	-0.241	0.696	-0.708	0.181

Table 2.9 Associations between brain HO-1 and type I IFN-stimulated genes in HIV-negative individuals

Correlations between HO-1 RNA or protein and *ISG15* or *MX1* RNA in individual regions were analyzed by Pearson's correlation. Bold and italicized text: $p<0.05$

	ICAM-1 protein vs. HO-1 RNA		ICAM-1 protein vs. HO-1 protein		VCAM-1 protein vs. HO-1 RNA		VCAM-1 protein vs. HO-1 protein		PECAM-1 protein vs. HO-1 RNA		PECAM-1 protein vs. HO-1 protein	
Region	**Pearson r**	**p-value**	**Pearson r**	**p-value**	**Pearson r**	**p-value**	**Pearson r**	**p-value**	**Pearson r**	**p-value**	**Pearson r**	**p-value**
FC	0.219	0.571	0.407	0.277	0.320	0.401	0.847	***0.004***	0.738	***0.023***	0.258	0.503
TC	0.049	0.900	0.180	0.644	0.385	0.306	0.827	***0.006***	0.870	***0.002***	0.752	***0.020***
OC	-0.324	0.395	0.141	0.719	0.285	0.458	0.039	0.921	0.768	***0.016***	0.888	***0.001***
MC	0.279	0.468	0.114	0.771	0.611	0.081	0.626	0.071	0.753	***0.019***	0.513	0.158
SC	0.435	0.242	0.132	0.735	0.497	0.173	0.535	0.138	0.777	***0.014***	0.175	0.652
ACC	0.199	0.607	0.294	0.443	0.556	0.120	0.906	***0.001***	0.751	***0.020***	0.569	0.110
PCC	-0.093	0.812	0.134	0.731	0.308	0.420	0.364	0.336	0.544	0.131	0.782	***0.013***
AM	-0.051	0.895	-0.275	0.474	0.807	***0.009***	0.439	0.238	0.571	0.108	0.659	0.054
CN	-0.190	0.625	-0.089	0.821	0.780	***0.013***	0.407	0.277	0.708	***0.033***	0.461	0.212
GP	0.161	0.679	0.125	0.748	0.615	0.078	0.619	0.076	0.623	0.073	0.679	***0.044***
PN	-0.215	0.578	0.186	0.633	0.207	0.592	0.748	***0.021***	0.768	***0.016***	0.551	0.125
MB	-0.039	0.920	0.293	0.481	0.243	0.528	0.778	***0.023***	0.299	0.435	0.562	0.147
MED	-0.160	0.706	0.332	0.422	0.556	0.152	0.686	0.060	0.493	0.214	0.364	0.375
CB	-0.401	0.285	-0.203	0.601	0.253	0.512	-0.065	0.869	0.497	0.174	-0.004	0.992
FWM	0.399	0.288	0.094	0.810	0.364	0.336	0.504	0.167	0.377	0.317	0.226	0.558
SPC	0.483	0.273	0.352	0.393	0.315	0.491	0.859	***0.006***	0.719	0.069	0.532	0.175

Table 2.10 Associations between brain HO-1 and endothelial adhesion molecules in PLWH

Correlations between HO-1 RNA or protein and ICAM-1, VCAM-1, or PECAM-1 protein in individual regions were analyzed by Pearson's correlation. Bold and italicized text: $p<0.05$

	ICAM-1 protein vs. HO-1 RNA		ICAM-1 protein vs. HO-1 protein		VCAM-1 protein vs. HO-1 RNA		VCAM-1 protein vs. HO-1 protein		PECAM-1 protein vs. HO-1 RNA		PECAM-1 protein vs. HO-1 protein	
Region	**Pearson r**	**p-value**	**Pearson r**	**p-value**	**Pearson r**	**p-value**	**Pearson r**	**p-value**	**Pearson r**	**p-value**	**Pearson r**	**p-value**
FC	-0.650	0.163	0.117	0.803	-0.166	0.753	0.420	0.349	-0.511	0.301	0.609	0.147
TC	0.642	0.243	0.155	0.741	-0.249	0.687	0.464	0.294	0.284	0.643	0.511	0.242
OC	0.625	0.133	0.443	0.319	-0.308	0.501	0.265	0.566	0.297	0.518	0.292	0.526
MC	0.293	0.523	0.013	0.978	-0.597	0.157	-0.018	0.970	0.551	0.200	0.172	0.713
SC	-0.776	0.070	-0.317	0.489	-0.774	0.071	0.294	0.522	-0.451	0.370	-0.230	0.619
ACC	0.200	0.668	0.629	0.130	-0.477	0.279	0.674	0.097	-0.129	0.784	0.363	0.424
PCC	-0.283	0.538	-0.221	0.634	-0.183	0.695	-0.035	0.941	0.401	0.373	0.752	0.051
AM	-0.083	0.860	0.255	0.581	-0.311	0.498	0.439	0.238	-0.240	0.604	0.184	0.694
CN	0.418	0.351	0.543	0.208	0.312	0.496	0.443	0.319	0.161	0.730	0.017	0.972
GP	-0.391	0.386	0.024	0.960	-0.350	0.441	-0.326	0.476	0.105	0.824	-0.084	0.857
PN	0.230	0.621	0.961	***0.001***	0.145	0.756	-0.466	0.292	-0.100	0.832	0.784	***0.037***
MB	-0.030	0.948	0.104	0.824	-0.609	0.147	0.379	0.402	-0.096	0.838	0.129	0.783
MED	-0.079	0.866	0.426	0.341	-0.062	0.896	0.199	0.669	-0.608	0.148	0.190	0.684
CB	0.100	0.851	0.004	0.993	-0.780	0.067	0.400	0.374	-0.418	0.409	0.468	0.290
FWM	-0.408	0.364	0.300	0.513	-0.667	0.102	0.389	0.388	-0.586	0.167	0.565	0.186
SPC	0.913	***0.030***	0.238	0.607	-0.488	0.404	0.000	0.999	0.162	0.795	0.368	0.417

Table 2.11 Associations between brain HO-1 and endothelial adhesion molecules in HIV-negative individuals

Correlations between HO-1 RNA or protein and ICAM-1, VCAM-1, or PECAM-1 protein in individual regions were analyzed by Pearson's correlation. Bold and italicized text: $p<0.05$

	PSD95 protein vs. HO-1 RNA		PSD95 protein vs. HO-1 protein		Synaptophysin protein vs. HO-1 RNA		Synaptophysin protein vs. HO-1 protein	
Region	**Pearson r**	**p-value**	**Pearson r**	**p-value**	**Pearson r**	**p-value**	**Pearson r**	**p-value**
FC	0.168	0.666	-0.063	0.872	-0.297	0.437	0.309	0.419
TC	0.396	0.291	0.171	0.660	-0.073	0.853	0.097	0.804
OC	0.647	0.060	0.666	0.050	-0.258	0.504	-0.526	0.145
MC	0.125	0.749	0.123	0.753	-0.184	0.635	-0.103	0.792
SC	0.433	0.244	-0.011	0.979	-0.293	0.445	-0.447	0.228
ACC	0.508	0.162	0.597	0.089	-0.222	0.566	-0.057	0.883
PCC	0.476	0.195	0.646	0.060	-0.279	0.467	-0.110	0.7774
AM	0.548	0.127	0.595	0.091	0.093	0.812	0.191	0.623
CN	0.379	0.315	0.686	***0.041***	0.254	0.509	0.222	0.566
GP	0.531	0.141	0.249	0.519	0.045	0.908	0.415	0.267
PN	0.617	0.077	0.185	0.634	0.057	0.884	-0.119	0.761
MB	0.421	0.260	0.468	0.243	0.561	0.116	0.323	0.435
MED	0.536	0.171	0.221	0.598	0.077	0.855	0.023	0.957
CB	0.292	0.445	-0.169	0.665	-0.545	0.129	0.040	0.919
FWM	-0.341	0.370	-0.466	0.206	-0.242	0.530	-0.571	0.108
SPC	0.527	0.224	0.438	0.278	-0.647	0.116	-0.532	0.175

Table 2.12 Associations between brain HO-1 and synaptic markers in PLWH

Correlations between HO-1 RNA or protein and PSD95 or synaptophysin protein in individual regions were analyzed by Pearson's correlation. Bold and italicized text: $p<0.05$

	PSD95 protein vs. HO-1 RNA		PSD95 protein vs. HO-1 protein		Synaptophysin protein vs. HO-1 RNA		Synaptophysin protein vs. HO-1 protein	
Region	**Pearson r**	**p-value**	**Pearson r**	**p-value**	**Pearson r**	**p-value**	**Pearson r**	**p-value**
FC	-0.184	0.727	0.003	0.995	0.215	0.682	0.791	***0.034***
TC	-0.431	0.469	0.546	0.205	-0.295	0.630	0.836	***0.019***
OC	0.717	0.070	0.753	0.051	0.057	0.903	0.381	0.399
MC	0.025	0.958	0.037	0.937	0.078	0.867	0.065	0.889
SC	-0.490	0.324	-0.209	0.653	0.489	0.325	0.130	0.781
ACC	-0.038	0.936	-0.100	0.831	0.205	0.660	-0.266	0.564
PCC	0.213	0.647	-0.149	0.749	-0.140	0.766	0.458	0.302
AM	0.286	0.534	0.056	0.905	0.286	0.535	0.770	***0.043***
CN	-0.057	0.903	-0.493	0.261	-0.400	0.374	-0.700	0.080
GP	-0.019	0.969	0.514	0.238	-0.307	0.503	0.589	0.164
PN	0.666	0.103	0.093	0.843	0.528	0.223	0.469	0.289
MB	-0.055	0.907	0.300	0.513	-0.170	0.716	0.503	0.250
MED	-0.552	0.199	0.537	0.214	-0.260	0.573	0.797	***0.032***
CB	0.339	0.511	-0.423	0.344	-0.409	0.421	0.360	0.428
FWM	0.133	0.776	0.756	***0.049***	0.178	0.702	0.639	0.123
SPC	-0.647	0.238	-0.246	0.595	-0.829	0.083	0.248	0.592

Table 2.13 Associations between brain HO-1 and synaptic markers in HIV-negative individuals

Correlations between HO-1 RNA or protein and PSD95 or synaptophysin protein in individual regions were analyzed by Pearson's correlation. Bold and italicized text: $p<0.05$

CHAPTER 3: Analysis of the role for HO-1 in endothelial cell function using *in vitro* blood-brain barrier models

Analise L. Gruenewald[1], Dennis L. Kolson[1]

[1]Deparment of Neurology, Perelman School of Medicine, University of Pennsylvania, Philadelphia, PA, USA

Unpublished

3.1 Abstract

Blood-brain barrier (BBB) disruption is well-known in HIV infection and may contribute to development of HIV-associated neurocognitive impairment (HIV NCI). Host antioxidant response enzyme HO-1 has been shown to support key functions of endothelial cells, which comprise the main structural component of the BBB, including tight junction permeability and transendothelial migration (116, 216). We have previously demonstrated that reduced HO-1 expression in prefrontal cortex associates with HIV NCI, and that HO-1 expression associates with expression of endothelial adhesion molecules throughout the brain in PLWH (**Table 2.10**) (36). Whether reduction of endothelial HO-1 contributes to BBB disruption in HIV infection is unknown. Similarly, the potential of induction of HO-1 as a therapeutic strategy to support BBB function in HIV infection is unclear. Here, we used two human brain endothelial cell models (hCMEC/D3 cell line (217) and primary human brain microvascular endothelial cells [HBMECs]) to interrogate the role for HO-1 expression in tight junction permeability and transendothelial migration. We modulated HO-1 expression pharmacologically and genetically in each model. HO-1 induction and knockdown, however, did not affect tight junction permeability or expression of adhesion molecules in response to pro-inflammatory stimuli. We successfully modeled chemotactic transendothelial migration of monocytes in both hCMEC/D3 cells and HBMECs. Our results indicate that each of these cell types can be utilized to determine HO-1-specific effects on BBB functions. Further development of experimental paradigms modeling inflammatory stimuli relevant to HIV infection is required to better understand the role for HO-1 in these functions.

3.2 Introduction

Despite the introduction of highly active combination antiretroviral therapy (ART), HIV-associated neurocognitive impairment (HIV NCI) affecting activities of daily functioning persists in ~15% of persons living with HIV (PLWH) (9). While transient increases in HIV RNA in the CSF, known as "blips," occur in up to 21% of PLWH on ART(153, 218), there is not a clear relationship between systemic or CNS replication and HIV NCI in individuals on ART(219), suggesting distinct or additional factors contributing to HIV NCI. Disruption to the blood-brain barrier (BBB), evidenced *in vivo* by increased neurofilament light chain protein (NFL) in CSF, increased CSF/plasma albumin ratio, and contrast enhanced MRI in infected individuals, is well-known in HIV infection (29, 220-225). Brain microvascular endothelial cells (HBMECs) are the primary structural component of the BBB. HBMECs are supported by smooth-muscle like pericytes embedded within the basement membrane and astrocyte endfeet that secrete supportive and regulatory factors; these cells are also considered components of the BBB (32, 33). The BBB possesses selective tight junctions (TJs), high transendothelial electrical resistance (TEER), and tight regulation of adhesion and transmigration of leukocytes, protecting the CNS from potentially harmful elements in the circulation(30, 32, 34, 226, 227). Increased BBB permeability and infiltration of activated and/or infected leukocytes into the CNS perpetuates inflammation and oxidative stress in the CNS compartment that likely contributes to neurocognitive impairment(31, 56, 154, 228).

A critical host response to inflammation and oxidative stress is the coordinated induction of genes regulated through the antioxidant response element (ARE) pathway (105). An array of genes encoding detoxifying and cytoprotective effector proteins contain this common promoter element (the ARE), and are induced in response to changes in cellular redox status (71, 72). A growing body of work supports a protective role for a particular ARE effector protein, heme oxygenase-1 (HO-1), against HIV NCI. HO-1 is a highly inducible, cytoprotective, and has potent anti-inflammatory and antioxidant effects (92, 229). HO-1 is critical to the host antioxidant response, catalyzing the rate-limiting first step of heme metabolism, cleaving heme to biliverdin, ferrous iron,

and carbon monoxide (92). HO-1 is induced by its substrate heme, as well as many other cellular stressors including microbial products and pro-inflammatory cytokines (92). HO-1 transcription is partially regulated by a $(GT)_n$ dinucleotide repeat polymorphism in its promoter region that modulates basal transcription and inducibility of HO-1 in response to stimuli (90). Shorter repeat length allele genotypes associate with better outcomes in numerous systemic and CNS disease states, as well as systemic HIV (89, 107, 113). We recently found that shorter repeat length alleles also associate with reduced risk for HIV NCI and HIV encephalitis (114, 115). Furthermore, HO-1 protein expression is reduced in dorsolateral prefrontal cortex of PLWH with HIV NCI, and this decreased HO-1 expression associates with increased neuroinflammation and HIV NCI. HIV-induced glial loss of HO-1 expression associates with the release of neurotoxic levels of glutamate (36, 166). Most recently, we have shown that HO-1 associates with expression of endothelial adhesion molecules throughout the brain in PLWH (Chapter 2).

In the brain, HO-1 is expressed in glial cells (astrocytes, microglia) as well as the highly specialized brain microvascular endothelial cells that comprise the primary structural component of the BBB. Endothelial HO-1 expression has been shown to have protective effects in several pathologic conditions, including cerebral ischemia and oxygen toxicity (230, 231). Additionally, HO-1 has been found to modulate expression of inflammatory cytokine-induced adhesion molecules in aortic endothelial cells (232). The contribution of HO-1 to the maintenance of barrier integrity and function in endothelial cells suggests that modulation of HO-1 expression might affect BBB functions relevant to the development of HIV NCI. We hypothesized that modulation of endothelial HO-1 expression affects the BBB's functional response to inflammation through TJ integrity and leukocyte adhesion and transmigration.

In order to interrogate the role for endothelial HO-1 expression in BBB function, we employed two *in vitro* models: a well-established endothelial cell line (hCMEC/D3 cells) and primary human brain microvascular endothelial cells (HBMECs). The hCMEC/D3 line is derived from culture of primary

adult temporal lobe microvessels, immortalized by lentiviral transduction of hTERT and SV40 large T antigen (217). In their initial development, hCMEC/D3s were shown to express TJ markers claudin-5 and ZO-1 and adhesion molecule PECAM-1 (217). However, hCMEC/D3 monolayer TEER is not as high as those observed *in vivo* or using primary endothelial cells or induced pluripotent stem cell-derived models, representing a limitation of this model (233). BBB models employed here consisted of endothelial cells seeded onto transwell inserts, mimicking the HBMEC barrier between plasma and CNS. Primary HBMEC models included human fetal astrocytes, adding another BBB component to the model. We lacked inclusion of pericytes and perivascular macrophages/microglia. In each model, we *i)* determined basal HO-1 expression; *ii)* defined the response to pharmacologic HO-1 inducers; and *iii)* specifically modulated HO-1 expression using siRNAs. Finally, we used each cell type to model critical BBB functions: monolayer impermeability, and transendothelial migration of monocytes. Our data suggest that hCMEC/D3 cells, HO-1 induction may ameliorate TNFα-induced monolayer permeability. Using HBMECs, we confirmed that human primary endothelial-astrocyte co-cultures can reliably model monocyte transmigration in response to CCL2, and that HO-1 can be genetically manipulated within this model.

3.3 Materials and Methods

hCMEC/D3 cell culture

hCMEC/D3 cells (217) were obtained courtesy of Dr. Jorge Alvarez (University of Pennsylvania). Cells were cultured in endothelial cell media (ECM): EBM-2 basal media (Lonza) with 5% fetal bovine serum, 1.4uM hydrocortisone (Sigma), 5ug/mL ascorbic acid (Sigma), 1% Chemically Defined Lipid Concentrate (Gibco), 10mM HEPES (Sigma), 200ng/mL Fibroblast Growth Factor-basic (Millipore). Cells were passaged every 4-6 days to T25 flasks coated with 1:500 rat tail collagen type I (Lonza) in PBS and used between P14-P28. Cells were maintained at 37°C and 6% CO_2.

Human brain microvascular endothelial cell culture

Human brain microvascular endothelial cells (HBMEC) (P1-P3) were obtained from ScienCell (cat. #1000) and cultured in M199C media: Media 199 (Gibco) with 200mM L-glutamine, 50mg/mL ascorbic acid (Sigma), 1% pen/strep, 25mg/mL heparin (Sigma), 3mg/mL Sigma Growth Factor (Sigma), 9mg/mL bovine brain extract (Clonetics), 5% human serum type AB (Corning), 20% newborn calf serum (Gibco). Cells were subcultured every 3-6 days to 100mm dishes coated with 0.2% laboratory grade gelatin (Fisher). Cells were maintained at 37°C and 5% CO_2.

Human fetal astrocyte cell culture

Primary human fetal astrocyte cultures were prepared and frozen down by the Basic Science Core I of the Comprehensive NeuroAIDS Center (CNAC) at Temple University School of Medicine. Fetal brain tissues (gestational age 16-18 weeks) obtained from elective abortion procedures were washed in Hank's balanced salt solution (HBSS), meninges and blood vessels were removed, and tissues were mechanically disrupted then digested with 0.25% trypsin (Life Technologies) and 10U/mL DNASE I (Sigma-Aldrich). Single cell suspensions were plated in mixed glial growth media (Dulbecco's modified eagle medium/Ham's F-12 nutrient mixture with HEPES (DMEM/F-12, Gibco) supplemented with 10% FBS (HyClone), 50ug/mL Gentamicin (Gibco), 5ug/mL Fungizone (Gibco), 2mM L-glutamine (Gibco), and 10ug/mL Insulin (Sigma-Aldrich)) and maintained under 10% CO2 for 5 days. To enrich for astrocytes, the mixed glial cell cultures were shaken at 200rpm for 14-18 hours, medium containing detached cells was removed, and the remaining adherent monolayers of astrocytes were fed with astrocyte growth media (DMEM/F-12 supplemented with 15% FBS, 50ug/mL Gentamicin, 5ug/mL Fungizone, 2mM L-glutamine, and 10ug/mL insulin) and maintained at 37°C and 5% CO_2. Frozen cells were thawed and maintained at 37°C and 5% CO_2 in M199C media.

siRNA knockdown

hCMEC/D3 cells were transfected at 80% confluency with 20nM Silencer Select siRNAs (Ambion) using Lipofectamine RNAiMax (Invitrogen) for a transfection period of 24-96 hours. Lipofectamine and siRNAs were incubated for 5 minutes in OptiMEM (Invitrogen) at room temperature prior to addition to cells. Control conditions included Lipofectamine alone and transfection with Silencer negative control siRNA targeting a scramble sequence (#4390846). HBMECs were transfected with 20nM Silencer Select siRNAs (Ambion) using Amaxa Nucleofector Kit V (Lonza) according to manufacturer's instructions and as described, using program T-23 (234). Controls included cells not electroporated, cells electroporated without any siRNA, and electroporation with Silencer negative control siRNA. siRNA targeting HO-1 (s6673) was used to knock down HO-1, while siRNA targeting BACH1 (s1859), a transcriptional repressor of HO-1, was used to induce HO-1 expression (36, 215).

Protein extraction and Western blot analysis

Protein lysates from hCMEC/D3 cell cultures were prepared in radioimmunoprecipitation assay (RIPA) lysis buffer (Amresco) supplemented with Complete Protease Inhibitor Cocktail (Roche Applied Science). Protein concentration was quantified using the Detergent Compatible (DC) protein assay (BioRad). Proteins were resolved by SDS-PAGE and transferred to polyvinylidene fluoride (PVDF) membranes. Membranes were incubated with primary antibody overnight at 4°C. For infrared fluorescent detection of protein expression, membranes were incubated with IRDye-conjugated secondary antibody for one hour at room temperature and scanned with the Odyssey CLx Infrared Imagine System (LI-COR Biosciences). Background-corrected signal intensity of protein bands was measured using Image Studio Lite software (LI-COR Biosciences). Protein expression was normalized to GAPDH or β-tubulin and fold change was calculated relative to in-experiment control (untreated, vehicle, or scramble) condition.

Permeability assay

Permeability of hCMEC/D3 or HBMEC monolayers on PET transwell inserts (Falcon) was assessed by tracer molecule (70 kDa FITC-dextran) exclusion as previously described (217, 235). In experiments only testing permeability, 0.4um-pore inserts were used, while 3.0um inserts were used in experiments also testing monocyte transmigration. FITC-dextran in respective endothelial cell media (2ng/mL) was added to the upper chamber of inserts. Every 5 minutes for 30 minutes, 10uL of media from the lower chamber was sampled and transferred to individual wells of 96-well plates. Fluorescence intensity of these samples was measured using a flour metric plate reader. Permeability is represented as Arbitrary Fluorescent Units measured at 30 minutes or permeability coefficient (Pe). The permeability coefficient was calculated as follows: Pe = PS/s, where PS is the permeability surface area of the endothelial monolayer and s is the surface area of the filter. PS is calculated by 1/PS = 1/me – 1/mf, where me and mf are the slopes of the curves corresponding to endothelial cells on filters and to filters only, respectively, with me and mf calculated by plotting the cleared volume against time. Cleared volume was calculated by (AUa-AUb)/Fi, where AUa is the total fluorescence (arbitrary units) in the basal compartment, AUb is the background fluorescence and Fi is the fluorescence of the initial solution (AU/mL) (235).

Monocyte transmigration assay

Peripheral blood mononuclear cells (PMBC) were isolated from volunteer donors by Ficoll density gradient centrifugation, and monocytes were isolated by adherence to gelatin-coated flasks (167). Enriched monocytes were added to the upper chamber of 3.0um transwell inserts (Falcon) with hCMEC/D3 or HBMEC monolayers and CCL2 (100-400ng/mL), which is known to enhance leukocyte transmigration (167, 236), was added concurrently to the lower chamber or both the upper and lower chambers. Monocytes were allowed to migrate for 24h. **(Fig. 3.1A-B)**. Permeability assays were done in each condition before and after migration in order to ensure monolayer integrity. Monocyte transmigration was determined by counting cells in 5 10x fields per well in each of three technical replicate wells. Relative transmigration is represented as fold change in average number of monocytes per 10x field compared to the untreated condition.

Human BBB model

HBMECs and primary human fetal astrocytes were cultured on opposite surfaces of 0.2% gelatin-coated 3.0um-pore polyethylene terephthalate (PET) inserts (Falcon) in M199C+ media to model the BBB as previously described **(Fig. 3.1B)** (237). Astrocytes were seeded to the underside of inserts and allowed to adhere for 4 hours. Inserts were inverted and placed into appropriate plates, after which HBMECs were seeded to the upper surface. Co-cultures were incubated at 37°C and 5% CO_2 for 48 hours to obtain confluent endothelial monolayers. Co-cultures were then transferred to low-serum M199C media (M199 with 10% newborn calf serum and endothelial cell growth factors) for 24 hours before permeability and monocyte transmigration assays. Impermeability of monolayers to FITC-dextran was confirmed prior to experimental manipulation of co-culture preparations.

Statistics

All quantifications are expressed as mean ± standard error of the mean (SEM). Protein expression data were log transformed. Statistical comparisons of three or more groups were made by one-way ANOVA with Holm-Sidak post hoc test for multiple comparisons. Statistical comparisons determining effects of more than one independent variable were made by two-way ANOVA with Holm-Sidak post hoc test for multiple comparisons. All statistical analyses were performed using GraphPad Prism 8 software. Statistical significance was defined as *p<0.05, **p<0.01, ***p<0.001, ****p<0.0001.

3.4 Results

HO-1 responds predictably to pharmacologic manipulation in hCMEC/D3 cells

We first determined whether we could predictably and reliably manipulate HO-1 expression in hCMEC/D3 cells using small molecules and cytokines known to induce HO-1 in other models: cobalt protoporphyrin (CoPP), dimethyl fumarate (DMF) and monomethyl fumarate (MMF) (**Fig.**

1.1). CoPP robustly induces HO-1 by both destabilizing BACH1 and stabilizing Nrf2, effectively deprepressing HO-1 transcription and enhancing it simultaneously (117). As expected, 24-hour treatment with 10uM CoPP robustly induced HO-1 expression (**Fig. 3.2A-B**). We next tested DMF and MMF, which induce HO-1 expression in monocyte-derived macrophages (MDM) and other cell types via electrophilic interactions with Keap1 (167, 238, 239). Both DMF and MMF treatment increased HO-1 expression in hCMEC/D3 cells, but with different kinetics (**Fig. 3.2C-D**). Treatment with 10uM DMF increased HO-1 expression to about four-fold when compared to untreated hCMEC/D3 cells, with peak expression occurring at 8 hours post-treatment. Treatment with 10uM MMF increased HO-1 expression to a similar magnitude, but with peak expression occurring at 24 hours post-treatment. HO-1 expression at 48 hours post-treatment was similar with DMF and MMF treatment. Finally, we treated hCMEC/D3 cells with interferon-beta (IFNβ), which has been reported to support BBB function in MS studies (240), to determine its effect on HO-1 expression. Using a dose-response approach over the course of 6 days, we found modest increases in HO-1 expression with 0.1, 0.5, and 1ng/mL IFNβ treatment at 24 hours post-treatment (**Fig. 3.2E-F**). There was no difference in HO-1 expression between untreated cells and those exposed to any dose of IFNβ at 4 or 6 days post-treatment.

hCMEC/D3 cell blood-brain barrier model recapitulates cytokine-induced monocyte chemotaxis, but not barrier permeability

With confirmation that we could observe and predictably manipulate HO-1 expression in hCMEC/D3 cells with known inducers, we next sought to use these cells to model the BBB using a transwell system. Based on previous reports, we hypothesized that hCMEC/D3 barrier permeability would increase in response to pro-inflammatory cytokines TNFα and IFNγ (241), and that monocyte transmigration across the hCMEC/D3 monolayer would increase in response to monocyte chemoattractant protein 1 (CCL2) (237). We seeded hCMEC/D3 cells onto polyethylene terephthalate (PET) membrane inserts, and determined monolayer integrity by measuring permeation of 70kDa FITC-tagged dextran from the upper chamber to the lower chamber over time

(30 minutes). Permeability of the hCMEC/D3 monolayer to FITC-dextran progressively decreased over time after plating, reaching equilibrium between 6 to 8 days, and thus monolayers were assayed at least 6 days after plating in subsequent experiments (**Fig. 3.3A**). Pore size (0.4um or 3.0 um) did not influence monolayer permeability, but serum content of the media did, suggesting that we had achieved a functional monolayer that would respond to soluble factors in media (**Fig. 3.3B**). We next tested the monolayer's response to pro-inflammatory cytokine treatment, with the hypothesis that exposure to IFNγ and TNFα would increase permeability as previously reported (241). hCMEC/D3 cells seeded to 0.4um-pore transwell inserts were transferred to serum-free media 24h prior to treatment. We exposed the monolayers to TNFα or IFNγ for 24h, after which we tested their permeability using 70kDa FITC-dextran. Contrary to our expectations, treatment with 5-10ng/mL TNFα did not significantly increase monolayer permeability (**Fig. 3.3C**). Because hydrocortisone pre-treatment can prevent increased permeability of hCMEC/D3 cells in response to TNFα (242), we repeated this experiment using serum- and hydrocortisone-free media. Still, TNFα treatment did not increase monolayer permeability (**Fig. 3.3C**). Similarly, we did not find any significant increase in permeability when we treated hCMEC/D3 monolayers with 5-10ng/mL IFNγ (**Fig. 3.3D**).

In addition to permeability, we aimed to use hCMEC/D3 cells to model transendothelial migration of lymphocytes. To do this, we measured migration of primary human monocytes across hCMEC/D3 monolayers in response to CCL2. We established hCMEC/D3 monolayers on 3um-pore transwell inserts using media suitable for co-culture with primary human monocytes (RPMI 5% FBS), which we had previously determined not to negatively impact monolayer permeability (**Fig. 3.2B**). To ensure that any observed increase in chemotaxis was due to diapedisis and not structural breakdown of the barrier, we first determined whether exposure to CCL2 would impact monolayer permeability. hCMEC/D3 monolayer permeability to 70kDa FITC-dextran after 24h exposure to 200ng/mL CCL2 in either the lower chamber or both upper and lower chambers (to differentiate between chemotaxis and chemikinesis) was not different compared to vehicle-treated

or untreated monolayers (**Fig. 3.3E**). When we applied primary human monocytes to the upper chamber of the transwell system at the same time as CCL2 (**Fig. 3.1A**), we observed that a greater number of monocytes migrated to the lower chambers with CCL2 compared to those with vehicle in the lower chamber or CCL2 in the upper and lower chambers (**Fig. 3.3F**). These data suggested that we could successfully model monocyte chemotaxis across a monolayer of hCMEC/D3 cells in response to CCL2.

Genetic manipulation of HO-1 may prevent inflammation-induced permeability in hCMEC/D3 cells

To determine the role for HO-1 in barrier function in hCMEC/D3 cells, we genetically manipulated HO-1 expression using siRNAs and evaluated monolayer permeability in those conditions. Using Lipofectamine to deliver siRNAs specific to HO-1 and its transcriptional repressor BACH1 (36, 215), we observed significant knockdown and induction of HO-1 expression, respectively, that persisted from 24h to 96h-post transfection (**Fig. 3.4A**). We tested permeability of hCMEC/D3 monolayers to 70kDa FITC-dextran 72h post-transfection, and observed a modest increase in permeability in monolayers treated with siRNA against HO-1, although this observation was not significant (**Fig. 3.4B**). Finally, we tested whether knockdown or induction of HO-1 prior to exposure to TNFα would impact permeability of hCMEC/D3 monolayers using the timeline of transfection efficacy we had previously observed (**Fig. 3.4A**) (241). We transfected hCMEC/D3 cells with siRNAs against HO-1 or BACH1 in our transwell system, then treated with 10ng/mL TNFα for 24h. Interestingly, we observed modest increases in permeability in TNFα-treated monolayers that had been transfected with scrambled-control siRNA or siRNA against HO-1 compared to untreated monolayers of the same siRNA condition, but not in monolayers transfected with siRNA against BACH1 (**Fig. 3.4C**). These results suggest that induction of HO-1 prior to exposure to TNFα may protect against inflammation-induced permeability in hCMEC/D3 cells. However, increased permeability with TNFα treatment was not observed in the untreated condition, and further investigation is required to confirm this conclusion.

Primary human brain microvascular endothelial cells express HO-1 in response to pharmacologic and genetic manipulation

With confirmation that we could observe and manipulate HO-1 expression and model BBB functions (monolayer permeability and transendothelial migration) using hCMEC/D3 cells in a transwell system, we applied these techniques to a more biologically relevant co-culture model using all primary cells. Using primary human brain microvascular endothelial cells (HBMECs), we first determined whether these cells *i)* express HO-1 under basal conditions, and *ii)* increase HO-1 expression in response to CoPP. Indeed, 10uM CoPP robustly induced HO-1 expression in HBMECs after 24h, while basal HO-1 expression was low difficult to resolve by Western blot (**Fig. 3.5A**). We performed a dose response experiment and observed increased HO-1 expression in response to 10uM CoPP 12h post-treatment (**Fig. 3.5B**). HO-1 expression continued to increase 24h and 48h post-treatment with 10uM CoPP. 1uM CoPP increased HO-1 expression 24h and 48h post-treatment albeit to a lower degree than 10uM CoPP, while 100nM CoPP was not sufficient to increase HO-1 expression in HBMECs. We next attempted to genetically manipulate HO-1 expression in HBMECs with siRNAs, using the same Lipofectamine protocol we had used in hCMEC/D3 cells. However, Lipofectamine delivery of siRNAs was ineffective in HBMECs, regardless of siRNA concentration, plating density of cells, and well coating used (data not shown). Using electroporation for delivery instead, we successfully knocked down and increased HO-1 expression using siRNAs against HO-1 and BACH1, respectively (**Fig. 3.5C**).

Pro-inflammatory cytokines increase endothelial adhesion molecule expression in HBMECs

We next sought to determine whether HO-1 knockdown or induction would impact inflammation-driven adhesion and transendothelial migration in HBMECs. We first determined expression of endothelial adhesion molecules (VCAM-1, ICAM-1) in response to TNFα or IFNγ (**Fig. 3.6A-D**). Both VCAM-1 and ICAM-1 expression increased in a dose-dependent manner in response to TNFα, while only ICAM-1 expression increased in response to IFNγ (quantified in **Fig. 3.6C-D**). Next, we determined adhesion molecule expression in response to TNFα treatment in HBMECs

pre-transfected with siRNAs to manipulate HO-1 expression. siRNAs against either HO-1 or BACH1 were delivered to HBMECs by electroporation. After 24h, cells were exposed to 1 or 10ng/mL TNFα for another 24h after which we measured HO-1, VCAM-1, and ICAM-1 expression (**Fig. 3.6E-G**). VCAM-1 and ICAM-1 expression were both increased in cells treated with TNFα compared to untreated controls, as expected. However, there was no difference in adhesion molecule induction between siRNA conditions. We confirmed HO-1 induction in cells electroporated with siRNA against BACH1, however, at 48h post-transfection (time of lysate collection), this effect was modest (**Fig. 3.6E**), and the level of HO-1 induction may not have been sufficient to prevent adhesion molecule expression in response to TNFα.

HBMEC tri-culture blood-brain barrier model recapitulates cytokine-induced transendothelial migration of monocytes

Finally, we modeled transendothelial migration in a transwell system exclusively using primary human cells (**Fig. 3.7A**). We seeded human fetal astrocytes to the underside and HBMEC to the top side of 3.0 um PET membrane inserts to model the interaction of astrocytes and endothelial cells at the BBB. With the monolayer established, we added purified human monocytes to the upper chamber and CCL2 to the lower chamber (**Fig. 3.1B)**. After 24h of incubation, we observed a robust increase in monocyte migration to the lower chamber in preparations with CCL2 in the lower chamber (**Fig. 3.7B-C**). However, we observed no differences in permeability to 70kDa FITC-dextran post-migration in any condition (**Fig. 3.7D)**, suggesting that *i)* CCL2 did not disrupt the HBMEC monolayer and *ii)* monocytes migrated through diapedesis along the chemotactic gradient.

3.5 Discussion

Based on our prior work suggesting HO-1 loss as a risk for HIV NCI and literature describing the protective effect of HO-1 in endothelial cell function, we sought to determine the role for endothelial HO-1 expression in BBB functions in HIV infection. We evaluated the feasibility of specifically

manipulating HO-1 expression and modeling BBB functions in two *in vitro* brain endothelial models: the hCMEC/D3 cell line and primary human brain microvascular endothelial cells (HBMECs).

Both hCMEC/D3 cells and HBMECs demonstrated robust induction of HO-1 expression when exposed to CoPP, confirming that while basal endothelial HO-1 expression is low, its inducibility is similar to what we have observed in monocyte-derived macrophages (36). In hCMEC/D3 cells, we also observed increased HO-1 expression with ARE inducers DMF and MMF, as well as IFNβ. These data are relevant to future *in vitro* and *in vivo* experiments targeted toward exploring HO-1 inducers as adjunctive therapy in HIV infection; each is FDA-approved for treatment of multiple sclerosis (243-245). HO-1 induction by DMF and MMF through transcription factor Nrf2 is well-established in other cell types, including monocyte-derived macrophages and astrocytes (167, 246-248). Our results are consistent with data from Lim et al. showing HO-1 induction in response to MMF that was accompanied by decreased expression of adhesion molecules and transendothelial monocyte migration (216). We speculate that exposure of hCMEC/D3 cells to DMF and MMF would similarly limit transendothelial migration of HIV-infected CD4+ T cells.

IFNβ also supports BBB function by limiting adhesion molecule expression and tight junction destabilization in response to pro-inflammatory stimuli (240). The role for HO-1 in IFNβ-mediated BBB function has been explored in the context of multiple sclerosis, with conflicting results. HO-1 expression in the CNS is increased in multiple sclerosis, but whether this is protective or pathologic is unclear. In one study, PBMCs from patients with exacerbated disease had decreased HO-1 expression, and IFNβ administration surprisingly correlated with HO-1 reduction. However, here, we demonstrate modest induction of HO-1 expression in hCMEC/D3 cells with IFNβ exposure. HO-1 has also been shown to regulate IFNβ production (249, 250), suggesting bi-directionality and potential feedback regulation within this relationship.

Specific modulation of HO-1 without off-target effects introduced using pharmacologic or immunologic agents is required to define the role for HO-1 in endothelial cell functions. We established reliable induction and knockdown of HO-1 expression using siRNA in both hCMEC/D3 cells and HBMECs. In hCMEC/D3 cells, we were able to apply the Lipofectamine RNAiMax protocol that we have previously used successfully in primary human monocyte-derived macrophages and primary human fetal astrocytes to knock down HO-1 using siRNA directly targeting HO-1, and to induce it by targeting its transcriptional suppressor BACH1 (36, 215) (Kovacsics et al., unpublished). Effects of siRNA manipulation of HO-1 expression were long-lasting, over the course of several days. These data are a useful tool for future experiments involving HO-1 in hCMEC/D3 cells.

In HBMECs, however, siRNA delivery was more challenging. In experiments not shown here, we attempted to deliver siRNAs to HBMECs using Lipofectamine under many variable conditions: increased concentration of siRNA, decreased plating density of cells, alternative plate coating materials, and alternative media formulations. None of these adjustments were sufficient to facilitate siRNA delivery by Lipofectamine. Gresch and Altrogge described the challenges of transfecting primary cells, and detailed efficient transfection of human umbilical vein endothelial cells by electroporation instead (251). Similarly, Slanina et al. demonstrated that transfection with the Nucleofector II system from Lonza yielded significantly greater transfection efficiency compared to Lipofectamine and other similar transfection methods (234). We, too, had success using the Amaxa Nucleofector II system, with appreciable knockdown and induction of HO-1 24h post-transfection in HBMECs. However, in contrast to our results in hCMEC/D3 cells, our data temper expectations for future experiments specifically manipulating HO-1 in HBMECs. First, electroporation is considerably toxic (approximately 50%). Second, HO-1 knockdown and induction did not extend beyond 24h post-transfection (data not shown). Finally, the effects of siRNAs on HO-1 expression were more modest than we have observed in hCMEC/D3s and monocyte-derived macrophages. Thus, the window of time in which experiments can be done with certainty that HO-

1 is either induced or knocked down is relatively short, and the quantity of cells available in each preparation is limited. Indeed, against our hypothesis, HO-1 manipulation did not impact adhesion molecule expression in response to TNFα. We speculate that the modesty of HO-1 knockdown and induction by siRNA in HBMECs is the reason for these negative data. For more permanent HO-1 manipulation in HBMECs that will generate ample cells for experiments, lentiviral transduction might be considered.

In addition to manipulating endothelial HO-1 expression, we sought to model key endothelial cell functions, including regulation of tight junction permeability and transendothelial migration of monocytes. We used an assay measuring endothelial monolayer permeability to 70kDa FITC-Dextran to evaluate tight junction integrity in both hCMEC/D3 cells and HBMECs. In hCMEC/D3 cells, we sought to increase monolayer impermeability by exposing cells to pro-inflammatory cytokines (TNFα or IFNγ), as others have demonstrated (241). Based on data from Forster et al. describing that hydrocortisone inhibits pro-inflammatory effects of TNFα and IFNγ in hCMEC/D3 cells (242), we eliminated hydrocortisone from the media. Still, exposure to neither TNFα nor IFNγ consistently increased hCMEC/D3 cell monolayer permeability in our hands. Similarly, manipulation of HO-1 expression did not significantly impact hCMEC/D3 cell monolayer permeability. When we combined these techniques and transfected hCMEC/D3 cells prior to exposure to TNFα, our results suggested that HO-1 induction may protect against TNFα-induced permeability (**Figure 3**). However, these data are difficult to interpret because exposure to TNFα did not consistently increase hCMEC/D3 cell monolayer permeability, suggesting that this model may not recapitulate *in vivo* barrier properties that had been previously reported (241). Ultimately, these data led us to use this permeability assay to confirm monolayer integrity as opposed to as a functional readout.

Finally, and perhaps most importantly, we sought to model transendothelial migration of monocytes in both hCMEC/D3 cells and in HBMECs in co-culture with primary human fetal astrocytes. In each,

we successfully modeled enhanced monocyte transmigration in response to CCL2, as has been previously demonstrated (237). Due to the efficiency of siRNA transfection achievable in hCMEC/D3 cells, this model would be ideal for determining the role for endothelial HO-1 in modulating transendothelial migration of monocytes. The HBMEC co-culture model, on the other hand, would be ideal for determining the role of astrocytic HO-1 in this context, as we have previously demonstrated efficient siRNA transfection via Lipofectamine in primary human fetal astrocytes (Kovacsics et al., unpublished). We also demonstrated increased adhesion molecule expression in response to TNFα and IFNγ in HBMECs. Given these data, we expect that exposure to TNFα and IFNγ would enhance transendothelial migration of monocytes and potentially CD4+ T cells in each model (252). These proof-of concept experiments pave the way for future studies measuring transendothelial migration HIV-infected CD4+ T cells.

3.6 Figures

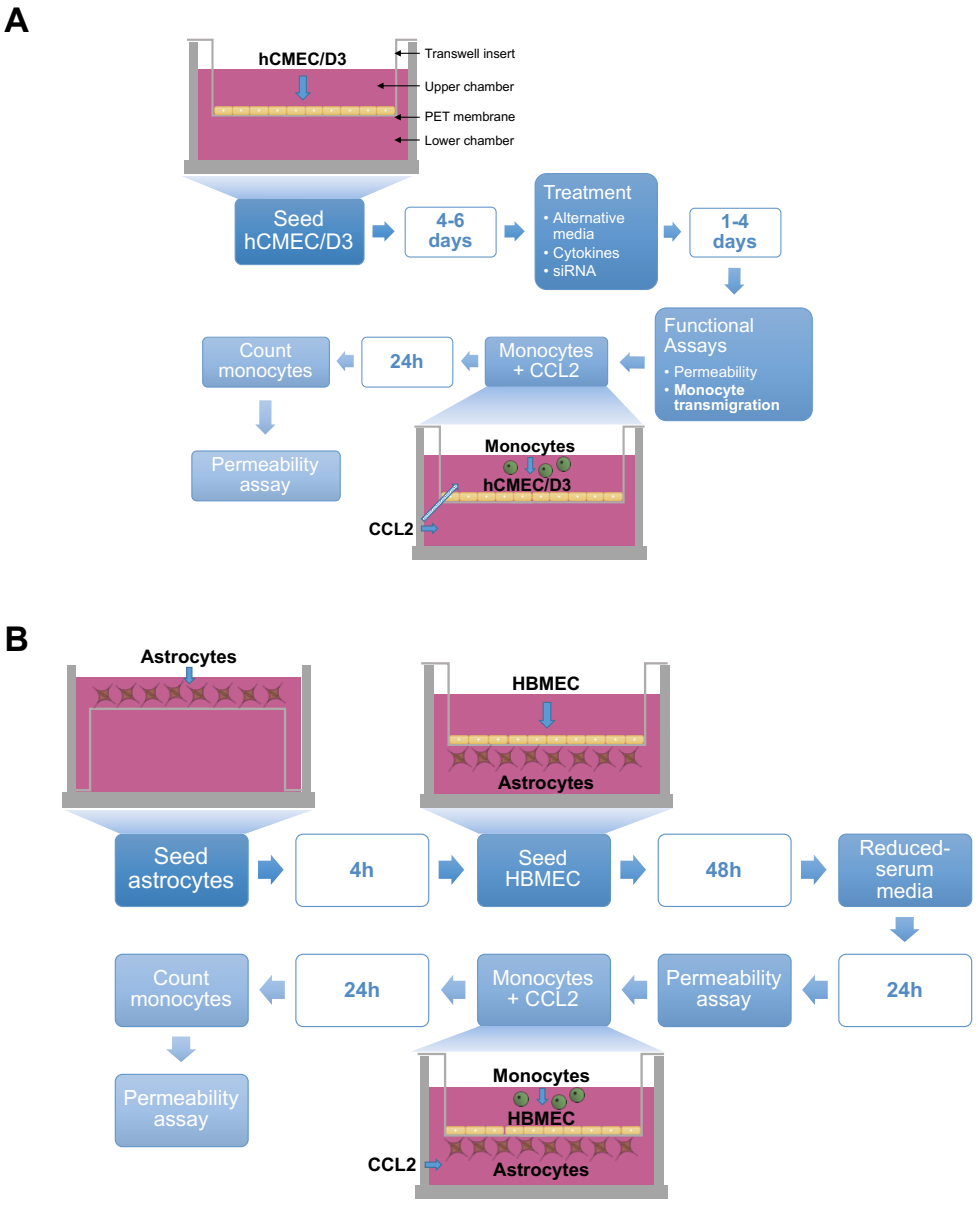

Figure 3.1 Functional modeling of the blood-brain barrier using a transwell system

(A) Schematic illustrating processes used to evaluate blood-brain barrier functions in hCMEC/D3 cells. **(B)** Schematic illustrating processes used to evaluate blood-brain barrier functions in tri-culture of HBMECs, HFAs, and monocytes.

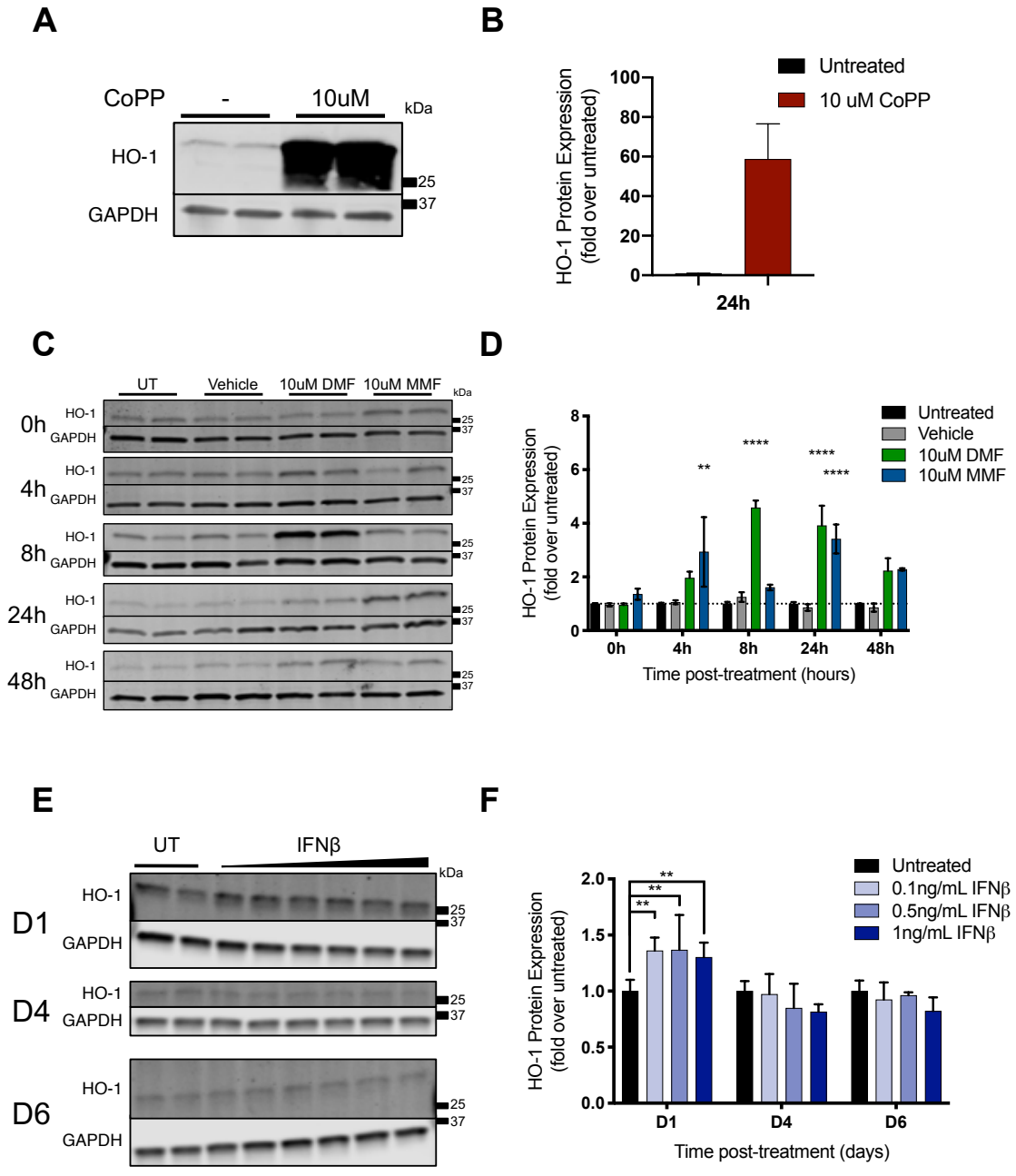

Figure 3.2 HO-1 responds predictably to pharmacologic manipulation in hCMEC/D3 cells

(A) Representative Western blot of hCMEC/D3 cell lysates collected 24h after exposure to 10uM CoPP. **(B)** HO-1 expression was determined by densitometry analysis normalized to GAPDH (n=2). **(C)** Representative Western blot of hCMEC/D3 cell lysates after exposure to 10uM DMF or 10uM

MMF for 0h, 4h, 8h, 24h, or 48h. **(D)** HO-1 expression was determined by densitometry analysis normalized to GAPDH (n=3). **(E)** Representative Western blot of hCMEC/D3 exposed to 0.1ng/mL, 0.5ng/mL, or 1ng/mL IFNβ for 1, 4, or 6 days. **(F)** HO-1 expression was determined by densitometry analysis normalized to GAPDH (n=2). Statistical comparisons to untreated were made by 2-way ANOVA with Holm-Sidak post hoc test for multiple comparisons. *p<0.05, **p<0.01, ***p<0.001, ****p<0.0001

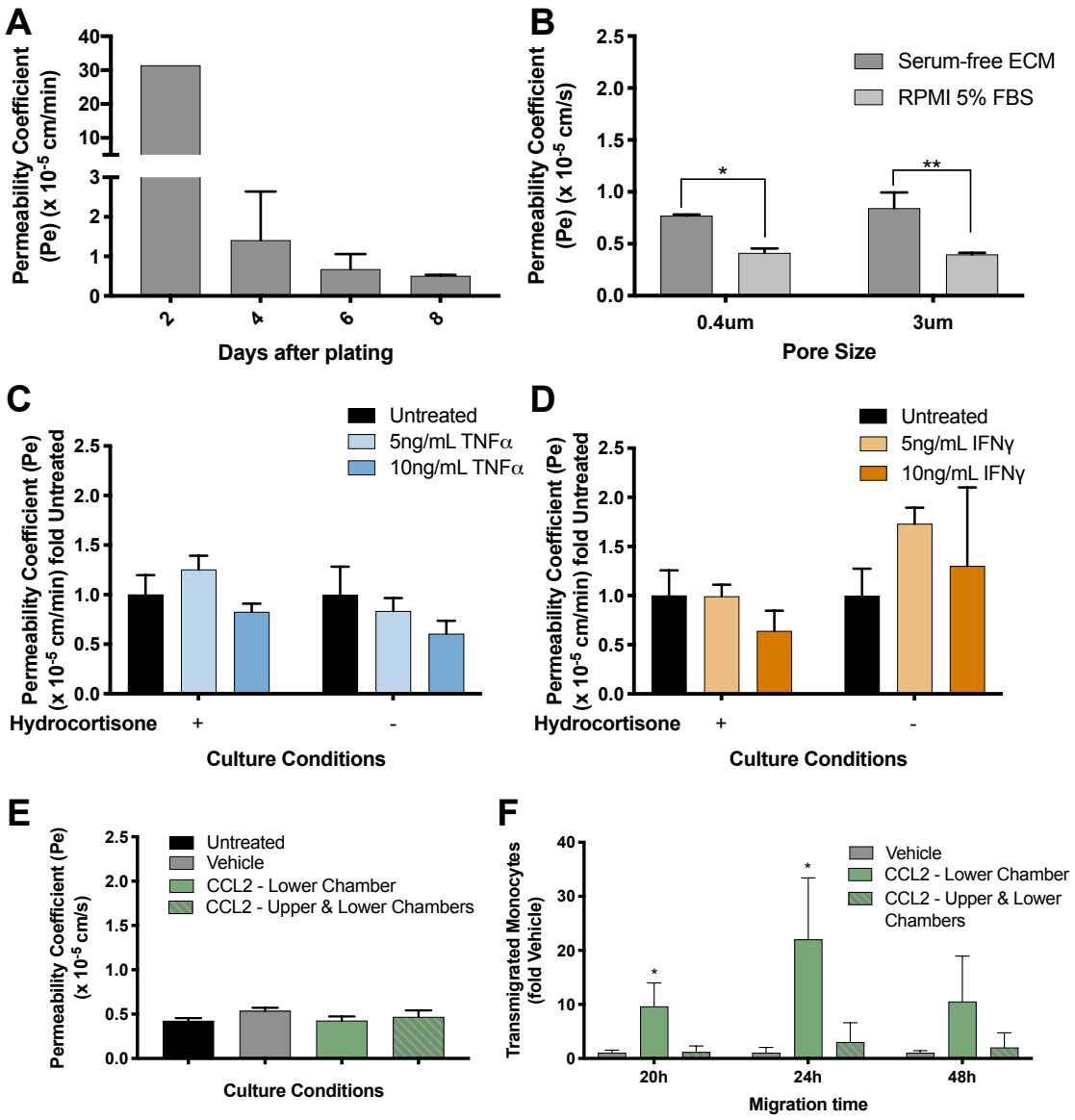

Figure 3.3 hCMEC/D3 cell blood-brain barrier model recapitulates cytokine-induced monocyte chemotaxis, but not barrier permeability

(A) hCMEC/D3 cells were seeded onto 0.4um-pore PET inserts and permeability was determined 2, 4, 6, or 8 days after plating (n=1-2). **(B)** hCMEC/D3 cells were seeded onto 0.4um- or 3.0um-pore PET inserts and transferred to either serum-free endothelial cell media or RPMI with 5% FBS for 24h before permeability assay. Statistical comparisons were made by two-way ANOVA with

Holm-Sidak post hoc test for multiple comparisons (n=2). **(C)** hCMEC/D3 cells seeded to 0.4um-pore PET inserts in ECM media with or without hydrocortisone were exposed to 5ng/mL or 10ng/mL TNFα for 24h prior to permeability assay. **(D)** hCMEC/D3 cells seeded to 0.4um-pore PET inserts in ECM media with and without hydrocortisone were exposed to 5ng/mL or 10ng/mL IFNγ for 24h prior to permeability assay. **(E)** hCMEC/D3 cells seeded to 0.4um-pore PET inserts in ECM media with and without hydrocortisone were exposed to vehicle (0.1% BSA) or 200ng/mL CCL2 24h prior to permeability assay. **(C, D, E)** Statistical comparisons in each culture condition to untreated were made by one-way ANOVA with Holm-Sidak post-hoc test for multiple comparisons (n=2-4). **(F)** Vehicle (0.1% BSA) or 200ng/mL CCL2 were added concurrently with monocytes to the indicated chambers. Monocytes in the lower chamber were counted after 20h, 24h, or 48h. Statistical comparisons to vehicle at each time point were made by one-way ANOVA with Holm-Sidak post-hoc test for multiple comparisons (n=3-4). *$p<0.05$, **$p<0.01$, ***$p<0.001$, ****$p<0.0001$

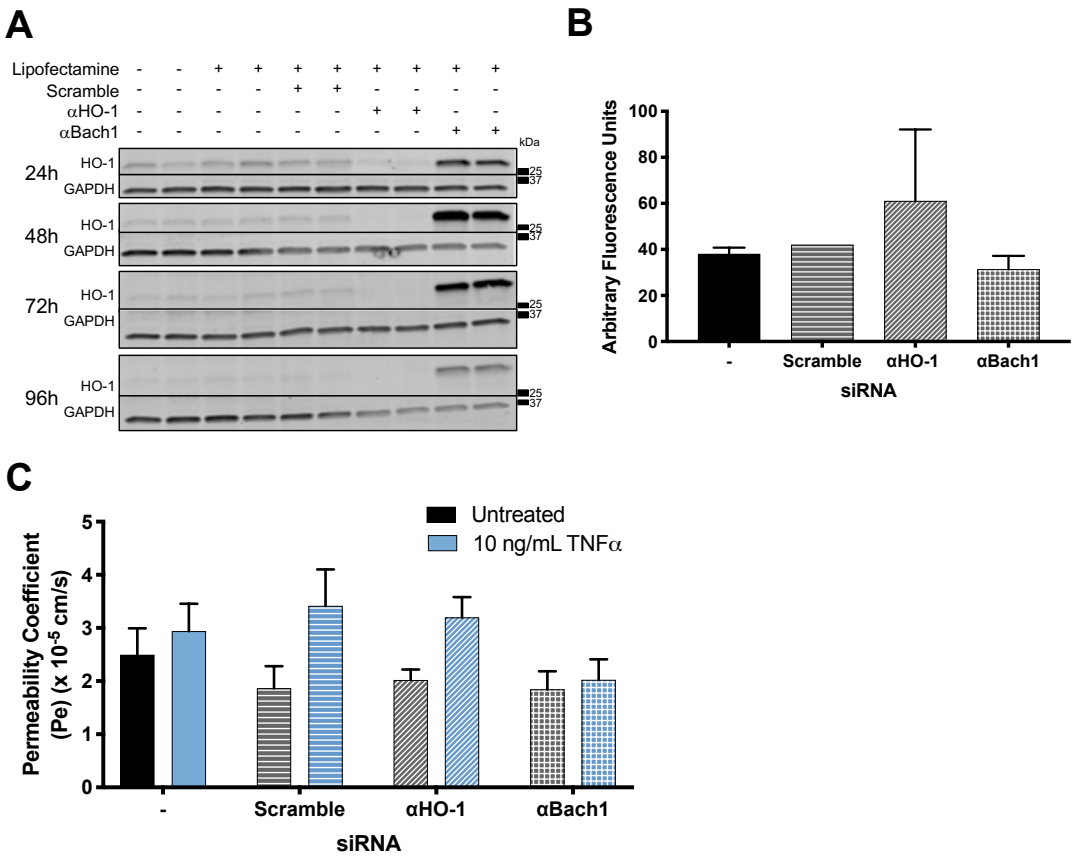

Figure 3.4 Genetic manipulation of HO-1 may prevent inflammation-induced permeability in hCMEC/D3 cells

(A) Representative Western blot of hCMEC/D3 cell lysates collected 24-96h after transfection with siRNA targeting HO-1 or BACH1. **(B)** Permeability assay was performed 72h post-transfection. Statistical comparisons to scramble were made by one-way ANOVA with Holm-Sidak post-hoc test for multiple comparisons (n=2). **(C)** 48h after siRNA transfection, hCMEC/D3 cells were exposed to 10ng/mL TNFα for 24h, followed by permeability assay. Statistical comparisons to untreated were made by two-way ANOVA with Holm-Sidak post-hoc test for multiple comparisons (n=2). *p<0.05, **p<0.01, ***p<0.001, ****p<0.0001

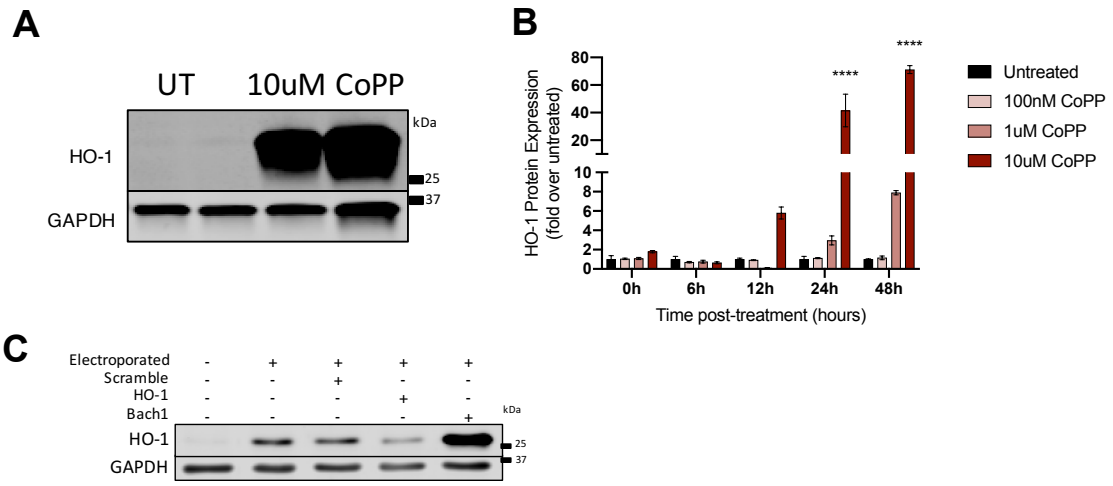

Figure 3.5 Primary human brain microvascular endothelial cells express HO-1 in response to pharmacologic and genetic manipulation

(A) Representative Western blot of HBMEC lysates collected 24h after exposure to 10uM CoPP. **(B)** Quantification of Western blot of HBMECs treated with 100nM, 1uM, or 10uM CoPP for 0h-48h. HO-1 expression was determined by densitometry analysis normalized to GAPDH. Statistical comparisons to untreated were made by 2-way ANOVA with Holm-Sidak post-hoc test for multiple comparisons, n=2. **(C)** Representative Western blot of HBMEC lysates collected 24h after electroporation with siRNA targeting HO-1 or BACH1. *p<0.05, **p<0.01, ***p<0.001, ****p<0.0001

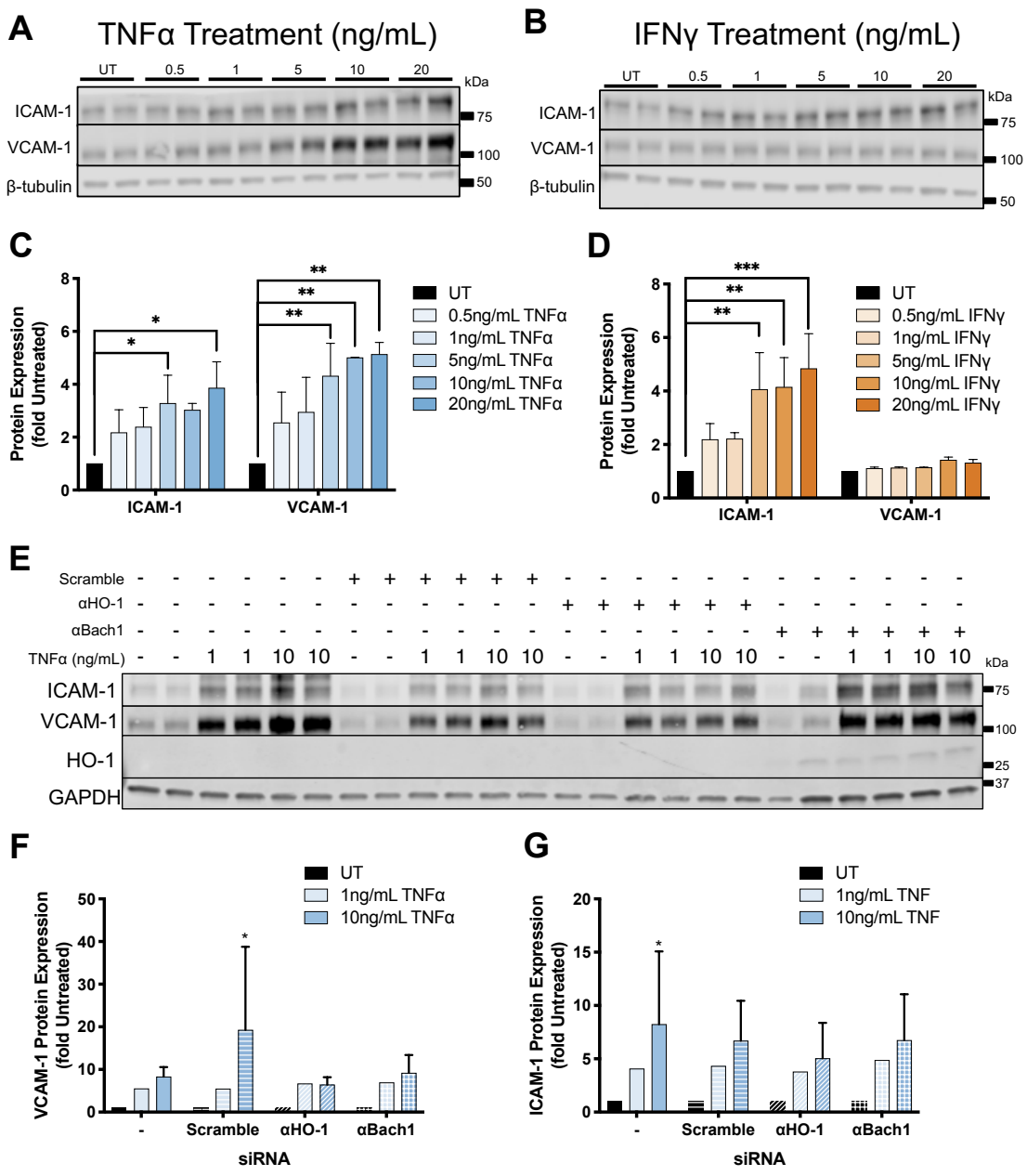

Figure 3.6 Pro-inflammatory cytokines increase endothelial adhesion molecule expression in HBMECs

(A) Representative Western blot of HMBEC lysates collected 24h after exposure to 0.5-20ng/mL TNFα or **(B)** IFNγ. **(C-D)** ICAM-1 and VCAM-1 expression were determined by densitometry analysis normalized to β-tubulin. Statistical comparisons to untreated were made by repeated

measures two-way ANOVA with Holm-Sidak post-hoc test for multiple comparisons (n=2). **(E)** Representative Western blot HBMEC lysates collected 24h after electroporation with siRNA targeting HO-1 or BACH1, followed by 24h exposure to 1 or 10ng/mL TNFα. **(F)** ICAM-1 and **(G)** VCAM-1 expression were measured by densitometry analysis normalized to GAPDH. Statistical comparisons to untreated were made by mixed-effects analysis with Holm-Sidak post-hoc test for multiple comparisons (n=1-3). *p<0.05, **p<0.01, ***p<0.001, ****p<0.0001

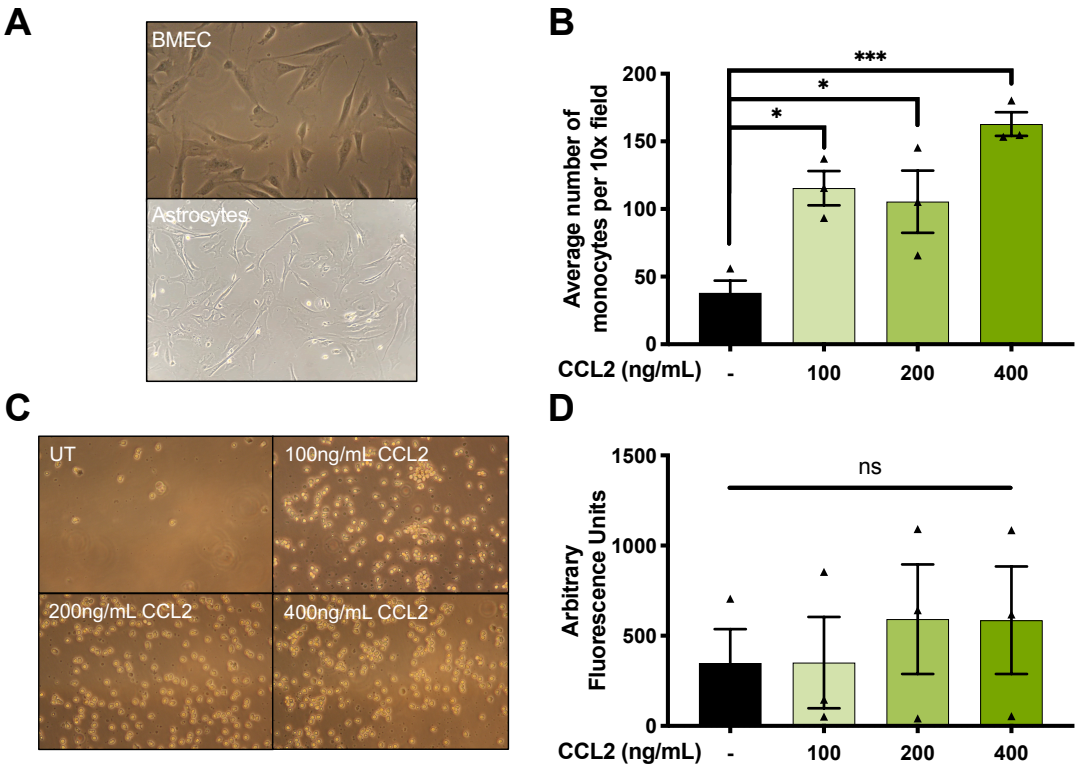

Figure 3.7 HBMEC tri-culture blood-brain barrier model recapitulates cytokine-induced transendothelial migration of monocytes

(A) Phase-contrast images of HBMECs and human fetal astrocytes (HFAs). **(B)** Monocyte transmigration assay was performed as described in Fig. 3.1B with 100-400ng/mL CCL2 in the lower chamber throughout the 24h migration period. **(D)** Phase-contrast images of representative 10x fields from each of the conditions in **(C)**. **(E)** Permeability of HBMEC-HFA monolayers was determined after the transmigration period. Statistical comparisons to untreated were made by one-way ANOVA with Holm-Sidak post-hoc test for multiple comparisons (n=3). *p<0.05, **p<0.01, ***p<0.001, ****p<0.0001

CHAPTER 4: Conclusions and Future Directions

The introduction of combination antiretroviral therapy (cART) has profoundly altered the prognosis associated with HIV infection, extending the life expectancy for persons living with HIV (PLWH) to nearly as long as that of HIV-negative population (1). Still, PLWH experience significant comorbidities to HIV infection, including HIV NCI, which associates with persistent inflammation and oxidative stress. In previous work, we have defined a novel role for antioxidant enzyme HO-1 in the pathogenesis of HIV NCI by identifying its deficiency in prefrontal cortex of individuals with HIV NCI. Building upon this study, we analyzed the distribution of genotypes for the $(GT)_n$ dinucleotide repeat polymorphism in PLWH stratified by CNS disease parameters. We found that shorter repeat length alleles associated with decreased risk for both HIV-encephalitis and HIV NCI (36, 114, 115). Short repeat length alleles associate with higher basal expression and inducibility of HO-1 in multiple cell types (90, 91). Together, these data suggest that individuals with shorter repeat length alleles, through relatively greater HO-1 expression and induction, have a greater antioxidant capacity that benefits disease outcomes *including* HIV NCI. These *ex vivo* findings are supported by *in vitro* studies demonstrating supernatant neurotoxicity of HIV-infected monocyte-derived macrophage associated with HO-1 deficiency, as well as post-translational degradation of HO-1 by the immunoproteasome in astrocytes chronically exposed to HIV-associated inflammatory cytokine IFNγ (36, 104). In the current work, we sought to develop our understanding of the role for HO-1 in HIV NCI in several areas not yet fully addressed: *i)* whether the HO-1 response to HIV infection is consistent throughout the brain; *ii)* how HO-1 expression relates to neuroinflammation in PLWH *without* HIV NCI; and *iii)* how HO-1 expression impacts brain microvascular endothelial cell (BMEC) and blood-brain barrier (BBB) functions in the context of HIV infection.

In the study described in Chapter 2, we established that HO-1 protein expression is stable or increased throughout the brain in PLWH without HIV NCI. This result is consistent with our previous study in prefrontal cortex, which found that prefrontal cortex HO-1 protein in PLWH without HIV NCI was not significantly different from HIV-negative individuals, but was significantly *higher* than in PLWH with HIV NCI (36). The reasons why HO-1 expression is higher in PLWH without HIV NCI

than in those with HIV NCI are unclear, although our prior studies suggest that the loss of HO-1 may be explained by immunoproteasome-mediated degradation in a subset of PLWH. We and others have reported elevated immunoproteasome expression and interferon responses in brains of PLWH irrespective of the concurrent diagnosis of HIV NCI (46, 105, 253). However, our subsequent study showed those with HIV NCI, HO-1 protein was low and this suggested that IFN-driven immunoproteasome expression enhances degradation of HO-1 protein in those individuals who develop HIV NCI, accounting for the discordance observed between brain HO-1 protein and RNA in those individuals (104). In this current study of PLWH without HIV NCI, we observed a positive association between brain HO-1 protein and RNA expression, despite elevated type I IFN-stimulated gene and immunoproteasome expression. The lower HO-1 protein expression in those with HIV NCI may reflect a threshold of immunoproteasome induction required for HO-1 degradation that is achieved only in PLWH who develop HIV NCI. Nonetheless, it is possible that mechanisms involved in HO-1 loss are triggered by duration of HIV infection or other unidentified, independent factors. Our data identified distinct regional patterns of neuroinflammation in brains of PLWH without HIV NCI. Posterior cingulate cortex, cerebellum, and globus pallidus each had higher immunoproteasome subunit and interferon-stimulated gene expression in PLWH compared to HIV-negative individuals. We believe that these data indicate a proclivity towards HIV-induced neuroinflammation in these regions, and HIV-induced abnormalities have been identified by others in each (147, 186, 198, 204).

PLWH in this cohort did not have HIV NCI, nor did any of these regions have altered expression of synaptic markers. However, there still may be functional consequences to such changes. In a preliminary analysis following up this study, we observed an association between poorer executive function and higher PCC MX1 expression (neuroinflammation) in this cohort of PLWH (**Fig. 4.1**).

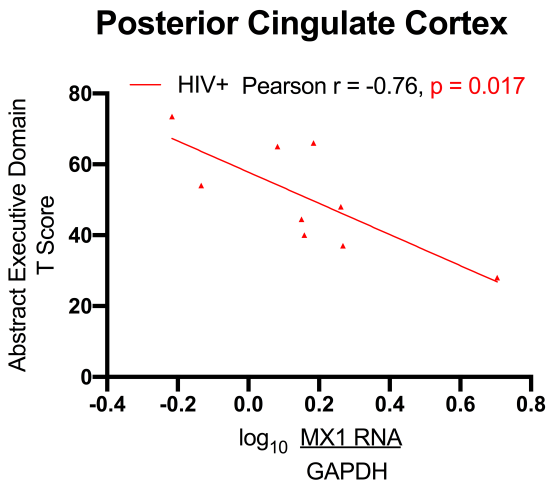

Figure 4.1 Higher IFN-stimulated gene MX1 expression in posterior cingulate cortex associates with poorer executive function in PLWH

Neurocognitive evaluation to determine assess performance in domains including executive functioning was performed by a neuropsychologist approximately 6 months before death. Test results were transformed to age-education-corrected scores (T scores) (254). MX1 RNA expression was measured by RT-qPCR. Associations between MX1 RNA expression and executive domain test T score were analyzed by Pearson's correlation with line of best fit by linear regression.

We recognize that the current cohort is underpowered to draw definitive conclusions from associations such as this. Prospective neuroimaging (MRS, PET) studies are more appropriate than post-mortem studies for analyses associating inflammatory biomarkers with neuropsychological testing performance, especially in the case of HIV NCI wherein the neurocognitive trajectory is not typically progressive (122). Longitudinal studies in which neuroimaging data collection and neuropsychological evaluation are temporally matched can more accurately define how potentially fluctuating local neuroinflammation can impact cognition (255). Nonetheless, our data are consistent with another report describing inflammation in the PCC that associates with poorer executive function in PLWH (147).

In this study, we also sought to determine the significance of brain regional variation of HO-1 expression in PLWH. Given the evidence for differential regional expression of HO-1 in the human

brain (164), we hypothesized that regions expressing lower HO-1 would be more vulnerable to HIV-mediated inflammation or neuronal damage. While we did observe statistically significant variation of HO-1 expression by brain region, regions with distinct neuroinflammation (posterior cingulate cortex, globus pallidus, and cerebellum) did not have consistently higher or lower HO-1 expression levels relative to the rest of the brain. These results do not necessarily rule out our original hypothesis. We previously showed that PLWH with HIV encephalitis have reduced HO-1 expression in the striatum (caudate) in addition to prefrontal cortex, but not the occipital cortex or cerebellum, suggesting that HIV NCI-associated HO-1 deficiency is regionally specific (36). However, these regions were not compared to one another, so their relative expression of HO-1 is unknown. It is possible that in PLWH with HIV NCI and deficient HO-1, those regions with lower HO-1 expression are more vulnerable to HIV-mediated inflammation and injury due to an insufficient antioxidant response. A future study including matched groups of HIV-negative individuals, PLWH without HIV NCI, and PLWH with confirmed HIV NCI in key brain regions identified here would more clearly define *i)* implications of regional differences in HO-1 expression in PLWH with and without HIV NCI; and *ii)* how HO-1 expression compares between PLWH with and without HIV NCI in each region.

The consequences of altered brain HO-1 expression in PLWH remain to be determined, and important relationships are suggested. We previously linked low HO-1 expression in the brain to HIV NCI, and low HO-1 expression in human macrophages to neurotoxin production, which could result in neuronal injury and dysfunction (36, 166). In this work, we extended observations to demonstrate increased expression of endothelial adhesion molecules (ICAM-1, PECAM-1, and VCAM-1) in PLWH and without HIV NCI compared to HIV-negative individuals, and associations with HO-1 expression. We speculate that this increase of endothelial adhesion molecules promotes increased adhesion and migration of immune cells through the blood-brain barrier, which could promote local inflammation. The clustering of ICAM-1 and VCAM-1 at the apical surface of endothelial cells and facilitation of leukocyte adhesion prior to diapedesis is well known (207).

Increased expression of ICAM-1 precedes transendothelial migration in ischemic stroke (209), and the duration and intensity of ICAM-1 expression not only promotes migration but also mediates the route of migration (210). Similarly, VCAM-1 is upregulated and facilitates migration of antigen-presenting cells into the CNS during viral infection (211). However, although PECAM-1 expression is not consistently increased during inflammation, its localization to tight junctions is, and this supports transendothelial diapedesis of cells (256).

Notably, our data indicate that HO-1 expression also associates positively with endothelial cell adhesion molecule expression in HIV-infected brain, and this suggests functional consequences. We suspect that this positive association, along with the higher levels of endothelial cell adhesion molecules in PLWH compared to HIV-negative individuals, represents the independent induction of each by HIV infection, but modulating effects of HO-1 on endothelial cell adhesion molecule expression are possible. Among endothelial cell functions, transendothelial immune cell adhesion and migration can be modulated by HO-1; HO-1 induction decreases monocyte transmigration in response to oxidized LDL in human aortic endothelial cells (257) and HO-1 induction in human umbilical vein endothelial cells before exposure to IFNγ reduces T-cell adhesion (258). Astrocytic HO-1 expression may mediate endothelial cell function through secreted factors (259). Additional *in vitro* analyses are required to model and define mechanisms by which HO-1 expression might also modulate endothelial cell function in HIV-infected brain.

We have shown that HO-1 protein expression throughout the brain in PLWH without NCI is comparable to or higher than that in HIV-negative individuals, in contrast to lower brain HO-1 protein levels in PLWH with NCI observed in our prior studies. This finding, coupled with our previous *in vitro* and *in vivo* studies demonstrating a strong protective effect of HO-1 on HIV-associated neuronal injury, neuroinflammation, and neurocognitive impairment suggest that maintaining, or even increasing, brain HO-1 expression in PLWH may delay or even prevent the development of these HIV-associated pathologies. We speculate that targeting the transcriptional

regulation of HO-1 or post-translational degradation of HO-1 offer therapeutic opportunities for neuroprotection against HIV.

One useful class of HO-1-inducing drugs that penetrate into the CNS is the class of fumaric acid esters, namely dimethyl fumarate (DMF) and its primary *in vivo* metabolite monomethyl fumarate (MMF). Oral DMF, formulated as the FDA-approved drug, Tecfidera, is now commonly used for effective treatment of multiple sclerosis, a disease characterized by neuroinflammation and oxidative stress (260, 261). Just this year, oral MMF has also been FDA-approved for multiple sclerosis treatment in the United States, under the proprietary name Bafiertam (262, 263). DMF and MMF induce HO-1 expression through activation of the Nrf2-dependent antioxidant response as well as inhibition of NF-kB signaling (reviewed in (264)). We have confirmed that DMF and MMF each induce HO-1 in HIV-infected human macrophages (36, 167) and human brain microvascular endothelial cells (HBMECs) (Chapter 3). Pre-treatment of HIV-infected macrophages with DMF or MMF significantly inhibits HIV infection and reduces neurotoxin production (167). Furthermore, DMF and MMF treatment of HIV-infected macrophages after HIV infection is established does not alter HIV replication, but does significantly reduce glutamate release and associated neurotoxicity, similar to other HO-1 inducing strategies (167). Additionally, DMF and MMF inhibit macrophage NF-κB nuclear translocation, decrease TNFα release, and reduce CCL2-mediated monocyte translocation (265), each of which could limit macrophage-mediated neuroinflammation in ART-treated individuals. Whether DMF and MMF support BBB function *in vivo* is controversial. Exposure of HBMECs to DMF *in vitro* supports tight junction integrity, and exposure of activated HBMECs to MMF reduced expression of VCAM-1 transendothelial migration of monocytes (266, 267). However, another *in vitro* study found that neither DMF nor MMF altered adhesion molecule expression or T cell adhesion to HBMECs (268). Furthermore, DMF treatment had no effect on structural tight junction protein claudin-5 expression in experimental autoimmune encephalomyelitis (EAE), a commonly used animal model for multiple sclerosis (269). Still, considerable evidence supports the study of HO-1 inducers such as DMF as adjunctive therapy in

ART-treated HIV-infected subjects to limit neuroinflammation, oxidative stress, blood-brain barrier disruption, and associated neurocognitive impairment. In a study in progress, we have treated rhesus macaques with DMF prior to infection with simian immunodeficiency virus (SIV). DMF-treated macaques had higher expression of Nrf2 antioxidant response element genes, including NQO1, GPX1, and a clear trend towards increased HO-1 expression although this was not statistically significant. Confirmation of induction of antioxidant response element genes in the brain to DMF within this model warrants further study.

Another candidate drug of interest for HO-1 induction is bardoxolone-methyl, a semi-synthetic triterpenoid that has been investigated for treatment of chronic kidney disease and some cancers. Similar to DMF and MMF, bardoxolone-methyl induces antioxidant response element proteins through activation of the Keap1/Nrf2 pathway and inhibition of NFκB nuclear translocation (270). Bardoxolone-methyl has also demonstrated antiviral effects, limiting replication of hepatitis B and C *in vitro* (271). In a model of ischemia reperfusion injury, treatment with bardoxolone-methyl decreased infarction volume and improved neurological symptoms after injury (272). Further study found that the protective effects of bardoxolone-methyl in this model were mediated in part by preventing BBB disruption, specifically through maintenance of tight junction molecule expression (273). In preliminary studies, we found that treatment of monocyte-derived macrophages with bardoxolone-methyl prior to HIV infection suppressed viral replication and limited supernatant neurotoxicity of HIV-exposed monocyte-derived macrophages. Further study of bardoxolone-methyl within HIV-infected monocyte derived macrophages and BBB models are required to determine its potential as an HO-1-modulating adjunctive therapy.

BIBLIOGRAPHY

1. Antiretroviral Therapy Cohort C. Survival of HIV-positive patients starting antiretroviral therapy between 1996 and 2013: a collaborative analysis of cohort studies. Lancet HIV. 2017;4(8):e349-e56.

2. (UNAIDS) JUNPoHA. 90-90-90 An ambitious treatment target to help end the AIDS epidemic. 2014 October, 2014.

3. Marsh K, Eaton JW, Mahy M, Sabin K, Autenrieth CS, Wanyeki I, et al. Global, regional and country-level 90-90-90 estimates for 2018: assessing progress towards the 2020 target. AIDS. 2019;33 Suppl 3:S213-S26.

4. Ghosn J, Taiwo B, Seedat S, Autran B, Katlama C. Hiv. Lancet. 2018;392(10148):685-97.

5. Kolson D. Neurologic Complications in Persons With HIV Infection in the Era of Antiretroviral Therapy. Top Antivir Med. 2017;25(3):97-101.

6. Budka H. Multinucleated giant cells in brain: a hallmark of the acquired immune deficiency syndrome (AIDS). Acta Neuropathol. 1986;69(3-4):253-8.

7. Budka H, Wiley CA, Kleihues P, Artigas J, Asbury AK, Cho ES, et al. HIV-associated disease of the nervous system: review of nomenclature and proposal for neuropathology-based terminology. Brain Pathol. 1991;1(3):143-52.

8. Vago L, Bonetto S, Nebuloni M, Duca P, Carsana L, Zerbi P, et al. Pathological findings in the central nervous system of AIDS patients on assumed antiretroviral therapeutic regimens: retrospective study of 1597 autopsies. AIDS. 2002;16(14):1925-8.

9. Saylor D, Dickens AM, Sacktor N, Haughey N, Slusher B, Pletnikov M, et al. HIV-associated neurocognitive disorder - pathogenesis and prospects for treatment. Nat Rev Neurol. 2016;12(5):309.

10. Gelman BB. Neuropathology of HAND With Suppressive Antiretroviral Therapy: Encephalitis and Neurodegeneration Reconsidered. Current HIV/AIDS reports. 2015;12(2):272-9.

11. Antinori A, Arendt G, Becker JT, Brew BJ, Byrd DA, Cherner M, et al. Updated research nosology for HIV-associated neurocognitive disorders. Neurology. 2007;69(18):1789-99.

12. Grant I, Franklin DR, Jr., Deutsch R, Woods SP, Vaida F, Ellis RJ, et al. Asymptomatic HIV-associated neurocognitive impairment increases risk for symptomatic decline. Neurology. 2014;82(23):2055-62.

13. Underwood J, De Francesco D, Leech R, Sabin CA, Winston A, Pharmacokinetic, et al. Medicalising normality? Using a simulated dataset to assess the performance of different diagnostic criteria of HIV-associated cognitive impairment. PLoS One. 2018;13(4):e0194760.

14. Jessen Krut J, Mellberg T, Price RW, Hagberg L, Fuchs D, Rosengren L, et al. Biomarker evidence of axonal injury in neuroasymptomatic HIV-1 patients. PLoS One. 2014;9(2):e88591.

15. Peterson J, Gisslen M, Zetterberg H, Fuchs D, Shacklett BL, Hagberg L, et al. Cerebrospinal fluid (CSF) neuronal biomarkers across the spectrum of HIV infection: hierarchy of injury and detection. PLoS One. 2014;9(12):e116081.

16. Gisslen M, Price RW, Andreasson U, Norgren N, Nilsson S, Hagberg L, et al. Plasma Concentration of the Neurofilament Light Protein (NFL) is a Biomarker of CNS Injury in HIV Infection: A Cross-Sectional Study. EBioMedicine. 2016;3:135-40.

17. Anderson AM, Easley KA, Kasher N, Franklin D, Heaton RK, Zetterberg H, et al. Neurofilament light chain in blood is negatively associated with neuropsychological performance in HIV-infected adults and declines with initiation of antiretroviral therapy. J Neurovirol. 2018;24(6):695-701.

18. Tambussi G, Gori A, Capiluppi B, Balotta C, Papagno L, Morandini B, et al. Neurological symptoms during primary human immunodeficiency virus (HIV) infection correlate with high levels of HIV RNA in cerebrospinal fluid. Clin Infect Dis. 2000;30(6):962-5.

19. Kamal S, Locatelli I, Wandeler G, Sehhat A, Bugnon O, Metral M, et al. The Presence of Human Immunodeficiency Virus-Associated Neurocognitive Disorders Is Associated With a Lower Adherence to Combined Antiretroviral Treatment. Open Forum Infect Dis. 2017;4(2):ofx070.

20. Calcagno A, Barco A, Trunfio M, Bonora S. CNS-Targeted Antiretroviral Strategies: When Are They Needed and What to Choose. Current HIV/AIDS reports. 2018;15(1):84-91.

21. McArthur JC, Johnson TP. Chronic inflammation mediates brain injury in HIV infection: relevance for cure strategies. Curr Opin Neurol. 2020;33(3):397-404.

22. Alford K, Vera JH. Cognitive Impairment in people living with HIV in the ART era: A Review. Br Med Bull. 2018;127(1):55-68.

23. Valcour VG, Ananworanich J, Agsalda M, Sailasuta N, Chalermchai T, Schuetz A, et al. HIV DNA reservoir increases risk for cognitive disorders in cART-naive patients. PLoS One. 2013;8(7):e70164.

24. Davis LE, Hjelle BL, Miller VE, Palmer DL, Llewellyn AL, Merlin TL, et al. Early viral brain invasion in iatrogenic human immunodeficiency virus infection. Neurology. 1992;42(9):1736-9.

25. Valcour V, Chalermchai T, Sailasuta N, Marovich M, Lerdlum S, Suttichom D, et al. Central nervous system viral invasion and inflammation during acute HIV infection. J Infect Dis. 2012;206(2):275-82.

26. Pilcher CD, Shugars DC, Fiscus SA, Miller WC, Menezes P, Giner J, et al. HIV in body fluids during primary HIV infection: implications for pathogenesis, treatment and public health. AIDS. 2001;15(7):837-45.

27. Sturdevant CB, Joseph SB, Schnell G, Price RW, Swanstrom R, Spudich S. Compartmentalized replication of R5 T cell-tropic HIV-1 in the central nervous system early in the course of infection. PLoS Pathog. 2015;11(3):e1004720.

28. Spudich S, Gisslen M, Hagberg L, Lee E, Liegler T, Brew B, et al. Central nervous system immune activation characterizes primary human immunodeficiency virus 1 infection even in participants with minimal cerebrospinal fluid viral burden. J Infect Dis. 2011;204(5):753-60.

29. Williams DW, Eugenin EA, Calderon TM, Berman JW. Monocyte maturation, HIV susceptibility, and transmigration across the blood brain barrier are critical in HIV neuropathogenesis. J Leukoc Biol. 2012;91(3):401-15.

30. Miner JJ, Diamond MS. Mechanisms of restriction of viral neuroinvasion at the blood-brain barrier. Curr Opin Immunol. 2016;38:18-23.

31. Hong S, Banks WA. Role of the immune system in HIV-associated neuroinflammation and neurocognitive implications. Brain Behav Immun. 2015;45:1-12.

32. Hawkins BT, Davis TP. The blood-brain barrier/neurovascular unit in health and disease. Pharmacol Rev. 2005;57(2):173-85.

33. Zhao Z, Nelson AR, Betsholtz C, Zlokovic BV. Establishment and Dysfunction of the Blood-Brain Barrier. Cell. 2015;163(5):1064-78.

34. Banks WA. The blood-brain barrier in neuroimmunology: Tales of separation and assimilation. Brain Behav Immun. 2015;44:1-8.

35. Wong ME, Jaworowski A, Hearps AC. The HIV Reservoir in Monocytes and Macrophages. Front Immunol. 2019;10:1435.

36. Gill AJ, Kovacsics CE, Cross SA, Vance PJ, Kolson LL, Jordan-Sciutto KL, et al. Heme oxygenase-1 deficiency accompanies neuropathogenesis of HIV-associated neurocognitive disorders. J Clin Invest. 2014;124(10):4459-72.

37. Guadalupe M, Reay E, Sankaran S, Prindiville T, Flamm J, McNeil A, et al. Severe CD4+ T-cell depletion in gut lymphoid tissue during primary human immunodeficiency virus type 1 infection and substantial delay in restoration following highly active antiretroviral therapy. J Virol. 2003;77(21):11708-17.

38. Klatt NR, Funderburg NT, Brenchley JM. Microbial translocation, immune activation, and HIV disease. Trends Microbiol. 2013;21(1):6-13.

39. Marchetti G, Tincati C, Silvestri G. Microbial translocation in the pathogenesis of HIV infection and AIDS. Clin Microbiol Rev. 2013;26(1):2-18.

40. Brenchley JM, Price DA, Douek DC. HIV disease: fallout from a mucosal catastrophe? Nat Immunol. 2006;7(3):235-9.

41. Brenchley JM, Price DA, Schacker TW, Asher TE, Silvestri G, Rao S, et al. Microbial translocation is a cause of systemic immune activation in chronic HIV infection. Nat Med. 2006;12(12):1365-71.

42. Veszelka S, Pasztoi M, Farkas AE, Krizbai I, Ngo TK, Niwa M, et al. Pentosan polysulfate protects brain endothelial cells against bacterial lipopolysaccharide-induced damages. Neurochem Int. 2007;50(1):219-28.

43. Logsdon AF, Erickson MA, Rhea EM, Salameh TS, Banks WA. Gut reactions: How the blood-brain barrier connects the microbiome and the brain. Exp Biol Med (Maywood). 2018;243(2):159-65.

44. Fiebig EW, Wright DJ, Rawal BD, Garrett PE, Schumacher RT, Peddada L, et al. Dynamics of HIV viremia and antibody seroconversion in plasma donors: implications for diagnosis and staging of primary HIV infection. AIDS. 2003;17(13):1871-9.

45. Gray F, Scaravilli F, Everall I, Chretien F, An S, Boche D, et al. Neuropathology of early HIV-1 infection. Brain Pathol. 1996;6(1):1-15.

46. Gelman BB, Chen T, Lisinicchia JG, Soukup VM, Carmical JR, Starkey JM, et al. The National NeuroAIDS Tissue Consortium brain gene array: two types of HIV-associated neurocognitive impairment. PLoS One. 2012;7(9):e46178.

47. Boven LA, Middel J, Verhoef J, De Groot CJ, Nottet HS. Monocyte infiltration is highly associated with loss of the tight junction protein zonula occludens in HIV-1-associated dementia. Neuropathol Appl Neurobiol. 2000;26(4):356-60.

48. Mollace V, Nottet HS, Clayette P, Turco MC, Muscoli C, Salvemini D, et al. Oxidative stress and neuroAIDS: triggers, modulators and novel antioxidants. Trends Neurosci. 2001;24(7):411-6.

49. de Quay B, Malinverni R, Lauterburg BH. Glutathione depletion in HIV-infected patients: role of cysteine deficiency and effect of oral N-acetylcysteine. AIDS. 1992;6(8):815-9.

50. Castagna A, Le Grazie C, Accordini A, Giulidori P, Cavalli G, Bottiglieri T, et al. Cerebrospinal fluid S-adenosylmethionine (SAMe) and glutathione concentrations in HIV infection: effect of parenteral treatment with SAMe. Neurology. 1995;45(9):1678-83.

51. Herzenberg LA, De Rosa SC, Dubs JG, Roederer M, Anderson MT, Ela SW, et al. Glutathione deficiency is associated with impaired survival in HIV disease. Proc Natl Acad Sci U S A. 1997;94(5):1967-72.

52. Andersson LM, Hagberg L, Fuchs D, Svennerholm B, Gisslen M. Increased blood-brain barrier permeability in neuro-asymptomatic HIV-1-infected individuals--correlation with cerebrospinal fluid HIV-1 RNA and neopterin levels. J Neurovirol. 2001;7(6):542-7.

53. Calcagno A, Romito A, Atzori C, Ghisetti V, Cardellino C, Audagnotto S, et al. Blood Brain Barrier Impairment in HIV-Positive Naive and Effectively Treated Patients: Immune Activation Versus Astrocytosis. J Neuroimmune Pharmacol. 2017;12(1):187-93.

54. Eden A, Price RW, Spudich S, Fuchs D, Hagberg L, Gisslen M. Immune activation of the central nervous system is still present after >4 years of effective highly active antiretroviral therapy. J Infect Dis. 2007;196(12):1779-83.

55. Roc AC, Ances BM, Chawla S, Korczykowski M, Wolf RL, Kolson DL, et al. Detection of human immunodeficiency virus induced inflammation and oxidative stress in lenticular nuclei with magnetic resonance spectroscopy despite antiretroviral therapy. Arch Neurol. 2007;64(9):1249-57.

56. Chaganti J, Marripudi K, Staub LP, Rae CD, Gates TM, Moffat KJ, et al. Imaging correlates of the Blood Brain Barrier disruption in HIV associated neurocognitive disorder and therapeutic implications. AIDS. 2019.

57. Avison MJ, Nath A, Greene-Avison R, Schmitt FA, Bales RA, Ethisham A, et al. Inflammatory changes and breakdown of microvascular integrity in early human immunodeficiency virus dementia. J Neurovirol. 2004;10(4):223-32.

58. Avison MJ, Nath A, Greene-Avison R, Schmitt FA, Greenberg RN, Berger JR. Neuroimaging correlates of HIV-associated BBB compromise. J Neuroimmunol. 2004;157(1-2):140-6.

59. Wolf K, Tsakiris DA, Weber R, Erb P, Battegay M, Swiss HIVCS. Antiretroviral therapy reduces markers of endothelial and coagulation activation in patients infected with human immunodeficiency virus type 1. J Infect Dis. 2002;185(4):456-62.

60. Hill J, Rom S, Ramirez SH, Persidsky Y. Emerging roles of pericytes in the regulation of the neurovascular unit in health and disease. J Neuroimmune Pharmacol. 2014;9(5):591-605.

61. Krause BW, Wijtenburg SA, Holcomb HH, Kochunov P, Wang DJ, Hong LE, et al. Anterior cingulate GABA levels predict whole-brain cerebral blood flow. Neurosci Lett. 2014;561:188-91.

62. Ances BM, Sisti D, Vaida F, Liang CL, Leontiev O, Perthen JE, et al. Resting cerebral blood flow: a potential biomarker of the effects of HIV in the brain. Neurology. 2009;73(9):702-8.

63. Tao-Cheng JH, Nagy Z, Brightman MW. Tight junctions of brain endothelium in vitro are enhanced by astroglia. J Neurosci. 1987;7(10):3293-9.

64. Neuhaus J, Risau W, Wolburg H. Induction of blood-brain barrier characteristics in bovine brain endothelial cells by rat astroglial cells in transfilter coculture. Ann N Y Acad Sci. 1991;633:578-80.

65. Janzer RC, Raff MC. Astrocytes induce blood-brain barrier properties in endothelial cells. Nature. 1987;325(6101):253-7.

66. Alvarez JI, Dodelet-Devillers A, Kebir H, Ifergan I, Fabre PJ, Terouz S, et al. The Hedgehog pathway promotes blood-brain barrier integrity and CNS immune quiescence. Science. 2011;334(6063):1727-31.

67. Eugenin EA, Clements JE, Zink MC, Berman JW. Human immunodeficiency virus infection of human astrocytes disrupts blood-brain barrier integrity by a gap junction-dependent mechanism. J Neurosci. 2011;31(26):9456-65.

68. Cysique LA, Brew BJ. Vascular cognitive impairment and HIV-associated neurocognitive disorder: a new paradigm. J Neurovirol. 2019.

69. Ishii T, Itoh K, Takahashi S, Sato H, Yanagawa T, Katoh Y, et al. Transcription factor Nrf2 coordinately regulates a group of oxidative stress-inducible genes in macrophages. J Biol Chem. 2000;275(21):16023-9.

70. Friling RS, Bensimon A, Tichauer Y, Daniel V. Xenobiotic-inducible expression of murine glutathione S-transferase Ya subunit gene is controlled by an electrophile-responsive element. Proc Natl Acad Sci U S A. 1990;87(16):6258-62.

71. Nguyen T, Nioi P, Pickett CB. The Nrf2-antioxidant response element signaling pathway and its activation by oxidative stress. J Biol Chem. 2009;284(20):13291-5.

72. Baird L, Dinkova-Kostova AT. The cytoprotective role of the Keap1-Nrf2 pathway. Arch Toxicol. 2011;85(4):241-72.

73. Itoh K, Wakabayashi N, Katoh Y, Ishii T, Igarashi K, Engel JD, et al. Keap1 represses nuclear activation of antioxidant responsive elements by Nrf2 through binding to the amino-terminal Neh2 domain. Genes Dev. 1999;13(1):76-86.

74. de Freitas Silva M, Pruccoli L, Morroni F, Sita G, Seghetti F, Viegas C, et al. The Keap1/Nrf2-ARE Pathway as a Pharmacological Target for Chalcones. Molecules. 2018;23(7).

75. Linnenbaum M, Busker M, Kraehling JR, Behrends S. Heme oxygenase isoforms differ in their subcellular trafficking during hypoxia and are differentially modulated by cytochrome P450 reductase. PLoS One. 2012;7(4):e35483.

76. Alam J, Cook JL. How many transcription factors does it take to turn on the heme oxygenase-1 gene? Am J Respir Cell Mol Biol. 2007;36(2):166-74.

77. Lavrovsky Y, Schwartzman ML, Levere RD, Kappas A, Abraham NG. Identification of binding sites for transcription factors NF-kappa B and AP-2 in the promoter region of the human heme oxygenase 1 gene. Proc Natl Acad Sci U S A. 1994;91(13):5987-91.

78. Lee PJ, Jiang BH, Chin BY, Iyer NV, Alam J, Semenza GL, et al. Hypoxia-inducible factor-1 mediates transcriptional activation of the heme oxygenase-1 gene in response to hypoxia. J Biol Chem. 1997;272(9):5375-81.

79. Ricchetti GA, Williams LM, Foxwell BM. Heme oxygenase 1 expression induced by IL-10 requires STAT-3 and phosphoinositol-3 kinase and is inhibited by lipopolysaccharide. J Leukoc Biol. 2004;76(3):719-26.

80. Weis N, Weigert A, von Knethen A, Brune B. Heme oxygenase-1 contributes to an alternative macrophage activation profile induced by apoptotic cell supernatants. Mol Biol Cell. 2009;20(5):1280-8.

81. Igarashi K, Sun J. The heme-Bach1 pathway in the regulation of oxidative stress response and erythroid differentiation. Antioxid Redox Signal. 2006;8(1-2):107-18.

82. Ogawa K, Sun J, Taketani S, Nakajima O, Nishitani C, Sassa S, et al. Heme mediates derepression of Maf recognition element through direct binding to transcription repressor Bach1. EMBO J. 2001;20(11):2835-43.

83. Ishikawa M, Numazawa S, Yoshida T. Redox regulation of the transcriptional repressor Bach1. Free Radic Biol Med. 2005;38(10):1344-52.

84. Reichard JF, Sartor MA, Puga A. BACH1 is a specific repressor of HMOX1 that is inactivated by arsenite. J Biol Chem. 2008;283(33):22363-70.

85. Kimpara T, Takeda A, Watanabe K, Itoyama Y, Ikawa S, Watanabe M, et al. Microsatellite polymorphism in the human heme oxygenase-1 gene promoter and its application in association studies with Alzheimer and Parkinson disease. Hum Genet. 1997;100(1):145-7.

86. Ono K, Goto Y, Takagi S, Baba S, Tago N, Nonogi H, et al. A promoter variant of the heme oxygenase-1 gene may reduce the incidence of ischemic heart disease in Japanese. Atherosclerosis. 2004;173(2):315-9.

87. Ono K, Mannami T, Iwai N. Association of a promoter variant of the haeme oxygenase-1 gene with hypertension in women. J Hypertens. 2003;21(8):1497-503.

88. Yamada N, Yamaya M, Okinaga S, Nakayama K, Sekizawa K, Shibahara S, et al. Microsatellite polymorphism in the heme oxygenase-1 gene promoter is associated with susceptibility to emphysema. Am J Hum Genet. 2000;66(1):187-95.

89. Chen YH, Lin SJ, Lin MW, Tsai HL, Kuo SS, Chen JW, et al. Microsatellite polymorphism in promoter of heme oxygenase-1 gene is associated with susceptibility to coronary artery disease in type 2 diabetic patients. Hum Genet. 2002;111(1):1-8.

90. Hirai H, Kubo H, Yamaya M, Nakayama K, Numasaki M, Kobayashi S, et al. Microsatellite polymorphism in heme oxygenase-1 gene promoter is associated with susceptibility to oxidant-induced apoptosis in lymphoblastoid cell lines. Blood. 2003;102(5):1619-21.

91. Taha H, Skrzypek K, Guevara I, Nigisch A, Mustafa S, Grochot-Przeczek A, et al. Role of heme oxygenase-1 in human endothelial cells: lesson from the promoter allelic variants. Arterioscler Thromb Vasc Biol. 2010;30(8):1634-41.

92. Gozzelino R, Jeney V, Soares MP. Mechanisms of cell protection by heme oxygenase-1. Annu Rev Pharmacol Toxicol. 2010;50:323-54.

93. Zhang Y, Furuyama K, Kaneko K, Ding Y, Ogawa K, Yoshizawa M, et al. Hypoxia reduces the expression of heme oxygenase-2 in various types of human cell lines. A possible strategy for the maintenance of intracellular heme level. FEBS J. 2006;273(14):3136-47.

94. Han F, Takeda K, Yokoyama S, Ueda H, Shinozawa Y, Furuyama K, et al. Dynamic changes in expression of heme oxygenases in mouse heart and liver during hypoxia. Biochem Biophys Res Commun. 2005;338(1):653-9.

95. Vukomanovic D, McLaughlin BE, Rahman MN, Szarek WA, Brien JF, Jia Z, et al. Selective activation of heme oxygenase-2 by menadione. Can J Physiol Pharmacol. 2011;89(11):861-4.

96. Hirose W, Ikematsu K, Tsuda R. Age-associated increases in heme oxygenase-1 and ferritin immunoreactivity in the autopsied brain. Leg Med (Tokyo). 2003;5 Suppl 1:S360-6.

97. Schipper HM. Heme oxygenase expression in human central nervous system disorders. Free Radic Biol Med. 2004;37(12):1995-2011.

98. Wu B, Wu Y, Tang W. Heme Catabolic Pathway in Inflammation and Immune Disorders. Front Pharmacol. 2019;10:825.

99. Schaer DJ, Buehler PW, Alayash AI, Belcher JD, Vercellotti GM. Hemolysis and free hemoglobin revisited: exploring hemoglobin and hemin scavengers as a novel class of therapeutic proteins. Blood. 2013;121(8):1276-84.

100. Brouard S, Otterbein LE, Anrather J, Tobiasch E, Bach FH, Choi AM, et al. Carbon monoxide generated by heme oxygenase 1 suppresses endothelial cell apoptosis. J Exp Med. 2000;192(7):1015-26.

101. Otterbein LE, Bach FH, Alam J, Soares M, Tao Lu H, Wysk M, et al. Carbon monoxide has anti-inflammatory effects involving the mitogen-activated protein kinase pathway. Nat Med. 2000;6(4):422-8.

102. Arai T, Yoshikai Y, Kamiya J, Nagino M, Uesaka K, Yuasa N, et al. Bilirubin impairs bactericidal activity of neutrophils through an antioxidant mechanism in vitro. J Surg Res. 2001;96(1):107-13.

103. Mazzone GL, Rigato I, Ostrow JD, Bossi F, Bortoluzzi A, Sukowati CH, et al. Bilirubin inhibits the TNFalpha-related induction of three endothelial adhesion molecules. Biochem Biophys Res Commun. 2009;386(2):338-44.

104. Kovacsics CE, Gill AJ, Ambegaokar SS, Gelman BB, Kolson DL. Degradation of heme oxygenase-1 by the immunoproteasome in astrocytes: A potential interferon-gamma-dependent mechanism contributing to HIV neuropathogenesis. Glia. 2017;65(8):1264-77.

105. Nguyen TP, Soukup VM, Gelman BB. Persistent hijacking of brain proteasomes in HIV-associated dementia. Am J Pathol. 2010;176(2):893-902.

106. Exner M, Minar E, Wagner O, Schillinger M. The role of heme oxygenase-1 promoter polymorphisms in human disease. Free Radic Biol Med. 2004;37(8):1097-104.

107. Bai CH, Chen JR, Chiu HC, Chou CC, Chau LY, Pan WH. Shorter GT repeat polymorphism in the heme oxygenase-1 gene promoter has protective effect on ischemic stroke in dyslipidemia patients. J Biomed Sci. 2010;17:12.

108. Chen M, Zhou L, Ding H, Huang S, He M, Zhang X, et al. Short (GT) (n) repeats in heme oxygenase-1 gene promoter are associated with lower risk of coronary heart disease in subjects with high levels of oxidative stress. Cell Stress Chaperones. 2012;17(3):329-38.

109. Gulla A, Evans BJ, Navenot JM, Pundzius J, Barauskas G, Gulbinas A, et al. Heme oxygenase-1 gene promoter polymorphism is associated with the development of necrotizing acute pancreatitis. Pancreas. 2014;43(8):1271-6.

110. Rueda B, Oliver J, Robledo G, Lopez-Nevot MA, Balsa A, Pascual-Salcedo D, et al. HO-1 promoter polymorphism associated with rheumatoid arthritis. Arthritis Rheum. 2007;56(12):3953-8.

111. Vazquez-Armenta G, Gonzalez-Leal N, M JV-dlT, Munoz-Valle JF, Ramos-Marquez ME, Hernandez-Canaveral I, et al. Short (GT)n microsatellite repeats in the heme oxygenase-1 gene promoter are associated with antioxidant and anti-inflammatory status in Mexican pediatric patients with sepsis. Tohoku J Exp Med. 2013;231(3):201-9.

112. Yasuda H, Okinaga S, Yamaya M, Ohrui T, Higuchi M, Shinkawa M, et al. Association of susceptibility to the development of pneumonia in the older Japanese population with haem oxygenase-1 gene promoter polymorphism. J Med Genet. 2006;43(4):e17.

113. Seu L, Burt TD, Witte JS, Martin JN, Deeks SG, McCune JM. Variations in the heme oxygenase-1 microsatellite polymorphism are associated with plasma CD14 and viral load in HIV-infected African-Americans. Genes Immun. 2012;13(3):258-67.

114. Gill AJ, Garza R, Ambegaokar SS, Gelman BB, Kolson DL. Heme oxygenase-1 promoter region (GT)n polymorphism associates with increased neuroimmune activation and risk for encephalitis in HIV infection. J Neuroinflammation. 2018;15(1):70.

115. Garza R, Gill AJ, Bastien BL, Garcia-Mesa Y, Gruenewald AL, Gelman BB, et al. Heme oxygenase-1 promoter (GT) n polymorphism associates with HIV neurocognitive impairment. Neurol Neuroimmunol Neuroinflamm. 2020;7(3).

116. Wang YF, Gu YT, Qin GH, Zhong L, Meng YN. Curcumin ameliorates the permeability of the blood-brain barrier during hypoxia by upregulating heme oxygenase-1 expression in brain microvascular endothelial cells. J Mol Neurosci. 2013;51(2):344-51.

117. Shan Y, Lambrecht RW, Donohue SE, Bonkovsky HL. Role of Bach1 and Nrf2 in up-regulation of the heme oxygenase-1 gene by cobalt protoporphyrin. FASEB J. 2006;20(14):2651-3.

118. Parfenova H, Basuroy S, Bhattacharya S, Tcheranova D, Qu Y, Regan RF, et al. Glutamate induces oxidative stress and apoptosis in cerebral vascular endothelial cells: contributions of HO-1 and HO-2 to cytoprotection. Am J Physiol Cell Physiol. 2006;290(5):C1399-410.

119. McArthur JC, Steiner J, Sacktor N, Nath A. Human immunodeficiency virus-associated neurocognitive disorders: Mind the gap. Ann Neurol. 2010;67(6):699-714.

120. Dore GJ, McDonald A, Li Y, Kaldor JM, Brew BJ, National HIVSC. Marked improvement in survival following AIDS dementia complex in the era of highly active antiretroviral therapy. AIDS. 2003;17(10):1539-45.

121. Sacktor N. Changing clinical phenotypes of HIV-associated neurocognitive disorders. J Neurovirol. 2018;24(2):141-5.

122. Sacktor N, Skolasky RL, Seaberg E, Munro C, Becker JT, Martin E, et al. Prevalence of HIV-associated neurocognitive disorders in the Multicenter AIDS Cohort Study. Neurology. 2016;86(4):334-40.

123. Wiley CA, Soontornniyomkij V, Radhakrishnan L, Masliah E, Mellors J, Hermann SA, et al. Distribution of brain HIV load in AIDS. Brain Pathol. 1998;8(2):277-84.

124. Zhou L, Rua R, Ng T, Vongrad V, Ho YS, Geczy C, et al. Evidence for predilection of macrophage infiltration patterns in the deeper midline and mesial temporal structures of the brain uniquely in patients with HIV-associated dementia. BMC Infect Dis. 2009;9:192.

125. Nebuloni M, Pellegrinelli A, Ferri A, Bonetto S, Boldorini R, Vago L, et al. Beta amyloid precursor protein and patterns of HIV p24 immunohistochemistry in different brain areas of AIDS patients. AIDS. 2001;15(5):571-5.

126. Krivine A, Force G, Servan J, Cabee A, Rozenberg F, Dighiero L, et al. Measuring HIV-1 RNA and interferon-alpha in the cerebrospinal fluid of AIDS patients: insights into the pathogenesis of AIDS Dementia Complex. J Neurovirol. 1999;5(5):500-6.

127. Archibald SL, Masliah E, Fennema-Notestine C, Marcotte TD, Ellis RJ, McCutchan JA, et al. Correlation of in vivo neuroimaging abnormalities with postmortem human immunodeficiency virus encephalitis and dendritic loss. Arch Neurol. 2004;61(3):369-76.

128. Aylward EH, Henderer JD, McArthur JC, Brettschneider PD, Harris GJ, Barta PE, et al. Reduced basal ganglia volume in HIV-1-associated dementia: results from quantitative neuroimaging. Neurology. 1993;43(10):2099-104.

129. Dal Pan GJ, McArthur JH, Aylward E, Selnes OA, Nance-Sproson TE, Kumar AJ, et al. Patterns of cerebral atrophy in HIV-1-infected individuals: results of a quantitative MRI analysis. Neurology. 1992;42(11):2125-30.

130. Hestad K, McArthur JH, Dal Pan GJ, Selnes OA, Nance-Sproson TE, Aylward E, et al. Regional brain atrophy in HIV-1 infection: association with specific neuropsychological test performance. Acta Neurol Scand. 1993;88(2):112-8.

131. Kieburtz K, Ketonen L, Cox C, Grossman H, Holloway R, Booth H, et al. Cognitive performance and regional brain volume in human immunodeficiency virus type 1 infection. Arch Neurol. 1996;53(2):155-8.

132. Stout JC, Ellis RJ, Jernigan TL, Archibald SL, Abramson I, Wolfson T, et al. Progressive cerebral volume loss in human immunodeficiency virus infection: a longitudinal volumetric magnetic resonance imaging study. HIV Neurobehavioral Research Center Group. Arch Neurol. 1998;55(2):161-8.

133. Correa DG, Zimmermann N, Netto TM, Tukamoto G, Ventura N, de Castro Bellini Leite S, et al. Regional Cerebral Gray Matter Volume in HIV-Positive Patients with Executive Function Deficits. J Neuroimaging. 2016;26(4):450-7.

134. Clifford KM, Samboju V, Cobigo Y, Milanini B, Marx GA, Hellmuth JM, et al. Progressive Brain Atrophy Despite Persistent Viral Suppression in HIV Patients Older Than 60 Years. J Acquir Immune Defic Syndr. 2017;76(3):289-97.

135. Kuhn T, Schonfeld D, Sayegh P, Arentoft A, Jones JD, Hinkin CH, et al. The effects of HIV and aging on subcortical shape alterations: A 3D morphometric study. Hum Brain Mapp. 2017;38(2):1025-37.

136. Shin NY, Hong J, Choi JY, Lee SK, Lim SM, Yoon U. Retrosplenial cortical thinning as a possible major contributor for cognitive impairment in HIV patients. Eur Radiol. 2017;27(11):4721-9.

137. Rubin LH, Meyer VJ, R JC, Sundermann EE, Wu M, Weber KM, et al. Prefrontal cortical volume loss is associated with stress-related deficits in verbal learning and memory in HIV-infected women. Neurobiol Dis. 2016;92(Pt B):166-74.

138. Ann HW, Jun S, Shin NY, Han S, Ahn JY, Ahn MY, et al. Characteristics of Resting-State Functional Connectivity in HIV-Associated Neurocognitive Disorder. PLoS One. 2016;11(4):e0153493.

139. du Plessis S, Vink M, Joska JA, Koutsilieri E, Bagadia A, Stein DJ, et al. Prefrontal cortical thinning in HIV infection is associated with impaired striatal functioning. J Neural Transm (Vienna). 2016;123(6):643-51.

140. Melrose RJ, Tinaz S, Castelo JM, Courtney MG, Stern CE. Compromised fronto-striatal functioning in HIV: an fMRI investigation of semantic event sequencing. Behav Brain Res. 2008;188(2):337-47.

141. Ipser JC, Brown GG, Bischoff-Grethe A, Connolly CG, Ellis RJ, Heaton RK, et al. HIV infection is associated with attenuated frontostriatal intrinsic connectivity: a preliminary study. J Int Neuropsychol Soc. 2015;21(3):203-13.

142. O'Connor EE, Zeffiro TA, Zeffiro TA. Brain Structural Changes following HIV Infection: Meta-Analysis. AJNR Am J Neuroradiol. 2018;39(1):54-62.

143. Sanford R, Ances BM, Meyerhoff DJ, Price RW, Fuchs D, Zetterberg H, et al. Longitudinal Trajectories of Brain Volume and Cortical Thickness in Treated and Untreated Primary Human Immunodeficiency Virus Infection. Clin Infect Dis. 2018;67(11):1697-704.

144. Haddow LJ, Godi C, Sokolska M, Cardoso MJ, Oliver R, Winston A, et al. Brain Perfusion, Regional Volumes, and Cognitive Function in Human Immunodeficiency Virus-positive Patients Treated With Protease Inhibitor Monotherapy. Clin Infect Dis. 2019;68(6):1031-40.

145. Jiang X, Barasky R, Olsen H, Riesenhuber M, Magnus M. Behavioral and neuroimaging evidence for impaired executive function in "cognitively normal" older HIV-infected adults. AIDS Care. 2016;28(4):436-40.

146. Adeli E, Kwon D, Zhao Q, Pfefferbaum A, Zahr NM, Sullivan EV, et al. Chained regularization for identifying brain patterns specific to HIV infection. Neuroimage. 2018;183:425-37.

147. Garvey LJ, Pavese N, Politis M, Ramlackhansingh A, Brooks DJ, Taylor-Robinson SD, et al. Increased microglia activation in neurologically asymptomatic HIV-infected patients receiving effective ART. AIDS. 2014;28(1):67-72.

148. Kallianpur KJ, Valcour VG, Lerdlum S, Busovaca E, Agsalda M, Sithinamsuwan P, et al. HIV DNA in CD14+ reservoirs is associated with regional brain atrophy in patients naive to combination antiretroviral therapy. AIDS. 2014;28(11):1619-24.

149. Navia BA, Cho ES, Petito CK, Price RW. The AIDS dementia complex: II. Neuropathology. Ann Neurol. 1986;19(6):525-35.

150. Ortega M, Heaps JM, Joska J, Vaida F, Seedat S, Stein DJ, et al. HIV clades B and C are associated with reduced brain volumetrics. J Neurovirol. 2013;19(5):479-87.

151. Jensen BK, Roth LM, Grinspan JB, Jordan-Sciutto KL. White matter loss and oligodendrocyte dysfunction in HIV: A consequence of the infection, the antiretroviral therapy or both? Brain Res. 2019;1724:146397.

152. Solomon IH, Chettimada S, Misra V, Lorenz DR, Gorelick RJ, Gelman BB, et al. White Matter Abnormalities Linked to Interferon, Stress Response, and Energy Metabolism Gene Expression Changes in Older HIV-Positive Patients on Antiretroviral Therapy. Mol Neurobiol. 2020;57(2):1115-30.

153. Chen MF, Gill AJ, Kolson DL. Neuropathogenesis of HIV-associated neurocognitive disorders: roles for immune activation, HIV blipping and viral tropism. Curr Opin HIV AIDS. 2014;9(6):559-64.

154. Tavazzi E, Morrison D, Sullivan P, Morgello S, Fischer T. Brain inflammation is a common feature of HIV-infected patients without HIV encephalitis or productive brain infection. Curr HIV Res. 2014;12(2):97-110.

155. Spudich SS. Immune activation in the central nervous system throughout the course of HIV infection. Curr Opin HIV AIDS. 2016;11(2):226-33.

156. Boerwinkle A, Ances BM. Molecular Imaging of Neuroinflammation in HIV. J Neuroimmune Pharmacol. 2019;14(1):9-15.

157. Dore S, Sampei K, Goto S, Alkayed NJ, Guastella D, Blackshaw S, et al. Heme oxygenase-2 is neuroprotective in cerebral ischemia. Mol Med. 1999;5(10):656-63.

158. Chang EF, Wong RJ, Vreman HJ, Igarashi T, Galo E, Sharp FR, et al. Heme oxygenase-2 protects against lipid peroxidation-mediated cell loss and impaired motor recovery after traumatic brain injury. J Neurosci. 2003;23(9):3689-96.

159. Wang J, Zhuang H, Dore S. Heme oxygenase 2 is neuroprotective against intracerebral hemorrhage. Neurobiol Dis. 2006;22(3):473-6.

160. Schipper HM, Song W. A heme oxygenase-1 transducer model of degenerative and developmental brain disorders. Int J Mol Sci. 2015;16(3):5400-19.

161. Chen J. Heme oxygenase in neuroprotection: from mechanisms to therapeutic implications. Rev Neurosci. 2014;25(2):269-80.

162. Chen J, Tu Y, Connolly EC, Ronnett GV. Heme oxygenase-2 protects against glutathione depletion-induced neuronal apoptosis mediated by bilirubin and cyclic GMP. Curr Neurovasc Res. 2005;2(2):121-31.

163. Dore S, Goto S, Sampei K, Blackshaw S, Hester LD, Ingi T, et al. Heme oxygenase-2 acts to prevent neuronal death in brain cultures and following transient cerebral ischemia. Neuroscience. 2000;99(4):587-92.

164. Takahashi K, Hara E, Suzuki H, Sasano H, Shibahara S. Expression of heme oxygenase isozyme mRNAs in the human brain and induction of heme oxygenase-1 by nitric oxide donors. J Neurochem. 1996;67(2):482-9.

165. Ambegaokar SS, Kolson DL. Heme oxygenase-1 dysregulation in the brain: implications for HIV-associated neurocognitive disorders. Curr HIV Res. 2014;12(3):174-88.

166. Gill AJ, Kovacsics CE, Vance PJ, Collman RG, Kolson DL. Induction of Heme Oxygenase-1 Deficiency and Associated Glutamate-Mediated Neurotoxicity Is a Highly Conserved HIV Phenotype of Chronic Macrophage Infection That Is Resistant to Antiretroviral Therapy. J Virol. 2015;89(20):10656-67.

167. Cross SA, Cook DR, Chi AW, Vance PJ, Kolson LL, Wong BJ, et al. Dimethyl fumarate, an immune modulator and inducer of the antioxidant response, suppresses HIV replication and

macrophage-mediated neurotoxicity: a novel candidate for HIV neuroprotection. J Immunol. 2011;187(10):5015-25.

168. Shevchenko A, Wilm M, Vorm O, Mann M. Mass spectrometric sequencing of proteins silver-stained polyacrylamide gels. Anal Chem. 1996;68(5):850-8.

169. He JZ, Ho JJ, Gingerich S, Courtman DW, Marsden PA, Ward ME. Enhanced translation of heme oxygenase-2 preserves human endothelial cell viability during hypoxia. J Biol Chem. 2010;285(13):9452-61.

170. Gelman BB, Endsley J, Kolson D. When do models of NeuroAIDS faithfully imitate "the real thing"? J Neurovirol. 2018;24(2):146-55.

171. Kaartokallio T, Utge S, Klemetti MM, Paananen J, Pulkki K, Romppanen J, et al. Fetal Microsatellite in the Heme Oxygenase 1 Promoter Is Associated With Severe and Early-Onset Preeclampsia. Hypertension. 2018;71(1):95-102.

172. Vilander LM, Vaara ST, Donner KM, Lakkisto P, Kaunisto MA, Pettila V, et al. Heme oxygenase-1 repeat polymorphism in septic acute kidney injury. PLoS One. 2019;14(5):e0217291.

173. Gelman BB, Lisinicchia JG, Chen T, Johnson KM, Jennings K, Freeman DH, Jr., et al. Prefrontal dopaminergic and enkephalinergic synaptic accommodation in HIV-associated neurocognitive disorders and encephalitis. J Neuroimmune Pharmacol. 2012;7(3):686-700.

174. Gelman BB, Nguyen TP. Synaptic proteins linked to HIV-1 infection and immunoproteasome induction: proteomic analysis of human synaptosomes. J Neuroimmune Pharmacol. 2010;5(1):92-102.

175. Espey MG, Basile AS, Heaton RK, Ellis RJ. Increased glutamate in CSF and plasma of patients with HIV dementia. Neurology. 2002;58(9):1439; author reply -40.

176. Espey MG, Ellis RJ, Heaton RK, Basile AS. Relevance of glutamate levels in the CSF of patients with HIV-1-associated dementia complex. Neurology. 1999;53(5):1144-5.

177. Ferrarese C, Aliprandi A, Tremolizzo L, Stanzani L, De Micheli A, Dolara A, et al. Increased glutamate in CSF and plasma of patients with HIV dementia. Neurology. 2001;57(4):671-5.

178. Tremolizzo L, Aliprandi A, Longoni M, Stanzani L, Ferrarese C. Glutamate may be the soluble cerebrospinal fluid factor that induces calcium dysregulation in cultured astrocytes in HIV dementia. AIDS. 2002;16(12):1691-2; author reply 2-3.

179. Peluso MJ, Meyerhoff DJ, Price RW, Peterson J, Lee E, Young AC, et al. Cerebrospinal fluid and neuroimaging biomarker abnormalities suggest early neurological injury in a subset of individuals during primary HIV infection. J Infect Dis. 2013;207(11):1703-12.

180. Sailasuta N, Ross W, Ananworanich J, Chalermchai T, DeGruttola V, Lerdlum S, et al. Change in brain magnetic resonance spectroscopy after treatment during acute HIV infection. PLoS One. 2012;7(11):e49272.

181. Saing T, Lagman M, Castrillon J, Gutierrez E, Guilford FT, Venketaraman V. Analysis of glutathione levels in the brain tissue samples from HIV-1-positive individuals and subject with

Alzheimer's disease and its implication in the pathophysiology of the disease process. BBA Clin. 2016;6:38-44.

182. Cassol E, Misra V, Dutta A, Morgello S, Gabuzda D. Cerebrospinal fluid metabolomics reveals altered waste clearance and accelerated aging in HIV patients with neurocognitive impairment. AIDS. 2014;28(11):1579-91.

183. Abidin AZ, D'Souza AM, Nagarajan MB, Wismuller A. Investigating Changes in Brain Network Properties in HIV-Associated Neurocognitive Disease (HAND) using Mutual Connectivity Analysis (MCA). Proc SPIE Int Soc Opt Eng. 2016;9788.

184. Kumar AM, Fernandez JB, Singer EJ, Commins D, Waldrop-Valverde D, Ownby RL, et al. Human immunodeficiency virus type 1 in the central nervous system leads to decreased dopamine in different regions of postmortem human brains. J Neurovirol. 2009;15(3):257-74.

185. Kumar AM, Ownby RL, Waldrop-Valverde D, Fernandez B, Kumar M. Human immunodeficiency virus infection in the CNS and decreased dopamine availability: relationship with neuropsychological performance. J Neurovirol. 2011;17(1):26-40.

186. Cysique LA, Juge L, Gates T, Tobia M, Moffat K, Brew BJ, et al. Covertly active and progressing neurochemical abnormalities in suppressed HIV infection. Neurol Neuroimmunol Neuroinflamm. 2018;5(1):e430.

187. Cysique LA, Maruff P, Brew BJ. Prevalence and pattern of neuropsychological impairment in human immunodeficiency virus-infected/acquired immunodeficiency syndrome (HIV/AIDS) patients across pre- and post-highly active antiretroviral therapy eras: a combined study of two cohorts. J Neurovirol. 2004;10(6):350-7.

188. Cysique LA, Moffat K, Moore DM, Lane TA, Davies NW, Carr A, et al. HIV, vascular and aging injuries in the brain of clinically stable HIV-infected adults: a (1)H MRS study. PLoS One. 2013;8(4):e61738.

189. Mohamed M, Barker PB, Skolasky RL, Sacktor N. 7T Brain MRS in HIV Infection: Correlation with Cognitive Impairment and Performance on Neuropsychological Tests. AJNR Am J Neuroradiol. 2018;39(4):704-12.

190. Chockanathan U, AM DS, Abidin AZ, Schifitto G, Wismuller A. Automated diagnosis of HIV-associated neurocognitive disorders using large-scale Granger causality analysis of resting-state functional MRI. Comput Biol Med. 2019;106:24-30.

191. Bladowska J, Zimny A, Koltowska A, Szewczyk P, Knysz B, Gasiorowski J, et al. Evaluation of metabolic changes within the normal appearing gray and white matters in neurologically asymptomatic HIV-1-positive and HCV-positive patients: magnetic resonance spectroscopy and immunologic correlation. Eur J Radiol. 2013;82(4):686-92.

192. Murray ME, Przybelski SA, Lesnick TG, Liesinger AM, Spychalla A, Zhang B, et al. Early Alzheimer's disease neuropathology detected by proton MR spectroscopy. J Neurosci. 2014;34(49):16247-55.

193. Garvey L. Microglial cell activation is visualized with 11C-[R]-PK11195-PET scans in neuroasymptomatic HIV infected subjects on effective antiretroviral therapy. Conference on Retroviruses and Opportunistic Infections. Seattle, WA2012.

194. Lopez OL, Smith G, Meltzer CC, Becker JT. Dopamine systems in human immunodeficiency virus-associated dementia. Neuropsychiatry Neuropsychol Behav Neurol. 1999;12(3):184-92.

195. Meltzer CC, Wells SW, Becher MW, Flanigan KM, Oyler GA, Lee RR. AIDS-related MR hyperintensity of the basal ganglia. AJNR Am J Neuroradiol. 1998;19(1):83-9.

196. Berger JR, Arendt G. HIV dementia: the role of the basal ganglia and dopaminergic systems. J Psychopharmacol. 2000;14(3):214-21.

197. Israel SM, Hassanzadeh-Behbahani S, Turkeltaub PE, Moore DJ, Ellis RJ, Jiang X. Different roles of frontal versus striatal atrophy in HIV-associated neurocognitive disorders. Hum Brain Mapp. 2019;40(10):3010-26.

198. Vera JH, Guo Q, Cole JH, Boasso A, Greathead L, Kelleher P, et al. Neuroinflammation in treated HIV-positive individuals: A TSPO PET study. Neurology. 2016;86(15):1425-32.

199. Brew BJ, Rosenblum M, Cronin K, Price RW. AIDS dementia complex and HIV-1 brain infection: clinical-virological correlations. Ann Neurol. 1995;38(4):563-70.

200. Chang L, Lee PL, Yiannoutsos CT, Ernst T, Marra CM, Richards T, et al. A multicenter in vivo proton-MRS study of HIV-associated dementia and its relationship to age. Neuroimage. 2004;23(4):1336-47.

201. Moore DJ, Masliah E, Rippeth JD, Gonzalez R, Carey CL, Cherner M, et al. Cortical and subcortical neurodegeneration is associated with HIV neurocognitive impairment. AIDS. 2006;20(6):879-87.

202. Ances BM, Ortega M, Vaida F, Heaps J, Paul R. Independent effects of HIV, aging, and HAART on brain volumetric measures. J Acquir Immune Defic Syndr. 2012;59(5):469-77.

203. Alakkas A, Ellis RJ, Watson CW, Umlauf A, Heaton RK, Letendre S, et al. White matter damage, neuroinflammation, and neuronal integrity in HAND. J Neurovirol. 2018.

204. Tagliati M, Simpson D, Morgello S, Clifford D, Schwartz RL, Berger JR. Cerebellar degeneration associated with human immunodeficiency virus infection. Neurology. 1998;50(1):244-51.

205. Wang H, Li R, Zhou Y, Wang Y, Cui J, Nguchu BA, et al. Altered cerebro-cerebellum resting-state functional connectivity in HIV-infected male patients. J Neurovirol. 2018;24(5):587-96.

206. Elsheikh BH, Maher WE, Kissel JT. Cerebellar atrophy associated with human immunodeficiency virus infection. Arch Neurol. 2010;67(5):634-5.

207. Muller WA. Mechanisms of leukocyte transendothelial migration. Annu Rev Pathol. 2011;6:323-44.

208. Muller WA. The regulation of transendothelial migration: new knowledge and new questions. Cardiovasc Res. 2015;107(3):310-20.

209. Rossi B, Angiari S, Zenaro E, Budui SL, Constantin G. Vascular inflammation in central nervous system diseases: adhesion receptors controlling leukocyte-endothelial interactions. J Leukoc Biol. 2011;89(4):539-56.

210. Rahman A, Fazal F. Hug tightly and say goodbye: role of endothelial ICAM-1 in leukocyte transmigration. Antioxid Redox Signal. 2009;11(4):823-39.

211. Ou R, Zhang M, Huang L, Flavell RA, Koni PA, Moskophidis D. Regulation of immune response and inflammatory reactions against viral infection by VCAM-1. J Virol. 2008;82(6):2952-65.

212. Thaney VE, Kaul M. Type I Interferons in NeuroHIV. Viral Immunol. 2019;32(1):7-14.

213. Jansen AH, Reits EA, Hol EM. The ubiquitin proteasome system in glia and its role in neurodegenerative diseases. Front Mol Neurosci. 2014;7:73.

214. Limanaqi F, Biagioni F, Gaglione A, Busceti CL, Fornai F. A Sentinel in the Crosstalk Between the Nervous and Immune System: The (Immuno)-Proteasome. Front Immunol. 2019;10:628.

215. Sun J, Hoshino H, Takaku K, Nakajima O, Muto A, Suzuki H, et al. Hemoprotein Bach1 regulates enhancer availability of heme oxygenase-1 gene. EMBO J. 2002;21(19):5216-24.

216. Lim JL, van der Pol SM, Di Dio F, van Het Hof B, Kooij G, de Vries HE, et al. Protective effects of monomethyl fumarate at the inflamed blood-brain barrier. Microvasc Res. 2015;105:61-9.

217. Weksler BB, Subileau EA, Perriere N, Charneau P, Holloway K, Leveque M, et al. Blood-brain barrier-specific properties of a human adult brain endothelial cell line. FASEB J. 2005;19(13):1872-4.

218. Grennan JT, Loutfy MR, Su D, Harrigan PR, Cooper C, Klein M, et al. Magnitude of virologic blips is associated with a higher risk for virologic rebound in HIV-infected individuals: a recurrent events analysis. J Infect Dis. 2012;205(8):1230-8.

219. Price RW. Impact of antiretroviral therapy on HIV-related brain injury. Clin Infect Dis. 2011;52(2):244-7.

220. Anesten B, Yilmaz A, Hagberg L, Zetterberg H, Nilsson S, Brew BJ, et al. Blood-brain barrier integrity, intrathecal immunoactivation, and neuronal injury in HIV. Neurol Neuroimmunol Neuroinflamm. 2016;3(6):e300.

221. Toborek M, Lee YW, Flora G, Pu H, Andras IE, Wylegala E, et al. Mechanisms of the blood-brain barrier disruption in HIV-1 infection. Cell Mol Neurobiol. 2005;25(1):181-99.

222. Atluri VS, Hidalgo M, Samikkannu T, Kurapati KR, Jayant RD, Sagar V, et al. Effect of human immunodeficiency virus on blood-brain barrier integrity and function: an update. Front Cell Neurosci. 2015;9:212.

223. Nakagawa S, Castro V, Toborek M. Infection of human pericytes by HIV-1 disrupts the integrity of the blood-brain barrier. J Cell Mol Med. 2012;16(12):2950-7.

224. Persidsky Y, Stins M, Way D, Witte MH, Weinand M, Kim KS, et al. A model for monocyte migration through the blood-brain barrier during HIV-1 encephalitis. J Immunol. 1997;158(7):3499-510.

225. Williams DW, Byrd D, Rubin LH, Anastos K, Morgello S, Berman JW. CCR2 on CD14(+)CD16(+) monocytes is a biomarker of HIV-associated neurocognitive disorders. Neurol Neuroimmunol Neuroinflamm. 2014;1(3):e36.

226. Luissint AC, Artus C, Glacial F, Ganeshamoorthy K, Couraud PO. Tight junctions at the blood brain barrier: physiological architecture and disease-associated dysregulation. Fluids Barriers CNS. 2012;9(1):23.

227. Chiba H, Osanai M, Murata M, Kojima T, Sawada N. Transmembrane proteins of tight junctions. Biochim Biophys Acta. 2008;1778(3):588-600.

228. Burdo TH, Lackner A, Williams KC. Monocyte/macrophages and their role in HIV neuropathogenesis. Immunol Rev. 2013;254(1):102-13.

229. Dwyer BE, Nishimura RN, Lu SY. Differential localization of heme oxygenase and NADPH-diaphorase in spinal cord neurons. Neuroreport. 1995;6(7):973-6.

230. Yoo SJ, Nakra NK, Ronnett GV, Moon C. Protective Effects of Inducible HO-1 on Oxygen Toxicity in Rat Brain Endothelial Microvessel Cells. Endocrinol Metab (Seoul). 2014;29(3):356-62.

231. Aztatzi-Santillan E, Nares-Lopez FE, Marquez-Valadez B, Aguilera P, Chanez-Cardenas ME. The protective role of heme oxygenase-1 in cerebral ischemia. Cent Nerv Syst Agents Med Chem. 2010;10(4):310-6.

232. Soares MP, Seldon MP, Gregoire IP, Vassilevskaia T, Berberat PO, Yu J, et al. Heme oxygenase-1 modulates the expression of adhesion molecules associated with endothelial cell activation. J Immunol. 2004;172(6):3553-63.

233. Wilhelm I, Fazakas C, Krizbai IA. In vitro models of the blood-brain barrier. Acta Neurobiol Exp (Wars). 2011;71(1):113-28.

234. Slanina H, Schmutzler M, Christodoulides M, Kim KS, Schubert-Unkmeir A. Effective plasmid DNA and small interfering RNA delivery to diseased human brain microvascular endothelial cells. J Mol Microbiol Biotechnol. 2012;22(4):245-57.

235. Strazza M, Maubert ME, Pirrone V, Wigdahl B, Nonnemacher MR. Co-culture model consisting of human brain microvascular endothelial and peripheral blood mononuclear cells. J Neurosci Methods. 2016;269:39-45.

236. Eugenin EA, Gamss R, Buckner C, Buono D, Klein RS, Schoenbaum EE, et al. Shedding of PECAM-1 during HIV infection: a potential role for soluble PECAM-1 in the pathogenesis of NeuroAIDS. J Leukoc Biol. 2006;79(3):444-52.

237. Eugenin EA, Osiecki K, Lopez L, Goldstein H, Calderon TM, Berman JW. CCL2/monocyte chemoattractant protein-1 mediates enhanced transmigration of human immunodeficiency virus (HIV)-infected leukocytes across the blood-brain barrier: a potential mechanism of HIV-CNS invasion and NeuroAIDS. J Neurosci. 2006;26(4):1098-106.

238. Poganik JR, Aye Y. Electrophile Signaling and Emerging Immuno- and Neuro-modulatory Electrophilic Pharmaceuticals. Front Aging Neurosci. 2020;12:1.

239. Fu CY, Chen J, Lu XY, Zheng MZ, Wang LL, Shen YL, et al. Dimethyl fumarate attenuates lipopolysaccharide-induced mitochondrial injury by activating Nrf2 pathway in cardiomyocytes. Life Sci. 2019;235:116863.

240. Kraus J, Oschmann P. The impact of interferon-beta treatment on the blood-brain barrier. Drug Discov Today. 2006;11(15-16):755-62.

241. Lopez-Ramirez MA, Fischer R, Torres-Badillo CC, Davies HA, Logan K, Pfizenmaier K, et al. Role of caspases in cytokine-induced barrier breakdown in human brain endothelial cells. J Immunol. 2012;189(6):3130-9.

242. Forster C, Burek M, Romero IA, Weksler B, Couraud PO, Drenckhahn D. Differential effects of hydrocortisone and TNFalpha on tight junction proteins in an in vitro model of the human blood-brain barrier. J Physiol. 2008;586(7):1937-49.

243. Jakimovski D, Kolb C, Ramanathan M, Zivadinov R, Weinstock-Guttman B. Interferon beta for Multiple Sclerosis. Cold Spring Harb Perspect Med. 2018;8(11).

244. Tintore M, Sastre-Garriga J. Multiple sclerosis: Dimethyl fumarate is coming of age. Nat Rev Neurol. 2016;12(8):436-7.

245. FDA Approves Oral Bafiertam™ (Monomethyl Fumarate), Similar to Tecfidera® for Relapsing MS - No Launch Date Yet National Multiple Sclerosis Society2020 [updated May 3, 2020. Available from: https://www.nationalmssociety.org/About-the-Society/News/FDA-Approves-Oral-Bafiertam™-(Monomethyl-Fumarate)?feed=AllNationalNews.

246. Lin SX, Lisi L, Dello Russo C, Polak PE, Sharp A, Weinberg G, et al. The anti-inflammatory effects of dimethyl fumarate in astrocytes involve glutathione and haem oxygenase-1. ASN Neuro. 2011;3(2).

247. Singh D, Reeta KH, Sharma U, Jagannathan NR, Dinda AK, Gupta YK. Neuro-protective effect of monomethyl fumarate on ischemia reperfusion injury in rats: Role of Nrf2/HO1 pathway in peri-infarct region. Neurochem Int. 2019;126:96-108.

248. Scannevin RH, Chollate S, Jung MY, Shackett M, Patel H, Bista P, et al. Fumarates promote cytoprotection of central nervous system cells against oxidative stress via the nuclear factor (erythroid-derived 2)-like 2 pathway. J Pharmacol Exp Ther. 2012;341(1):274-84.

249. Tsuchihashi S, Zhai Y, Fondevila C, Busuttil RW, Kupiec-Weglinski JW. HO-1 upregulation suppresses type 1 IFN pathway in hepatic ischemia/reperfusion injury. Transplant Proc. 2005;37(4):1677-8.

250. von Knethen A, Neb H, Morbitzer V, Schmidt MV, Kuhn AM, Kuchler L, et al. PPARgamma stabilizes HO-1 mRNA in monocytes/macrophages which affects IFN-beta expression. Free Radic Biol Med. 2011;51(2):396-405.

251. Gresch O, Altrogge L. Transfection of Difficult-to-Transfect Primary Mammalian Cells. In: Hartley JL, editor. Protein Expression in Mammalian Cells: Methods and Protocols. Totowa, NJ: Humana Press; 2012. p. 65-74.

252. Sonar SA, Shaikh S, Joshi N, Atre AN, Lal G. IFN-gamma promotes transendothelial migration of CD4(+) T cells across the blood-brain barrier. Immunol Cell Biol. 2017;95(9):843-53.

253. Sanna PP, Repunte-Canonigo V, Masliah E, Lefebvre C. Gene expression patterns associated with neurological disease in human HIV infection. PLoS One. 2017;12(4):e0175316.

254. Morgello S, Gelman BB, Kozlowski PB, Vinters HV, Masliah E, Cornford M, et al. The National NeuroAIDS Tissue Consortium: a new paradigm in brain banking with an emphasis on infectious disease. Neuropathol Appl Neurobiol. 2001;27(4):326-35.

255. Boban J, Thurnher MM, Brkic S, Lendak D, Bugarski Ignjatovic V, Todorovic A, et al. Neurometabolic Remodeling in Chronic Hiv Infection: a Five-Year Follow-up Multi-Voxel Mrs Study. Sci Rep. 2019;9(1):19799.

256. Muller WA. How endothelial cells regulate transmigration of leukocytes in the inflammatory response. Am J Pathol. 2014;184(4):886-96.

257. Ishikawa K, Navab M, Leitinger N, Fogelman AM, Lusis AJ. Induction of heme oxygenase-1 inhibits the monocyte transmigration induced by mildly oxidized LDL. J Clin Invest. 1997;100(5):1209-16.

258. Du D, Chang S, Chen B, Zhou H, Chen ZK. Heme oxygenase-1 protects INF-gamma primed endothelial cells from Jurkat T-cell adhesion. Transplant Proc. 2007;39(10):3449-51.

259. Chen-Roetling J, Kamalapathy P, Cao Y, Song W, Schipper HM, Regan RF. Astrocyte heme oxygenase-1 reduces mortality and improves outcome after collagenase-induced intracerebral hemorrhage. Neurobiol Dis. 2017;102:140-6.

260. Gold R, Kappos L, Arnold DL, Bar-Or A, Giovannoni G, Selmaj K, et al. Placebo-controlled phase 3 study of oral BG-12 for relapsing multiple sclerosis. N Engl J Med. 2012;367(12):1098-107.

261. Fox R. The New England Journal of Medicine publishes pivotal data demonstrating efficacy and safety of oral BG-12 (dimethyl fumarate) in multiple sclerosis. Can J Neurosci Nurs. 2012;34(3):7-11.

262. Bafiertam (monomethyl fumarate) delayed-release capsules, for oral use. 2020.

263. Banner Life Sciences Announces Final FDA Approval of BAFIERTAM for Multiple Sclerosis [press release]. Business Wire, April 30, 2020 2020.

264. Gill AJ, Kolson DL. Dimethyl fumarate modulation of immune and antioxidant responses: application to HIV therapy. Crit Rev Immunol. 2013;33(4):307-59.

265. Fernandez S, Tanaskovic S, Helbig K, Rajasuriar R, Kramski M, Murray JM, et al. CD4+ T-cell deficiency in HIV patients responding to antiretroviral therapy is associated with increased expression of interferon-stimulated genes in CD4+ T cells. J Infect Dis. 2011;204(12):1927-35.

266. Kunze R, Urrutia A, Hoffmann A, Liu H, Helluy X, Pham M, et al. Dimethyl fumarate attenuates cerebral edema formation by protecting the blood-brain barrier integrity. Exp Neurol. 2015;266:99-111.

267. Lim JL, van der Pol SM, Di Dio F, van Het Hof B, Kooij G, de Vries HE, et al. Protective effects of monomethyl fumarate at the inflamed blood-brain barrier. Microvasc Res. 2016;105:61-9.

268. Haarmann A, Nehen M, Deiss A, Buttmann M. Fumaric Acid Esters Do Not Reduce Inflammatory NF-kappaB/p65 Nuclear Translocation, ICAM-1 Expression and T-Cell Adhesiveness of Human Brain Microvascular Endothelial Cells. Int J Mol Sci. 2015;16(8):19086-95.

269. Benardais K, Pul R, Singh V, Skripuletz T, Lee DH, Linker RA, et al. Effects of fumaric acid esters on blood-brain barrier tight junction proteins. Neurosci Lett. 2013;555:165-70.

270. Wang YY, Yang YX, Zhe H, He ZX, Zhou SF. Bardoxolone methyl (CDDO-Me) as a therapeutic agent: an update on its pharmacokinetic and pharmacodynamic properties. Drug Des Devel Ther. 2014;8:2075-88.

271. Nio Y, Sasai M, Akahori Y, Okamura H, Hasegawa H, Oshima M, et al. Bardoxolone methyl as a novel potent antiviral agent against hepatitis B and C viruses in human hepatocyte cell culture systems. Antiviral Res. 2019;169:104537.

272. Takagi T, Kitashoji A, Iwawaki T, Tsuruma K, Shimazawa M, Yoshimura S, et al. Temporal activation of Nrf2 in the penumbra and Nrf2 activator-mediated neuroprotection in ischemia-reperfusion injury. Free Radic Biol Med. 2014;72:124-33.

273. Imai T, Takagi T, Kitashoji A, Yamauchi K, Shimazawa M, Hara H. Nrf2 activator ameliorates hemorrhagic transformation in focal cerebral ischemia under warfarin anticoagulation. Neurobiol Dis. 2016;89:136-46.